

TigerSat Blue

A High-Powered CubeSat for Demonstration of
Solid-Fuel Cylindrical Hall Thruster Capabilities

Critical Design Review

MAE 342: Blue Team

May 15, 2018

Contents

1	Introduction	4
1.1	Introduction to CubeSats	4
1.2	Cylindrical Hall Thrusters	4
1.3	Team Organization	5
2	Mission Design	6
2.1	Mission Concept	6
2.2	CONOPS	6
2.3	Mission Requirements	7
2.4	Space Environment	9
3	Orbit Analysis	13
3.1	Orbit Selection	13
3.2	Selection of Altitude Limits	18
3.3	Complete STK Simulation	24
3.4	Conclusion	28
4	Payload	29
4.1	Cylindrical Hall Thruster (CHT) Introduction	29
4.2	CHT Payload Characterization	30
4.3	Measurements and Devices	32
4.4	CHT Characteristic Relationships and Failure Modes	36
5	Power Systems	39
5.1	Requirements	39
5.2	System architecture	40
5.3	Component Selection	41

5.4	Analysis	48
6	Mechanisms	52
6.1	Introduction	52
6.2	Requirements	53
6.3	Component Selection	54
6.4	Mechanism Characteristics	56
6.5	Testing	58
6.6	Conclusion	59
7	Structures and Configuration	60
7.1	Configuration Overview	60
7.2	Structural Analysis	64
7.3	Mass Budget	67
8	Attitude Determination and Control System	69
8.1	Requirements and Modes	69
8.2	ADCS Package Selection and Specifications	69
8.3	Cubesat Coordinate System	71
8.4	Detumbling	72
8.5	Initial Location and Orientation Acquisition	74
8.6	Orbit Maintenance	76
8.7	Slews	76
8.8	Environmental Disturbance Torques	80
8.9	Torques from Error in Thruster Placement	82
8.10	Conclusion	84
9	Communications and Data Handling	86
9.1	Introduction	86
9.2	Requirements	86
9.3	Data Budget	91
9.4	Communications	92
9.5	Processing	97
9.6	Software	98
9.7	Testing	104
9.8	Conclusion	104

10 Thermal	105
10.1 Overview	105
10.2 Design Assumptions	105
10.3 Design Requirements	107
10.4 Heat Sources	108
10.5 Orbit Analysis	109
10.6 Thruster Calculation	114
10.7 Launch Temperature Transience	117
10.8 Conclusion	118
11 Bibliography	120
A Testing Procedures	128
A.1 Testing Procedure Overview	128
A.2 Subsystem Testing Procedures	129
A.3 Integration Testing Procedures	130
A.4 Environmental Testing Procedures	131
B External Requirements	133
B.1 NASA-LSP-REQ-317	133
B.2 NanoRacks CubeSat Deployer Interface Control Document	148
B.3 CubeSat Design Specification	177

Chapter 1

Introduction

1.1 Introduction to CubeSats

A CubeSat is a U-class (University-class) spacecraft with strict unit based size restrictions. The size classifications range from 1U to 27U, or 10x10x10cm to 34x35x36cm. CubeSats are widely used for educational purposes as they are an affordable and standardized method to experiment in space. The standardization allows potentially all components to be off the shelf.

1.2 Cylindrical Hall Thrusters

The Cylindrical Hall Thruster (CHT) is an approach to electric propulsion that can retain efficiency while scaling to smaller applications. It utilizes a permanent magnet and electromagnets to direct ions and create thrust. Typically, the CHT fuel will be an inert gas with low ionization energy such as xenon gas. Our payload thruster, however, is being designed to utilize a solid fuel, resulting in an increase in efficiency and a reduction in technical complications associated with incorporating a pressurized chamber on a small spacecraft. Furthermore, NASA regulations forbid the use of pressurized chambers on CubeSats without explicit permission. The CHT performs in the power range of 50-300W and generates thrust in the range of 2.5-12mN. The technical benefits of the CHT is an extremely high thrust to fuel-mass ratio and a relatively small size (7.3cm diameter, 3.5cm length).

1.3 Team Organization

Below are the assigned roles for each member in the team:

Subsystem	Member 1	Member 2
Chief Engineer	Michael Whitmore	
Program Manager	Gokulanand Iyer	
Mechanisms	Devon Hartsough	Mike Fuerst
Structures	John Van Orden	Michael Whitmore
Communications and Data Handling	Isabel Cleff	Matt Romer
Orbit Analysis	Bertha Wang	Jeff Diament
Payload	John Van Orden	
Thermal	Robbie Cohen	Fred Zheng
Power	Mark Scerbo	Dan Chao
Attitude Determination and Control System	Hemani Kalucha	Mrudhula Baskaran

Chapter 2

Mission Design

2.1 Mission Concept

The goal of the TigerSat mission is to demonstrate the capability of a novel solid-fuel Cylindrical Hall Thruster (CHT) by performing an orbit raising maneuver. The demonstration satellite will be a 3U CubeSat, deployed from the International Space Station via a NanoRacks deployer. The various criteria for mission success are:

- Partial mission success: The thruster fires properly and provides orbit station-keeping
- Minimum mission success: The thruster fires properly and is capable of raising and lowering the orbit at least once
- Full mission success: The thruster fires properly and is capable of raising and lowering the orbit nine times in two years of operation

2.2 CONOPS

The TigerSat Blue concept of operations is as follows:

- I. Deployment
 - A. Pre-Deployment: Power off (Main power system) - From delivery to Launch Vehicle (LV) through On-Orbit Deployment
 - B. On-Orbit Deployment: Power on (Main power system) - No RF radiation for first 45 minutes

- C. Mechanism deployment - solar arrays (minimum 30 minutes after on-orbit deployment)
 - i. Store mechanism status data for telemetry
- D. Communication systems power up - (minimum 45 minutes after on-orbit deployment)
 - i. Send telemetry to ground
 - ii. Receive commands from ground (if necessary)

II. Primary Mission Operation

- A. Battery Charging - no thruster firing
 - i. Perform sun-pointing control
 - ii. Store telemetry data
 - iii. Send telemetry to ground
- B. Thruster Firing - battery discharge
 - i. Control thrust vectoring
 - ii. Store telemetry data
- C. Safe Mode - emergency battery charging (when battery charge is critically low)
 - i. Turn off telemetry
 - ii. Charge with sun-pointing
 - iii. Receive communication from ground
 - iv. When battery levels are safe again, switch to normal charging

III. End-Of-Life (EOL) Operation

- A. De-orbit - after 2 years of mission operation
 - i. Lower orbit to naturally de-orbit within 25 years

2.3 Mission Requirements

Due to the modular and standardized nature of a CubeSat mission, requirements come from multiple sources. The first source is mission specific requirements. The remaining requirements and constraints come from standardized CubeSat deployers and Launch Service Programs (LSP), which facilitate these types of missions.

2.3.1 Mission Specific Requirements

The primary mission requirements are derived from the mission concept and the mission success parameters. The functional and operational requirements defined by the mission specifications are as follows:

Functional	
Performance	-Demonstrate 9 orbit raising/lowering maneuver cycles -Complete mission within 2 years
Responsiveness	-Must transmit telemetry/receive commands at minimum once a day -Capable of autonomous normal operation
End of Life	-Must de-orbit naturally within 25 years
Operational	
Duration	-Mission designed for a maximum duration of 2 years
Survivability	-Must survive LEO space environment while completing its primary mission
Data Content	-Must provide telemetry detailing TigerSat position, velocity, orientation -Must provide telemetry detailing fuel usage, relevant thruster usage data

2.3.2 External Requirements and Constraints

Deployer

The TigerSat Blue mission is designed to accommodate deployment from a NanoRacks CubeSat Deployer. The primary design constraints are derived from the NanoRacks CubeSat Deployer Interface Control Document Revision 0.36 as well as the Document Change Notices (DCN) 052 and 064. The document appears in Appendix B.2.

Additionally, the CubeSat Design Specification Revision 13 is used to provide further CubeSat design standards, in parallel with the NanoRacks constraints. The document appears in Appendix B.3.

Launch Service Provider

The TigerSat Blue mission will be deployed as a secondary payload on a resupply mission to the ISS, in accordance with the NASA CubeSat Launch Initiative (CSLI). The

design must also comply with the guidelines laid out in the NASA Launch Services Program Level Dispenser and CubeSat Requirements Document Revision B. This document lays out constraints on the TigerSat Blue design as well as required testing procedures. Testing procedures are collected in Appendix A. The document appears in Appendix B.1.

Sizing Requirements Overview

TigerSat will be a 3U sized CubeSat. A 3U CubeSat is 10 cm x 10 cm x 34.05 cm. The NanoRacks mass limit for a 3U sized CubeSat is 4.8 kg.

2.4 Space Environment

2.4.1 Injection Orbit Definition

The initial satellite orbit is constrained to approximately the orbit of the International Space Station due to the LV and deployment constraint. The orbital parameters are as follows [1]:

Orbit Parameters of ISS
Epoch (UTC): 02 April 2018 21:41:28
Eccentricity: 0.0001729
inclination: 51.6383°
perigee height: 403 km
apogee height: 406 km
right ascension of ascending node: 34.0210°
argument of perigee: 292.5230°
revolutions per day: 15.54147523
mean anomaly at epoch: 67.5739°
orbit number at epoch: 2680

The initial orbit of the CubeSat will be approximately a circular low earth orbit (LEO) orbit at or near 400 km altitude with 51.6 degree inclination.

2.4.2 Low Earth Orbit

The space environment that the TigerSat will encounter during its primary mission operation is LEO. Specifically the initial orbit altitude will be 400 km which is located

within the Thermosphere (85-500 km). The characteristic features of the Thermosphere are that it is the last layer of the atmosphere with continuous medium properties, and that it has increasing temperature with increasing altitude.

The primary implication of the CubeSat being in LEO is that it will be affected by the Earth's atmosphere. It will interact with atmospheric species including molecular nitrogen and oxygen, as well as atomic oxygen, hydrogen and helium. The CubeSat will move through this medium on the order of 8 km/s. A major effect of this interaction is that the satellite will experience drag. Drag will affect its orbital energy and lifetime. A second major effect is the erosion of material surfaces due to adsorption [2].

2.4.3 Ionosphere

The orbit is also located within the Ionosphere, specifically the F2 layer (250-500 km). The F2 layer is dominated by O+. It will be exposed to extreme ultraviolet radiation with a wavelength range from 10 to 91 nm[4]. At 400 km, the CubeSat's orbit will be above the F2 layer maximum electron density, which occurs at 300 km, and thus will encounter a lower electron density in its initial orbit. The satellite will be located within the Earth's atmosphere for the entire duration of its mission and thus it will not have a chance of encountering the Van Allen Belts.

2.4.4 Orbital Debris

Additionally, a major characteristic of LEO is substantial orbital debris. The distribution of debris at different altitudes and in LEO is depicted in Figure 3-1. At a 400 km orbit, the spatial density of orbital debris is about 2×10^{-9} particles/km³, which is about 2 orders of magnitude higher than the density at MEO, but comparable to density at GEO and GPS altitude. The density at the CubeSat's altitude is also an order of magnitude lower than the maximum debris density in LEO, which occurs at 800 km altitude. This means that the satellite's environment will have increasing debris at higher altitudes and decreasing debris at lower altitudes.

2.4.5 Operating Orbit

Because the CubeSat is performing an orbit raising maneuver, it will encounter a slightly different environment during the course of its mission. The alternative space environment is a higher orbit around 500-600 km altitude. This secondary space environment would

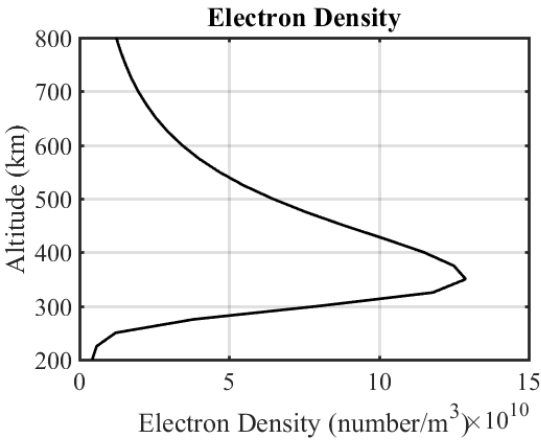
be located in the Exosphere (500-1000 km). In this environment, the satellite would no longer encounter an atmospheric continuous medium, and would also encounter lower ion density due to moving above the F2 layer into the Topside F layer. The satellite would then be less affected by drag and ionized particle fluence, but would face orbital debris density that is an order of magnitude higher. In both cases the satellite would have a high probability of collision with small particulate matter, with a 99.8+% chance of interference over the 2 year duration of the mission at 400 km, and effectively a 100% chance of collision at an orbit between 500-600 km (numbers based on Statistical Collision Hazard equation)[4]. The primary difference between environments is that the initial 400 km orbit will have fewer collisions with particulate matter, but the mission lifetime will be constrained by atmospheric drag. The secondary orbit would encounter significantly more debris, but would experience less atmospheric drag affecting the mission lifetime.

2.4.6 Qualitative Analysis

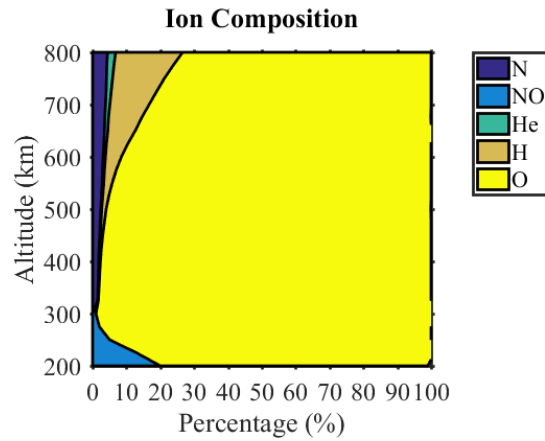
Since the CubeSat is performing an orbit raising maneuver, the environment it encounters will vary. If the orbit reaches too low of an altitude, it will be heavily affected by drag and will de-orbit rapidly. If the orbit reaches too high of an altitude, it would reach a point where it would not naturally de-orbit within the required timescale. These effects are detailed in chapter 3.

The TigerSat would experience higher electron density and Ionosphere effects at a lower altitude. These effects would decrease at increasing altitudes. This would suggest that the CubeSat should stay at a higher orbit to prevent damage to the outer structure from charged particles.

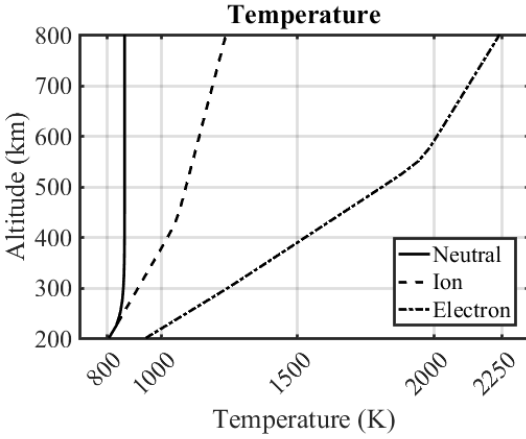
At increasing altitudes, the amount of orbital debris would increase, peaking around 800 km. This effect, however, would not be significant, since while the chance of encountering debris would be higher, it would still be at a safe level. This is also detailed in chapter 3.



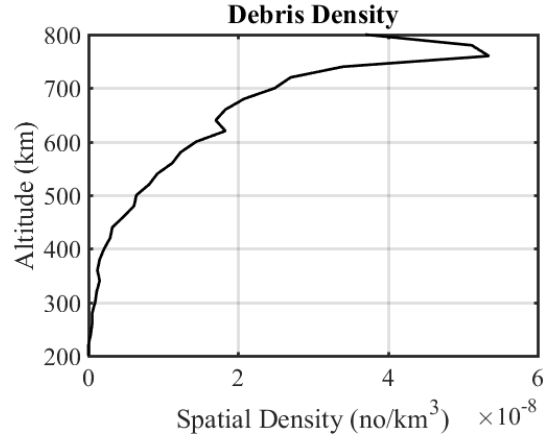
(a) Electron density range contains the F layer and topside F layer.



(b) Primary ion particles are elemental oxygen.



(c) Ionized particles become more highly energized with increasing altitude.



(d) Debris peak around 750 km is Iridium-Cosmos breakup.

Figure 2.1: Graphs of relevant environmental effects for the TigerSat Blue orbit altitude range. Data for Ionosphere effects from International Reference Ionosphere for 50°latitude and 40°longitude [3]. Data for orbital debris published by NASA from ORDEM 3.0 (Orbital Debris Engineering Model) [4].

Chapter 3

Orbit Analysis

The functionality of the cylindrical hall thruster can be demonstrated by performing following orbital maneuvers throughout the satellite's lifetime:

- I. **Altitude change:** Continuously raise and lower the altitude of the orbit by a certain distance (e.g. 200 km).
- II. **Inclination change:** Continuously raise and lower the inclination of the orbit by a certain value (e.g. 15°).
- III. **Station-keeping:** Maintain the initial orbit altitude to within a certain margin (e.g. +/- 10 km)

The following section details the trades associated with each orbital maneuver and discusses how the final selection of altitude change was decided.

3.1 Orbit Selection

3.1.1 Radiation

As discussed in Section 2.4, TigerSat is launched from the ISS orbit at an altitude above the earth of approximately 400 km. Whether the mission seeks to conduct altitude change, inclination change, or station-keeping, the orbit will remain in LEO, so only effects of radiation within LEO are considered. The radiation density below 1000 km altitude is low, and at 1000 km altitude, radiation density significantly increases due to the Van Allen belts.[5] The mission would not leave LEO, or more specifically, rise

above 600 km altitude, as determined in Section 3.2. Therefore, the radiation profile would remain approximately constant regardless of the chosen orbital maneuver, and thus would not affect orbit selection.

However, although radiation is not a limiting factor for one mission option compared to another, it is still a significant concern that must be appropriately dealt with by properly protecting the spacecraft from the damaging effects of ionized particles. Regardless of the type of mission, radiation hardening will protect the satellite against these damaging effects.

3.1.2 Orbital Debris

The risk of impacting orbital debris must be low to make the mission viable. Unlike radiation, it's much more difficult to protect the satellite from collisions with orbital debris. Thus, the best protective mechanism is to avoid high debris density regions of space. The following quantitative analysis evaluates how the debris field in LEO varies with altitude, and compares this with NASA requirements for debris collision risk. This analysis is conducted under the assumption that the debris density is relatively constant at a given altitude (and thus does not vary with inclination). A more detailed model of the debris field is necessary to quantify how debris density changes with inclination. Thus, this analysis is primarily used to determine if the altitude change mission option has increased risk of impacting orbital debris as compared to the inclination change and station-keeping mission options.

The Space Mission Analysis and Design, 3rd Edition (SMAD 3rd Ed.) Table 21-3 (see Figure 3.1 below) details the debris collision probability for a satellite with a cross section of 5-40 m² for altitudes from 300 km to 800 km for a one-year mission.[5]

While *SMAD 3rd Ed.* lists the probabilities for a cross sectional area of 5 m² and 40 m², TigerSat has a maximum cross sectional area of 0.1969 m². The probability of collision is proportional to cross sectional area, so the probability of collision for 5 m² listed by *SMAD 3rd Ed.* is simply scaled by a factor of 0.1959 m² divided by 5 m². Additionally, because TigerSat's mission is two years long, Equation 3.1 is used to redetermine the probability of collision for two years. With these corrections, the appropriate cross sectional area and mission length are taken into account and are used in the debris collision risk analysis.

$$p_{2\text{years}} = 1 - (1 - p_{1\text{year}})^2 \quad (3.1)$$

TABLE 21-3. Collision Probability per Year (in 1999). The table values are approximated over all inclinations for a cross-sectional area range of 5 to 40 m². The cross-sectional area is defined as the area viewed from one orientation, and is approximately 1/4 of the total surface area for simple convex shapes.

Altitude (km)	Collision Probability per Year		
	Trackable	1 cm diameter	1 mm diameter
300	10^{-6} - 10^{-5}	10^{-4} - 10^{-3}	10^{-2} - 10^{-1}
400	10^{-5} - 10^{-4}	10^{-4} - 10^{-3}	10^{-1} - 1
500	10^{-5} - 10^{-4}	10^{-4} - 10^{-3}	10^{-1} - 1
600	10^{-5} - 10^{-4}	10^{-4} - 10^{-3}	10^{-1} - 1
800	10^{-4} - 10^{-3}	10^{-3} - 10^{-2}	10^{-1} - 1
1,000	10^{-4} - 10^{-3}	10^{-3} - 10^{-2}	10^{-1} - 1
1,200	10^{-4} - 10^{-3}	10^{-3} - 10^{-2}	10^{-1} - 1
1,500	10^{-5} - 10^{-4}	10^{-3} - 10^{-2}	10^{-1} - 1
2,000	10^{-6} - 10^{-5}	10^{-5} - 10^{-3}	10^{-2} - 10^{-1}

Figure 3.1: Collision probability per year as tabulated in *SMAD 3rd Ed.*

NASA requirements for collision risk are listed in a document titled, "Process for Limiting Orbital Debris." They state that the probability of collision with debris that is larger than 10 cm in diameter must be less than 0.001, and that the probability of collision with debris less than 10 cm in diameter must be less than 0.01.[6] The mission must satisfy these requirements.

Figure 3.2 compares the actual probability of collision with TigerSat (solid lines) to the NASA probability thresholds (dashed lines). For LEO altitudes of 300 km to 800 km, the probability of collision with debris is entirely compliant with the required probability threshold, which is 0.01 for debris smaller than 10 cm in diameter, and 0.001 for debris larger than 10 cm in diameter. This indicates that orbital debris is not a limiting factor for altitude change, inclination change, or station-keeping.

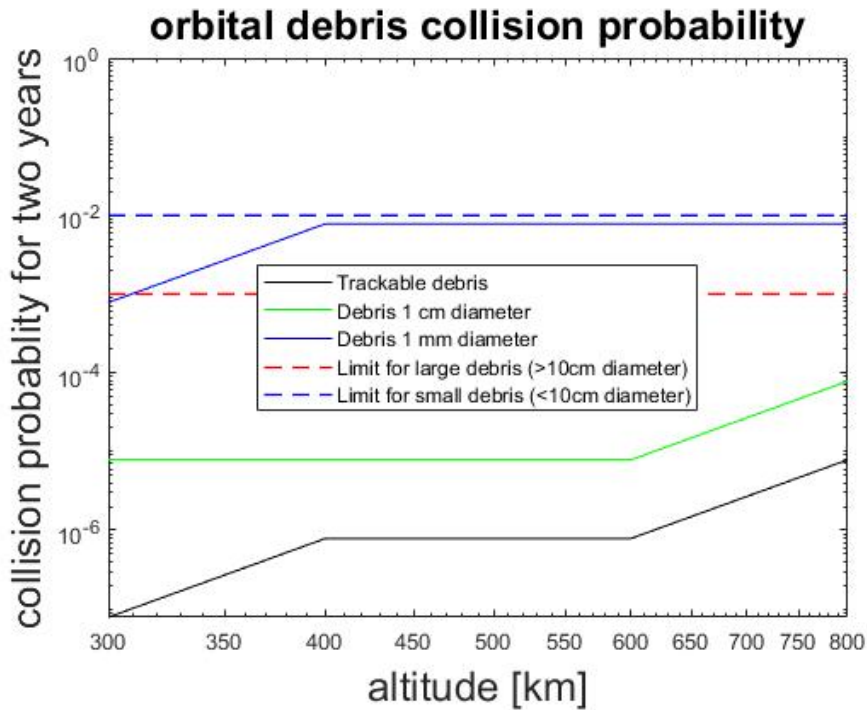


Figure 3.2: Probability of debris collision for the 0.1959 m^2 TigerSat for the 2-year mission compared to NASA probability limits.

3.1.3 Orbital Determination Sensors

The orbit parameters of each mission possibility must be determined within a certain accuracy in order to make the mission viable. For instance, if the orbit determination sensor was only accurate to an altitude within $+/- 100 \text{ km}$, it would be impractical to conduct a mission to raise and lower the altitude of the orbit by 50 km.

The GPS integrated on the flight computer (see Section 9.5 for more details) will be used as the primary orbital determination sensor. Its positional accuracy is less than 10 meters (3D RMS), and its velocity accuracy less than 25 cm/s (3D RMS), which is sufficient considering that the orbital maneuvers are in the magnitude of kilometers. Since the GPS provides a highly accurate position estimate, it is not a limiting factor for the altitude change, inclination change, or station-keeping mission profiles.

3.1.4 Delta-V Requirements

It is important to do an estimate of the delta-V requirements for altitude change and inclination change (the two mission options with the highest delta-V requirements) in order

to determine mission feasibility. Researchers from the Georgia Institute of Technology performed analysis for low thrust, high I_{sp} electric propulsion maneuvers beginning in LEO.[7] Equation 3.2 shows the delta-V (ΔV_{alt}) needed to raise the altitude of an orbit by 200 km. In this equation, μ is the standard gravitational parameter of the Earth and V_1 and V_2 are the circular orbit velocities at orbit radii of r_1 (400 km) and r_2 (600 km), respectively.

$$\begin{aligned}\Delta V_{alt} &= V_1 - V_2 \\ &= \sqrt{\frac{\mu}{r_1}} - \sqrt{\frac{\mu}{r_2}}\end{aligned}\tag{3.2}$$

Equation 3.3 shows the delta-V (ΔV_{inc}) needed to raise the inclination of an orbit by 15° . In this equation, μ is the standard gravitational parameter of the Earth, V_1 is the circular orbit velocities at orbit radii of r_1 (400 km), and Δi is the inclination change in radians.

$$\begin{aligned}\Delta V_{inc} &= V_1 \Delta i \frac{\pi}{2} \\ &= \sqrt{\frac{\mu}{r_1}} \Delta i \frac{\pi}{2}\end{aligned}\tag{3.3}$$

Raising the altitude of a circular orbit from 400 km to 600 km requires a delta-V of 111 m/s. To raise the inclination of a satellite by 15° requires a delta-V of 3155 m/s.

The rocket equation (Equation 3.4) can be used to compute the total delta-V (ΔV_{total}) capability of a 5 kg satellite (m_0) carrying 0.5 kg of fuel (m_{fuel}). For this calculation, the CHT is approximated to have an $I_{sp} = 2000$ s and $g_0 = 9.81$ m/s².

$$\Delta V_{total} = I_{sp} g_0 \ln\left(\frac{m_0}{m_0 - m_{fuel}}\right)\tag{3.4}$$

Equation 3.4 suggests that the $\Delta V_{total} = 2067$ m/s. Thus, the satellite contains enough fuel to perform up to 9 altitude change cycles (where raising and lowering 200 km is “one” cycle), but not enough fuel to change the inclination of the satellite by 15° even once. Because the mission can accommodate more cycles of altitude changes compared to inclination changes, it would be easier to fulfill partial mission success for altitude changes. This could obviously be accommodated by changing the value of the inclination change maneuver; however, changing inclination will always require significantly more delta-V than changing altitude.

Thus, the altitude change mission option allows for more interesting maneuvers than

the station-keeping option, but has significantly lower delta-V requirements than the inclination change option.

3.1.5 Interest

The Princeton CubeSat Team is currently designing a mission to demonstrate the efficacy of a CHT via altitude change, which gives it preference over the inclination change or station keeping. Choosing a parallel mission path to the Princeton CubeSat team gives the opportunity for collaboration and has the potential to bolster the purpose of this project

3.1.6 Mission Profile Selection

Altitude change (repeatedly raising and lowering the altitude of the orbit) was ultimately chosen as the primary orbital maneuver of the mission. Environmental factors were not deciding factors: radiation hardening of the vehicle is necessary for each mission option and the risk of colliding with orbital debris is low for each mission option. Orbit determination sensors were also not a deciding factor: the resolution of the GPS is significantly high enough to accurately track each mission option. The delta-V requirements suggest that between the delta-V intensive mission options (altitude change and inclination change), the altitude change option requires significantly less delta-V. This lower requirement makes it possible to repeat altitude raising and lowering cycles, and allows the opportunity to obtain partial mission success in the case of premature thruster failure. Ultimately, the greatest applicability of the altitude change mission option (in order to best parallel the path of the Princeton CubeSat Club) made it the preferential option for this mission.

3.2 Selection of Altitude Limits

This section details how the upper and lower limits of the orbit altitude were selected. In order to minimize orbital debris, there is a NASA requirement that all small satellites must naturally de-orbit themselves (primarily due to the effects of atmospheric drag) in 25 years. This translates into a constraint on the maximum altitude of the satellite, because above a certain altitude, the force due to atmospheric drag is not large enough to de-orbit the satellite within the allotted time (since the atmospheric density is too

low). Furthermore, atmospheric drag also places a constraint on the minimum altitude of the satellite. If the altitude of the satellite dips too low, then the thrusters may not be able to overcome atmospheric drag, and the orbit will decay prematurely. Throughout the mission, the satellite needs to maintain a certain critical distance away from this absolute minimum altitude in order to ensure that there is ample time to recover from any anomalies or malfunctions with the propulsion system. These altitude limits are determined using an atmospheric drag model and a software simulation.

3.2.1 SMAD Atmospheric Drag Model

To conduct a preliminary analysis of how atmospheric drag will affect the orbit of the satellite, the *Space Mission Engineering: The New SMAD (The New SMAD)* was used.[2] Section 6.2.3 in *The New SMAD* discusses how atmospheric properties limit the lifetime of a vehicle in Equation 3.5:

$$L \approx \frac{-H}{\Delta a_{rev}} \quad (3.5)$$

where H is the atmospheric density scale height and Δa_{rev} is the change in semi-major axis per revolution given by Equation 3.6 (assuming that the orbit is always nearly circular):

$$\Delta a_{rev} = -2\pi \left(\frac{C_D A}{m} \right) \rho a \quad (3.6)$$

where $\frac{C_D A}{m}$ is referred to as the ballistic coefficient of the satellite, ρ is the atmospheric density, and a is the average semi-major axis for that rotation of the satellite.

Atmospheric density is strongly dependent on both altitude and solar activity level. Broadly speaking, higher altitudes correspond to decreasing atmospheric density and higher solar activity corresponds to increasing atmospheric density. The solar cycle has a period of roughly 11 years, during which solar activity slowly oscillates between a minimum and maximum value. Thus, on timescales on the order of 25 years (which are used in the following analysis), the lifetime of a satellite becomes largely independent of the specific phase of the solar cycle, since all periods of solar activity are experienced by the satellite.

The New SMAD Table 8-3 tabulates the ballistic coefficients for various spacecraft (see Figure 3.3 below). The satellite can be approximated as having a similar mass, area, and drag coefficient to Oscar-1, which was a small amateur radio satellite.

TABLE 8-3. Typical Ballistic Coefficients for Low-Earth Orbit Satellites. Values for cross-sectional area and drag coefficients are estimated from the approximate shape, size, and orientation of the satellite and solar arrays. [XA = cross-sectional]

Satellite	Mass (kg)	Shape	Max. XA (m ²)	Min. XA (m ²)	Max. XA Drag Coef.	Min. XA Drag Coef.	Max. Ballistic Coef. (kg/m ²)	Min. Ballistic Coef. (kg/m ²)	Type of Mission
Oscar-1	5	box	0.075	0.0584	4	2	42.8	16.7	Comm.

Figure 3.3

Equation 3.5 was integrated over varying values of atmospheric drag (for changing altitude as well as minimum and maximum solar activity). The results were plotted in *The New SMAD* Figure 8-4, which is show in Figure 3.4 below.

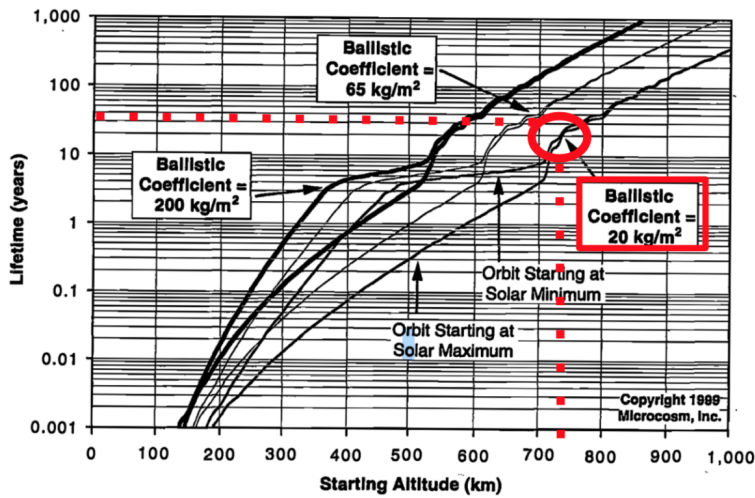


Fig. 8-4. Satellite Lifetimes as a Function of Altitude, Relationship to the Solar Cycle, and Representative Ballistic Coefficients. For each ballistic coefficient, the upper curve represents launch at the start of solar minimum when there will be a low level of decay and the lower curve represents launch at the start of solar maximum when the satellite will decay most rapidly for several years. Data generated with the *SatLife* program [1999].

Figure 3.4

If the satellite has a ballistic coefficient of approximately 20 kg/m^2 (as per Figure 3.3), then as long as the altitude of orbit never exceeds about 725 km, the orbit will decay in less than 25 years. This result is true regardless of whether the mission begins at a solar maximum or minimum. Furthermore, if the orbit altitude ever drops below approximately 200 km, then the orbit will decay within a matter of days. To summarize, this approximate analysis using SMAD produces the following constraints:

- I. Maximum altitude $\approx 725 \text{ km}$ (so that satellite naturally de-orbits in less than 25 years)

- II. Minimum altitude \approx 200 km (so that satellite does not prematurely de-orbit within a few days)

3.2.2 STK Simulation

Lifetime Tool

AGI's STK has a tool to approximate the lifetime of a satellite based on decay due to atmospheric drag. The following parameters were used for this tool:

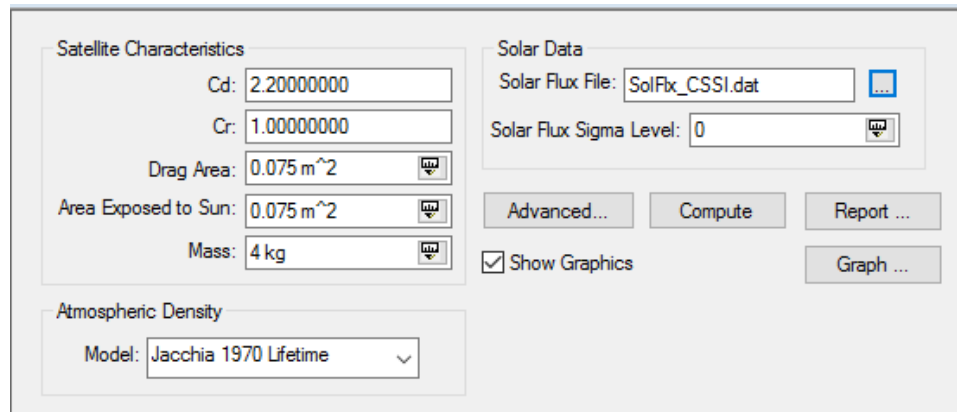


Figure 3.5: STK lifetime tool settings

The geometrical features of the satellite were estimated to match the parameters of the satellite (with Cd based on Oscar-1 from the previous SMAD-based analysis). The drag area is approximated as an approximate average of the minimum and maximum surface area of the vehicle (0.01 m^2 and 0.160 m^2). This is done to simulate a tumbling satellite with constantly varying orientations.

The lifetime tool was used to calculate the lifetime of satellites with starting altitudes ranging from 200 to 700 km. The results are plotted in Figure 3.6 below, shown with an exponential trendline. The lifetime tool takes into account variable atmospheric density due to the roughly eleven year solar cycle.

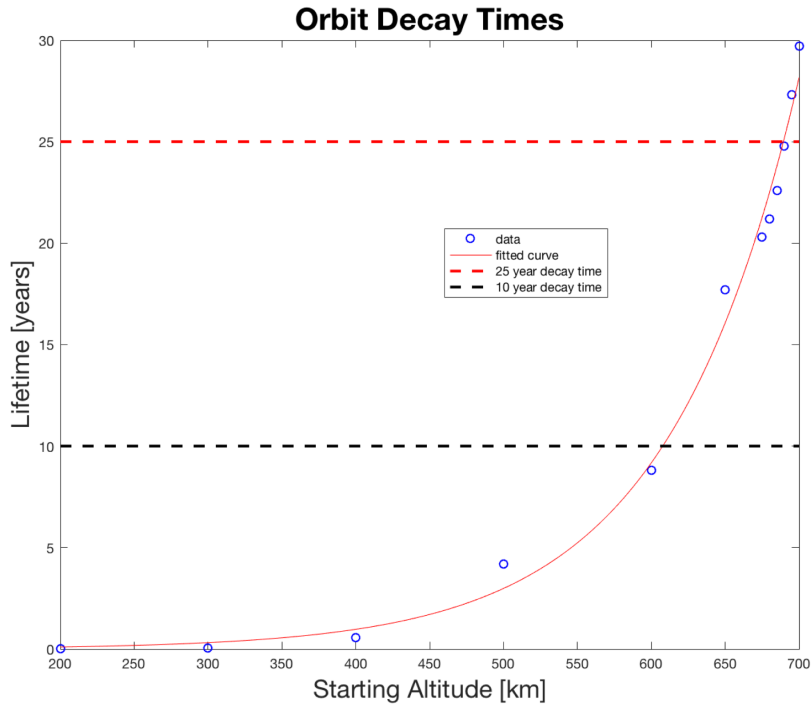


Figure 3.6: Satellite lifetime for different altitudes

In case the satellite de-orbited while somehow fixed in an orientation such that its maximum surface area was always perpendicular to its trajectory, a safety factor of 2.5 was added. Thus in Figure 3.6, the 25 year lifetime limit is shown as well as a 10 year lifetime limit, which accounts for this safety factor.

Full Decay Simulation

To verify the results of the lifetime tool discussed above, a full fidelity simulation was conducted (see Force settings in Figure 3.7) to model the decay of the satellite due to atmospheric drag from a starting altitude of 690 km. This full simulation took approximately 30 minutes and verified the results of the lifetime tool. The following plot (Figure 3.8) shows how this orbit decays over time (in terms of apogee radius, perigee radius, and eccentricity).

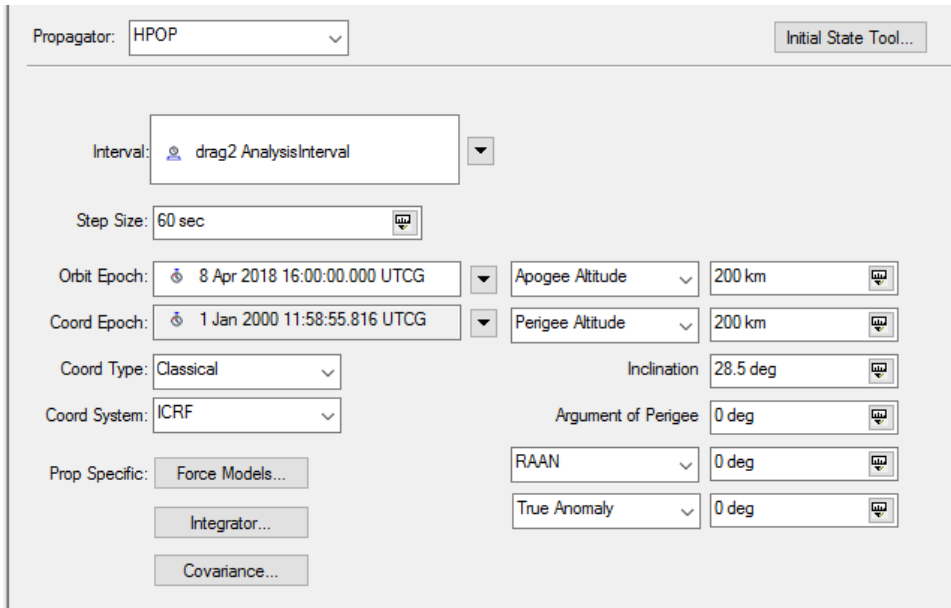


Figure 3.7: STK basic orbit settings

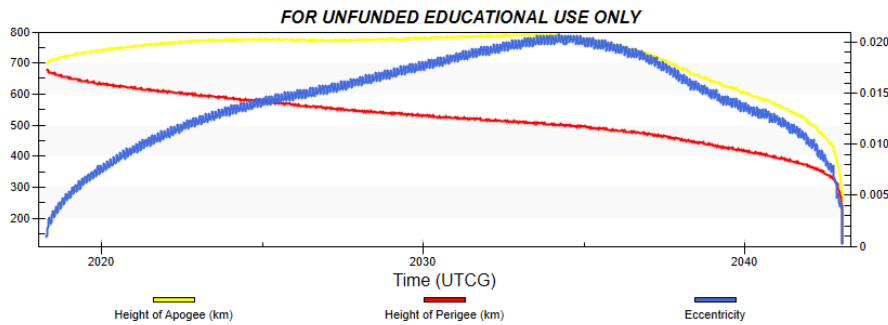


Figure 3.8: Orbit decay for starting altitude of 690km

The STK analysis further refines the SMAD approximations. To summarize,

- I. Maximum altitude \approx 690 km (so that satellite naturally de-orbits in less than 25 years)
- II. Minimum altitude \approx 200 km (so that satellite does not prematurely de-orbit within a few days)

3.2.3 Altitude Limits Selection

Based on *The New SMAD* and STK analysis, which give a range of the *maximum* upper altitude and *minimum* lower altitude, final values were chosen as the altitude bounds

for this mission.

The upper limit was chosen to be 600 km. This ensures that even if the thruster fails at this altitude, then the satellite will naturally decay due to atmospheric drag within 10 years (a safety factor of 2.5 compared to the 25 year NASA limit).

The lower limit was chosen to be 400 km. This ensures that if the thruster fails at this altitude, the satellite will have approximately 200 days to recover before the orbit fully decays. Furthermore, this is approximately the same altitude as the ISS (which varies between 403 and 406 km), which will be the starting altitude for the mission.

3.3 Complete STK Simulation

The mission is modeled using STK, and simulates thruster burn periods followed by propagation periods to raise and lower the satellite over the course of two years. The maximum burn time of the TigerSat is 10 minutes, which is limited by the on-board battery capacity. During the ten-minute burn periods, the thruster fires tangentially to the trajectory of the satellite. To raise the altitude, the burns are done in the same direction as the velocity vector and to lower the altitude, the burns are done in the opposite direction of the velocity vector; this allows for a “spiral out” or “spiral in” trajectory. After the batteries are depleted, the satellite cruises for a fixed time, which is when the batteries recharge. The initial state variables used in the simulations are shown in Figure 3.9. Note that a total initial mass of 5 kg was used to simulate a conservative scenario.

Coord. System:	Earth Inertial	<input type="button" value="..."/>
Coordinate Type:	Keplerian	<input type="button" value="..."/>
Orbit Epoch:	18 Apr 2018 16:00:00.000 UTCG	<input type="button" value="..."/>
Element Type:	Osculating	<input type="button" value="..."/>
Periapsis Altitude	403 km	<input type="button" value="..."/>
Apoapsis Altitude	406 km	<input type="button" value="..."/>
Inclination:	51.6 deg	<input type="button" value="..."/>
Right Asc. of Asc. Node	0 deg	<input type="button" value="..."/>
Argument of Periapsis:	0 deg	<input type="button" value="..."/>
True Anomaly	0 deg	<input type="button" value="..."/>
Dry Mass:	4.5 kg	<input type="button" value="..."/>
Drag		
Coefficient (Cd):	2.2	<input type="button" value="..."/>
Area:	0.1958 m^2	<input type="button" value="..."/>
Solar Radiation Pressure (Spherical)		
Coefficient (Cr):	1	<input type="button" value="..."/>
Area:	0.1958 m^2	<input type="button" value="..."/>
Radiation Pressure (Albedo/Thermal)		
Coefficient (Ck):	1	<input type="button" value="..."/>
Area:	0.1958 m^2	<input type="button" value="..."/>
GPS Solar Radiation Pressure		
K1:	1	<input type="button" value="..."/>
K2:	1	<input type="button" value="..."/>
Tank Pressure:	5000 Pa	<input type="button" value="..."/>
Tank Volume:	1.5 m^3	<input type="button" value="..."/>
Tank Temperature:	293.15 K	<input type="button" value="..."/>
Fuel Density:	1000 kg/m^3	<input type="button" value="..."/>
Fuel Mass:	0.5 kg	<input type="button" value="..."/>
Maximum Fuel Mass:	0.5 kg	<input type="button" value="..."/>

Figure 3.9: STK initial state variables for TigerSat mission.

3.3.1 Duty Cycle Selection

The ratio between the burn time and charge time is defined as the duty cycle and was selected based on mission time and power subsystem capabilities. To get a sense of how duty cycle affects mission time, altitude raising from 400 km to 600 km was simulated with different duty cycles using STK. The time it takes to raise the satellite once was simulated with varying duty cycles, and is plotted to show an *inversely* linear relationship in Figure 3.10. Lower duty cycles are preferable because they take fewer days to raise; however, the chosen duty cycle must comply with power subsystem constraints. Ultimately, a duty cycle of 1:30 was deemed appropriate, which would take less than 30 days for one altitude raise, and also provides a 1.82 safety factor with the minimum duty cycle for the worst-case scenario from the power subsystem (Table 5.7). This corresponds to up to 13 cycles over the course of the two year mission.

It is important to also note that while the mission is simulated with a consistent duty cycle, the actual mission may not adhere to the strict 1:30 duty cycle. As mentioned in Section 9.6, thruster firings are scheduled by the ground station. Due to thermal

constraints, thruster firings will only be scheduled while the satellite is in the eclipse portion of the orbit (in the shadow of the Earth). Thus, the *average* duty cycle will be 1:30, but the actual duty cycle will vary for each burn.

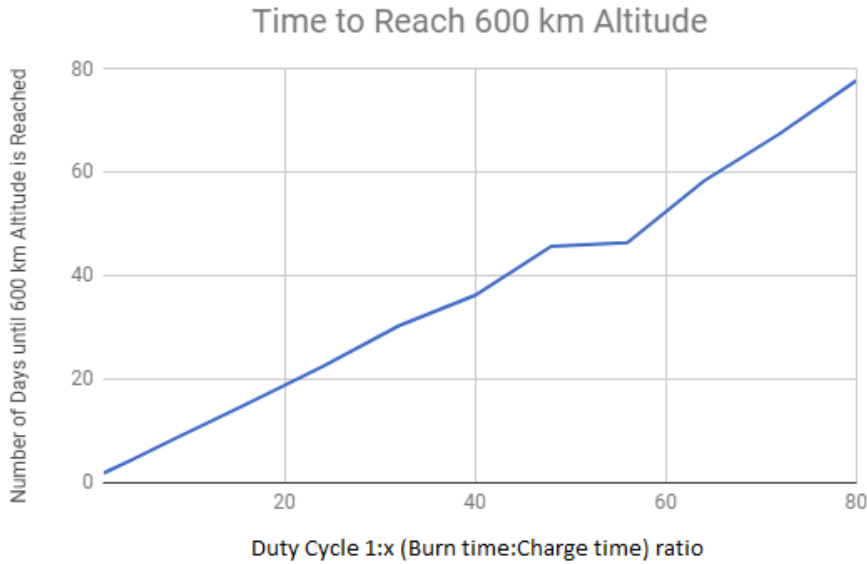


Figure 3.10: Raise time to reach 600 km based on duty cycle.

3.3.2 Full Mission Simulation

A full STK simulation of nine full raising and lowering cycles ($400\text{ km} \rightarrow 600\text{ km} \rightarrow 400\text{ km} \times 9$) was conducted and the results are displayed in Figures 3.11 and 3.12 below.

In Figure 3.11, the pink lines represent burn trajectories and the yellow lines represent charge time trajectories. The mission passes over all of Earth between 51.6° north and south of the equator, which is why there is no ground track over the poles in Figure 3.11, and reflects the fact that the orbit maintains an inclination of 51.6° . While the inclination remains constant, the node of the orbit precesses due to perturbations the oblateness of Earth. Furthermore, since the satellite is not in a geostationary orbit, the Earth rotates beneath the satellite at a different period than the orbit; thus, the ground track changes over the course of the mission.

One full cycle (raising and lowering the altitude by 200 km) nominally takes 52 days to complete, so in two years the satellite has time to complete 14 full cycles (Figure 3.12). However, due to payload constraints that are detailed in Section 3.1.4, the mission will only consist of 9 cycles. Based on the simulation, 9 cycles will take 467 days. Compared

to the allotted time of two years, this leaves a safety factor of 1.56 to fulfill the mission.

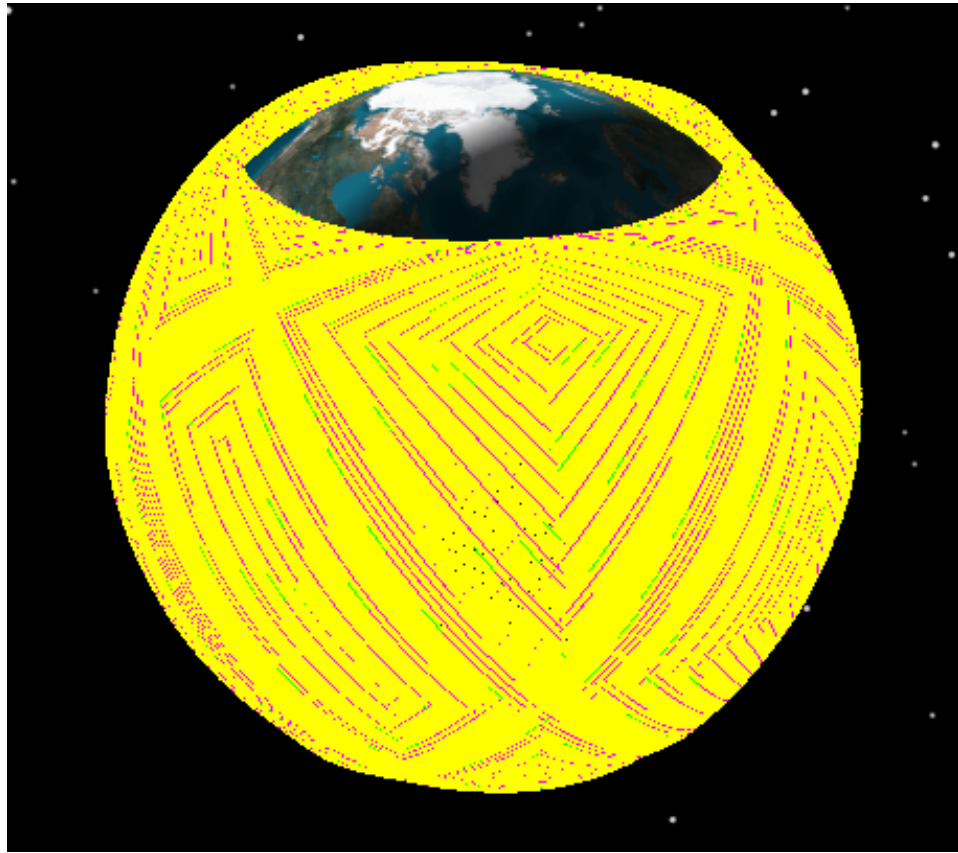


Figure 3.11: 3D graphic of the simulated mission using STK.

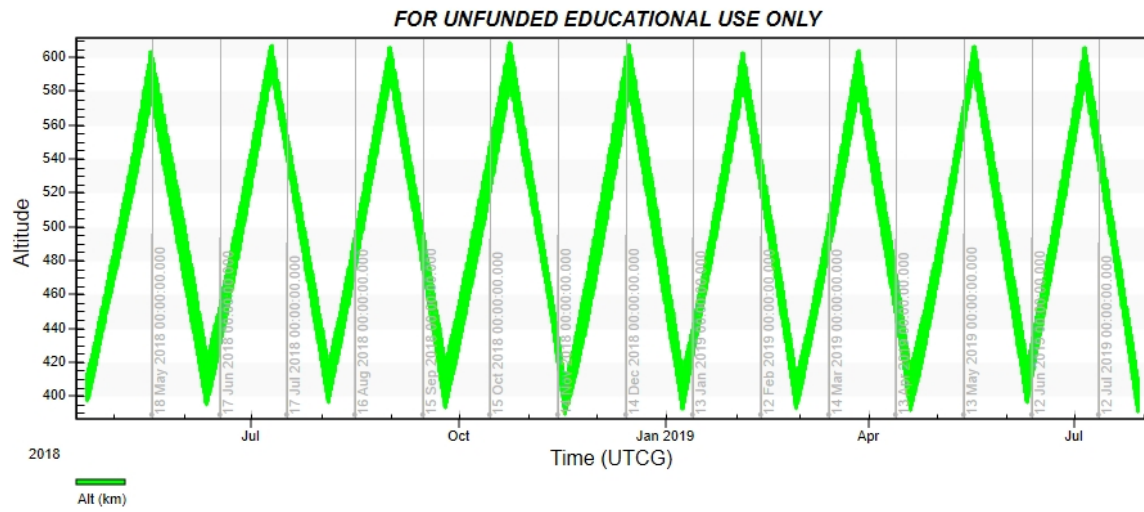


Figure 3.12: Altitude change over time throughout the entire mission.

Justification of Simulation Approximations

For this simulation, the satellite was modelled as always travelling perpendicular to its maximum cross sectional area. In reality, the attitude of the satellite will change, especially when it slews to remain sun-pointed during the charging phase. However, designing the simulation like this allows for a worst-case estimate of the time required to raise the altitude, since the satellite will be maximally fighting against atmospheric drag.

The duty cycle was modelled as constant (1:30). Burns will be scheduled by the ground station so that they occur only when the satellite is in eclipse. However, designing the simulation like this is a fair approximation, since the mission is designed such that the average duty cycle converges to 1:30.

The custom thruster is modelled as having a constant I_{sp} . Realistically, the performance of the thruster is predicted to degrade by approximately 2% throughout the 2 year mission. However, the thruster decay was not modelled in the simulation because it is predicted to be so small. However, ample margins are included into the mission time line to account for degraded thruster performance.

3.4 Conclusion

The mission will be to demonstrate 9 cycles of raising and lowering TigerSat between the initial ISS orbit at 400 km altitude and 600 km altitude. The maximum altitude of 600 km was based on the NASA requirement of de-orbiting in 25 years, and the minimum altitude of 400 km was selected in order to ensure that TigerSat would have ample time to recover its orbit if the cylindrical hall thruster temporarily failed. The mission will have on average a 1:30 duty cycle, which will take 52 days per raise/lower cycle, and would allow TigerSat to have enough *time* complete up to 13 complete cycles. However, if the mission proceeds nominally then the spacecraft will only have enough *fuel* to perform 9 complete cycles (see Section 3.1.4). Thus, the *fuel* capacity of the spacecraft is ultimately the limiting factor; if the mission goes completely according to plan then it will be completed in less than the allotted two years for the mission. This margin allows time for technical failures and recoveries and also accommodates errors in the STK simulation.

Chapter 4

Payload

4.1 Cylindrical Hall Thruster (CHT) Introduction

The mission objectives characterize the testing in a space environment of a cylindrical hall effect thruster. There are a variety of hall thrusters, each with slightly different thrust, mass, and power. This mission will make use of a solid fuel iodine cylindrical hall thruster with major characteristics enumerated in table 4.1.

Hall thrusters are classified as a mature electric propulsion method by NASA, with a TRL of 8 for pressurized xenon fuel and a TRL of 4 for gaseous iodine. [8] This payload will utilize a solid fuel mass management system that stores iodine as a solid fuel on the spacecraft. Solid iodine is 3 times more dense than pressurized xenon, and does not require heavy pressurized containment mechanism. [9] It therefore reduces space and mass on board the spacecraft. However, only one major prototype of this kind has been tested by NASA, a 12U solid fuel iodine hall thruster [9].

Hall thrusters contain an anode, usually combined with a fuel inlet, and a cathode with a fuel outlet. A voltage difference is applied to the anode and cathode in the range of 0-500 volts. The fuel is ionized as it passes through the inlet and these ions are then accelerated through the electric field generated by the voltage potential. Sm-CO magnets surround the thruster and create a magnetic field that guides the exit plume of ionized particles as they are accelerated out of the thruster. [10]

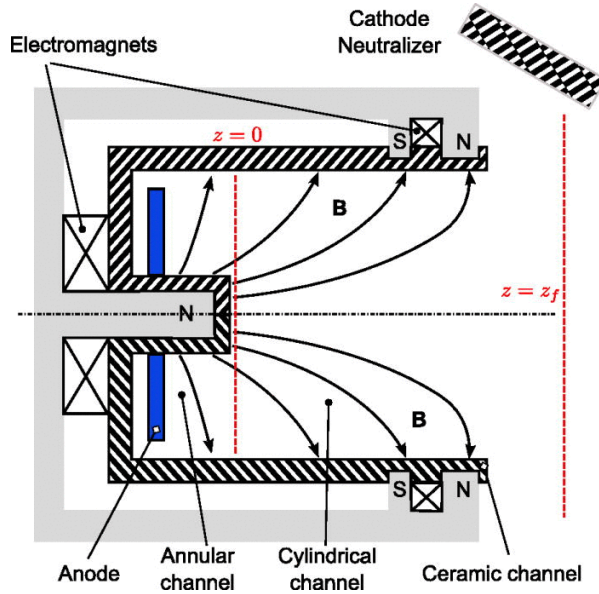


Figure 4.1: The inner workings of a cylindrical hall thruster with anode and fuel inlet on the left.

4.2 CHT Payload Characterization

Payload mission objectives differ slightly from overall mission objectives and are more focused toward the payload's specific functionality. The payload's objectives are as follows:

- I. **Full payload success:** 2 year orbit maneuver operations in space environment. Sufficient solid fuel for mission duration. Thermal regulation and control to prevent heat stress from cycling hot gas over cold metal. Ability to sample and transmit voltage, current, *thrust/Isp*, and thermal state without Loss of signal (LOS). No major anomalies detected during firing, with fewer than 6 minor anomalies during the two year period.
- II. **Partial payload success:** 1.5 – 2 year orbit maneuver operations in space environment. Sufficient solid fuel for mission duration. Partial thermal regulation and control to minimize heat stress from cycling hot gas over cold metal. Ability to sample and transmit voltage, current, and *thrust/Isp*, without LOS. 0 – 1 major anomalies detected during firing, with fewer than 10 minor anomalies during operation.
- III. **Minimum payload success:** < 1 year orbit maneuver operation in space envi-

ronment. Sufficient solid fuel for mission duration. Ability to sample and transmit voltage, current, and *thrust/Isp*, without LOS. 1 – 2 major anomalies detected during firing, with fewer than 15 minor anomalies during operation.

The anomaly specifications are derived from a study of hundreds of previously launched Hall Thrusters that lists mean time to anomaly for both major and minor anomalies. [11] Given a 2 year mission duration for full payload success, the mean time to anomaly leads to the expectation of fewer than 6 minor anomalies over this time period.

Characteristic	Value	Notes
Mass (kg)	546 (655.2 with margin)	Growth factor of 1.2 used.
Volume (cc)	146.4824	$D = 7.3\text{cm}, L = 3.5\text{cm}$
Power (W)	200	
Thrust (mN)	7	
Pointing	N/A	No Pointing Required
Data Rate (total)	792 hz	Voltage, current, time, external temperature, anode temperature, E-field
Thermal (Operating Temperature, Anode (K))	673	Based on experimental results of 200W thruster
Heat Flux (Anode) (W)	50	Based on experimental results of 5kW HET, ionized iodine
Structural Support	3U for Nanorack	See CAD drawing of chassis

Table 4.1: List of characteristics and parameters for on-board CHT.

The CHT is mounted to the rear of the satellite, opposite the antennas and battery, as seen in figure 7.1. The CHT’s structural support and general satellite structure is discussed in detail in chapter 7.

4.2.1 Fuel Management System

The use of iodine solid fuel is a relatively new area of study, and to date only one satellite has been designed with the intention of testing such a system. Such a system is desirable because the density of solid iodine is 3 times greater than that of pressurized Xenon, and as such the fuel management system does not need to be as heavy to support high pressures. [12] A reduction in pressure from 2500 psi to 2psi with the transition from xenon gas to solid iodine not only reduces weight, but it reduces the added challenge of meeting NASA’s requirements for pressurized containers on CubeSats.

TigerSat has one near predecessor with respect to its payload, NASA’s iSat (Iodine Satellite). iSat was first conceived in 2015 and is a 12U CubeSat. [12] [13] The stated goal of this mission was to prove that a fuel management system could be produced that had reduced mass by 80% and volume by 90%, compared to a xenon propellant based system. The mission utilized a mature technology, NASA stated TRL 8 Busek BHT-600 Hall Thruster and changed the fuel system to reduce mass and volume. [14] Given

this stated goal, it was then determined that the mass and volume of a xenon CHT comparable to the this project's payload should be equivalently reduced by 80% and 90% respectively, and the system components would be physically modelled on NASA's iSat.

A baseline mass was required for the fuel management system of a 3U CubeSat with a xenon Hall thruster. Such a baseline was found through a study at the University of Michigan, which listed the following masses on a 5kg, 3U CubeSat: 2kg chassis and structures, 0.5kg thruster, 1kg of fuel, 1kg of payload, and 0.5kg of dry mass fuel management system. [15] In order to account for the immaturity of the solid fuel technology, build in a mass margin, and account for other differences between TigerSat and the CubeSat used in this study, it was estimated that the fuel management system mass may be reduced by a factor of two-thirds instead of the full 80%.

The components were modelled based on relevant components of the iSat fuel delivery system, including a resovoir, pump, valves, and PPU. Due to limited documentation and a sample size of only one with which to compare previous technologies, the volume and placement of components were chosen to approximate the iSat design, which dedicates slightly less than 2U of space to the fuel system at the front of the satellite. [16]

4.3 Measurements and Devices

In order to determine the efficacy of this relatively untested solid fuel CHT, direct measurements during operation are required. A trade study was performed to determine exactly how many and which measurements were critical to understanding CHT performance. The following parameters were considered:

- Operating Current
- Operating Voltage
- Mass Flow Rate
- Anode Temperature
- Cathode Temperature
- Electric Field (Thrust)

- Magnetic Field
- Downstream Plume Temperature
- Space Environment Temperature

Each parameter was considered for ease of measurement with a low power, space environment measurement device, importance to researchers, and strain on the data handling system.

Measurement	Ease of Measurement*	Importance to Researchers
Operating Current	9	8
Operating Voltage	9	9
Mass Flow Rate	2	5
Anode Temperature	7	8
Cathode Temperature	5	6
Electric Field (Thrust)	5	9
Magnetic Field	7	5
Plume Temperature	3	6
Space Environment Temperature	9	7

Table 4.2: Trade on various quantities that may be measured and returned to Earth. Scale is 0-10 with 10 as best.

*Ease of Measurement includes availability of sensors, integration with circuitry, and ease of structural mounting.

Data handling is equivalent for all sensors because they will operate with DC current from on board batteries. It is therefore not included in the trade study. As a result, there is no need to sample at any particular rate to reconstruct the waves normally present in AC current. Data sampling then becomes a question of convenience and how frequently researchers would like to sample in order to observe fluctuations in data.

It is both natural and reasonable to utilize a sampling rate roughly equivalent to that which may be employed if reconstructing full AC waves. The frequency of the data stream would be 60hz maximum, which when multiplied by a 2.2 reconstruction factor, would result in a 132hz minimum sampling rate per sensor. [17] Finally, the trade study must be consulted before determining the ultimate number of sensors and equivalent total data rate that would be transmitted back to Earth.

A few measurements are prohibitively complicated or difficult and cannot be reasonably measured in a space environment. These are primarily the mass flow rate, and the plume temperature. In laboratory testing, measuring the plume temperature is often accomplished with a thermal camera or independently mounted thermocouple, which

can sample ion energy at various distances from the CHT cathode. [18] This is not possible in a space environment due to the lack of independent mounting locations.

Mass flow rate is equally untenable, because there are no reasonable devices available to make this measurement. By carefully testing the fuel pump on the ground, its efficiency and power in could be related to mass flow rate, but there would be no way to verify this in a space environment if only power in is measured (through current and voltage). These two measurements were therefore not considered for the final spacecraft design.

Of relatively low importance to researchers is the magnetic field produced by the hall thruster. The reliability of the magnetic field is not of concern to the thruster's performance. It is produced by reliable Sm-Co electromagnets that produce a constant magnetic field surrounding the hall thruster, directing the exhaust plume to exit the thruster normal to the exit plane. This measurement too was not considered for the final design.

All other measurements were included in the final design for their high ease of measurement and high importance except for the cathode temperature. This temperature is not as important to understanding the thruster's performance as the anode temperature, where fuel is vaporized and injected. Ground experiments easily and reliably relate the power into a thruster and anode temperature with the resultant cathode temperature. It is also not as easy to mount a thermocouple inside the CHT as it is at the rear. The cathode experiences temperatures that fluctuate near the top range of thermocouples, and may produce unreliable measurements without a specially designed thermocouple. Finally, the thermocouple may cause unwanted affects with the flow, from turbulence to thermo-acoustic instability.

This left operating current, operating voltage, anode temperature, electric field (2 sensors), and space environment temperature to be included in the design. With each sampling at 132hz, this led to a final sampling rate of 792hz, which is easily handled by the data handling system (section 9). Current and voltage are discussed in section 4.3.1, electric field measurement is discussed in section 4.3.2, and temperature measurement is discussed in section 4.3.3.

4.3.1 Power Measurement

Power into the thruster will be measured as the product of voltage and current to the anode. Efficiency will be measured in a laboratory environment and considered a known

function of input voltage throughout mission duration (see section 4.4 for change in efficiency with input voltage).

Measuring current is accomplished through a clamp on ammeter, which measures current through a magnetic field produced by a wire with current flowing through it. Such a device can be small and easily mounted outside the rear of the CHT, and because it is not integrated in the circuit, produces zero resistance and has no affect on the current measured. [19]

Measuring voltage is similarly accomplished with an extremely high impedance voltmeter mounted at the rear of the CHT anode. It is very important to use a high impedance voltmeter to prevent the build up of electrostatic charge over time. Such devices have been developed with resistance as high as $3e16$ Ohms and capacitance as low as $3e - 16$ F.[20]

During standard operation, the CHT will operate at voltages between 0-500 V, with current between 0-30A. [10] The voltmeter and ammeter will consume 0.1W of power maximum. [21]

4.3.2 Thrust and E-field Measurement

The thrust will be measured indirectly by measuring the electric field produced by the CHT. Because the CHT creates thrust by accelerating ions in an E-field, it can be shown that:

$$T = -F_{ion} = -0.5 * \epsilon_0 * (E_{accel}^2 - E_{screen}^2) \quad (4.1)$$

Measuring an electric field is aided by the development of very small DC electric field meters that can be unobtrusively mounted just outside the CHT.[22] Such a meter would easily be capable of measuring electric fields with up to 1 MV/m. [22].

4.3.3 Thermal Measurement

Potential devices to measure temperature include thermistors, thermocouples, and thermal cameras. However, thermistors have a highly limited range of operating temperatures, and thermal cameras require a mounting point that allows direct observation of the surface being measured. Because the anode is buried and not visible and the space environment has no surfaces, only a thermocouple can be used to obtain the required measurements.

One thermocouple will be placed inside the CHT next to the anode while the other will be placed far from the CHT, at the bottom of the satellite in order to reduce interference from on-board components that may produce heat. The thermocouples, depending on material and diameter, have temperature ranges from -275 to 2000 °.[23] A type K thermocouple would likely be used for the anode temperature, and a modified type T thermocouple would be used for space environment measurement.

Thermocouples have been designed and integrated in very lower power circuits, reducing the demand on the data handling system. For example, Texas Instruments has produced thermocouples with power drain as low as 8e-8. [24].

4.4 CHT Characteristic Relationships and Failure Modes

The most common way for CHTs to fail during operation is due to the degradation of the inner ceramic coating that acts as the barrier between the high energy ion plume and the rest of the CHT. The ions have enough energy to force the ceramic to eject atoms. resulting in thinner ceramic layers over time. This effect, called sputtering, can ultimately degrade the ceramic until the magnetic coils are exposed, causing CHT failure. [25] See figure 4.2 for a plot of ceramic coating over time.

The rate of erosion speeds up over time, and the thinner layer of ceramic insulation leads to a decrease in electric potential inside the thruster. This drop in potential leads directly to a drop in electric field strength, lowering the strength with which the ions are accelerated. This in turn results in a decrease in thrust over time, such as in figure 4.3.

For full mission success, the CHT will fire a cumulative 400 hours at most, which will result in an approximately 6.8% decrease in thrust by the end of the mission according to figure 4.3. While small, this phenomena will affect the final capability of the CHT to complete the orbit lowering and raising, but enough additional fuel in the form of safety mass margins are included such that the decrease in thrust may be compensated by firing for slightly longer than the current burn time of 10 minutes per cycle.

Finally, it is worth briefly discussing the trade between voltage and current when providing power to a CHT. It is widely accepted that high voltage, low current should be used for three of reasons:

- I. Lower current is safer and does not require high gauge wires
- II. It is easier to directly use the high voltage to generate a strong electric field.

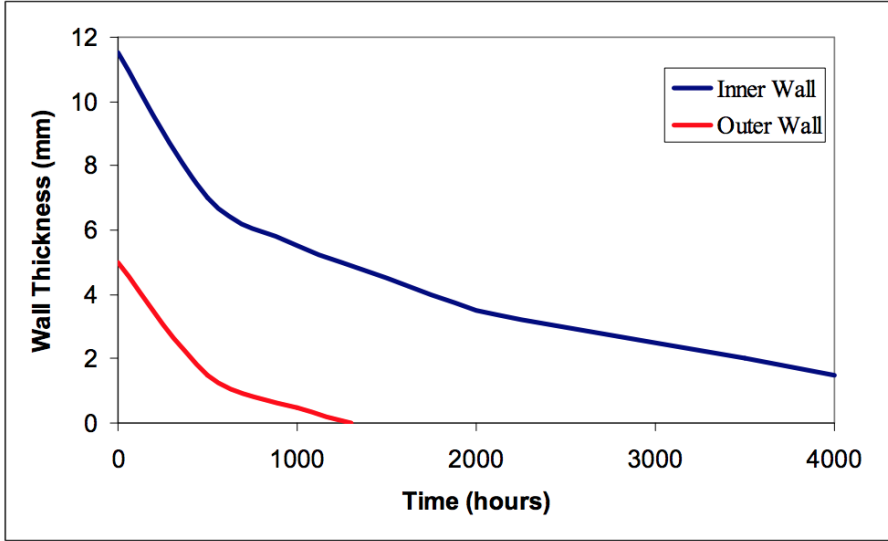


Figure 13. Wall Thickness versus Time at the Exit Plane²⁰

Figure 4.2: The ceramic wall of the CHT degrades over times due to friction and electrostatic forces from the high energy ions. Image from United States Air Force. [25]

III. The CHT Anode is most efficient when operating at high voltage.

This last point is perhaps the most interesting, and can be seen visually in Figure 4.4. Note this data is not for a CHT comparable to this project's payload, but is meant to show the general trend that can be expected from this propulsion technique.

The efficiency of the anode is actually greater at high voltage. The anode efficiency is a measure of the efficiency of mass, current, and voltage. [26] At higher voltage, a higher mass flow rate can be realized along with less relative heat loss due to lower currents at the same power rating. As a result, it is important to operate the CHT at the highest voltage achievable through a voltage converter, which is discussed in section 5.3.4.

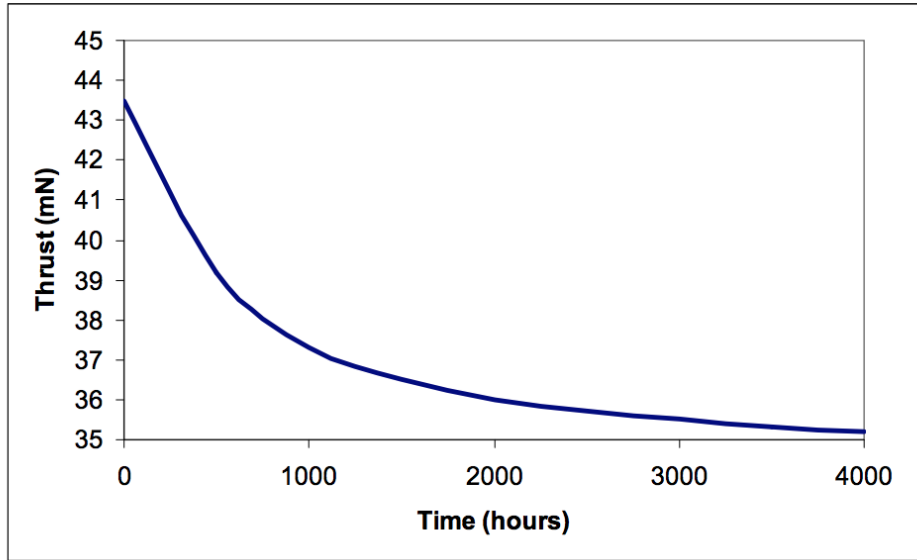


Figure 15. Thrust versus Time²⁰

Figure 4.3: The eroding ceramic insulation leads to a drop in electric potential and thrust in a CHT over time. Image from United States Air Force. [25]

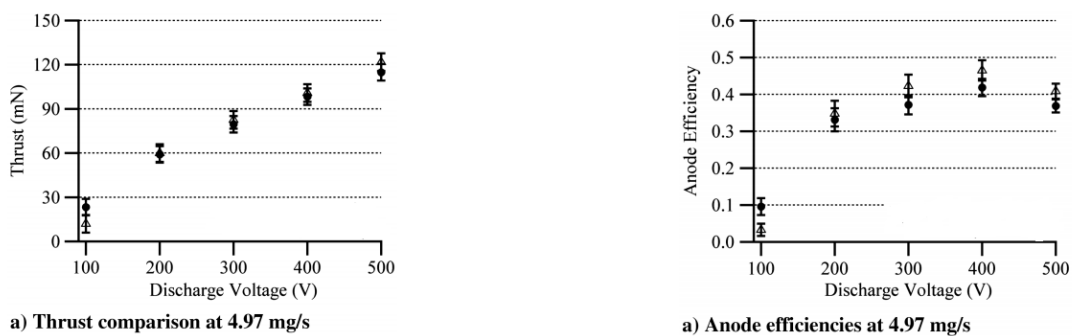


Figure 4.4: A comparison of CHT Anode Efficiency vs. Voltage (right) and Thrust vs. Voltage (left). Image from Georgia Institute of Technology. [26]

Chapter 5

Power Systems

The CHT payload makes use of the TigerSat Electrical Power System (EPS), which presents a unique design challenge. Typical 3U CubeSats provide only 10-40 W of power, so the TigerSat EPS will require careful modification of off-the-shelf (OTS) CubeSat components and custom design of new components to deliver 200 W to the payload when thrusting.

5.1 Requirements

Requirements imposed by the CubeSat Design Specification (see Appendix B.3) can be found in Table 5.1.

Electrical Power System	
C1	At minimum, one deployment switch to maintain power-off state
C2	At minimum, two RF inhibits (or one inhibit and <1.5 W RF)
C3	Provide telemetry detailing fuel, thruster, power usage
C4	Propulsion system must have at least 3 inhibits to activation
C5	Total chemical energy will not exceed 100 Watt-Hours
C6	Must include an RBF pin that disables all power

Table 5.1: EPS Requirements derived from CDS.

In addition, other requirements were derived from other subteams:

- Payload:
 - CHT maximum input power: 200 W
 - CHT input voltage: 100-300 V
 - CHT input current: 0-2 A

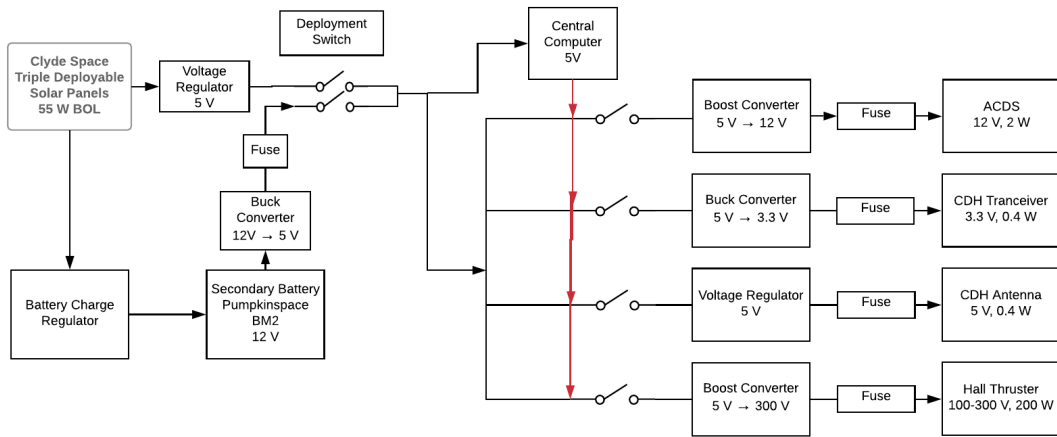


Figure 5.1: A block diagram showing the major components for the power system. All power flows through the lines. The red lines represent power flow from the computer to control the state of each switch, and consequently whether each subsystem is powered on or off. The black lines represent power flow from the solar panels and batteries to the various subsystems.

- Mechanisms:
 - Solar panels will not be actuated (though they may be deployed)
- Orbita:
 - Maximum charging duty cycle (defined as the ratio of charging time to thrusting time) for station-keeping: 60
 - Desired charging duty cycle for orbit raising: 30
 - Minimum thrust time: 10 minutes
 - Minimum umber orbit raising cycles: 9
- Thermal:
 - Operational temperature range: -15 to 30 °C
- The orbit-average power budget for all subsystems can be seen in Table 5.6

5.2 System architecture

Figure 5.1 shows a block diagram for how the major components of the electrical power system will be connected. Because of the relatively few number of subsystems, each with different operating power requirements, a distributed system will be used. Switches are required for deployment, to ensure that all power is cut off. Various other switches are controlled by a central computer that determines whether or not a subsystem should be

powered on or off.

5.3 Component Selection

5.3.1 Battery Chemistry

One of the first trade studies conducted was the selection of battery chemistry. Because CubeSats are rarely the primary launch priority, the TigerSat could sit in an integration facility for months or even years. This shelf time would significantly degrade the capacity of any primary batteries included in TigerSat, so only rechargeable secondary batteries were examined. High specific energy (measured in Wh/kg) was required, as the CHT payload would require significant quantities of energy for every firing. Cycle lifetime is also a key characteristic, as the batteries must continue to store enough energy to operate the thruster at the minimum mission success condition.

BATTERIES FOR SPACE POWER ¹							
CHEMISTRY:	PRIMARY			SECONDARY			
	LiCF	LiSOCl ₂	AgZn	AgZn	NiH2	NiCd	NiMH ²
Lifetime (cycles)	Not Applicable	Not Applicable	Not Applicable	200 ³	45K ⁴	40K ⁴	2
Watt-Hours/Kilogram	130	185	110	100	65	35	55
Watt-Hours/Liter	160	240	200	185	80	85	180
Discharge Rate	Low	Mod. ⁵	High	High	Mod+	High	High++
Charge Retention	Not Applicable	Not Applicable	Not Applicable	High	Low ⁶	Mod	Mod
Memory	Not Applicable	Not Applicable	Not Applicable	No	No	Yes	No
Wet Shelf Life	Long	Short ⁷	Short ⁷	Mod	Mod	Long	Long
Failure Tolerance	Low ⁸	High	High	High	Mod ⁹	High	Mod
Notes:	Not Sensitive within limits ^{9,10}		Activation req'd at time of use; May have free Electrolyte		Pressure Vessel; Capacity loss concerns after storage	Not Sensitive ¹⁰	Activation req'd at time of use; May have free Electrolyte ¹⁰
Operating Temp	0°C - 100°C		10°C - 50°C	0°C - 45°C	0°C - 20°C	0°C - 50°C	5°C - 10°C
Venting Requirements	Burst vent req'd		Can be sealed	Can be sealed	None	Can be sealed	None
Cell Voltage (Operating)	2.95V	3.1V	1.5V	1.5V	1.3V	1.25V	1.32V
Experience Level	High	Mod	High	Low	Moderate	High	Low-
Costs	Low	Low	Low	Low	High	Mod	High

¹ Based on MSFC applications (EB12)
² New Technology
³ Approximately 50% depth of discharge
⁴ Refers to 61 minute sun and 35 minute eclipse low earth orbit cycle with approximately 5500 cycles per year at less than 20% depth of discharge
⁵ Can be designed for high rate use
⁶ Significantly improves with lower temperature (0° C)
⁷ Lifetime is limited to 90 - 200 days depending on construction
⁸ High temperature buildup on "high-rate" overcharge
⁹ Unstable at very high temperatures and high rate of discharge
¹⁰ Environmental concerns with constituent materials

1992 EB12

Figure 5.2: NASA trade summary of various battery chemistries used in space applications. Information from [27].

NASA provides the table seen in Figure 5.2 as a summary of battery chemistries used in spacecraft; the document was assembled in 1992, however, and modern battery

Chemistry	LiPo	LFP	NiMH	AgZn
Specific Energy (Wh/kg)	100-265	90-110	60-120	130
Lifetime (Cycles, 100% DOD)	500 (80% DOD) 2000 capable if 4.1V max	2-7k	2000	1000
Operating Temp (C)	-20:30 (capacity loss below 10)	-20:40 (capacity loss below 10)	-20:60 (capacity loss below 10)	-20:55
Cell Voltage (V)	3.0-4.2	3-3.3	1.1-1.4	1.5
Pros	Lightweight; Heavily used in CubeSat applications	Stable discharge voltage (3.2V); Thermal & chemical stability	Low internal resistance→high discharge rate	Low self-discharge (5%/year); thermal stability
Cons	Explosion risk if overdrawn; Capacity highly affected by temp, DOD, discharge rate		High rates of self-discharge (5-20% on first day)	Older technologies have low cycle life (ZPower up to 1000 cycles)

Table 5.2: Comparison of modern battery chemistries. Also note that “Lithium Ion” is a confusing term that includes LiPo, LFP, NMC, INR, IMR, and many more chemistries. Many commercial specifications generically say “Li-Ion batteries” without specifying the chemistry. Data from: [28], [29], [30], [31], and [32].

science has made significant advances. For this reason, several of the battery chemistries listed there have been entirely superseded by more advanced chemistries. Today’s NiMH batteries are far superior to NiCd and NiH₂, and today’s Li-Ion varieties are superior to lead-acid batteries, resulting in the following traded battery chemistries: Lithium-Polymer (LiPo), Lithium Iron-Phosphate (LFP), Nickel Metal-Hydride (NiMH), and Silver-Zinc (AgZn). Note that cost was not a factor traded on, as the final cost of the battery module is highly dependent on other production, assembly, and market forces.

The battery chemistries traded for TigerSat can be seen in Table 5.2. LiPo batteries typically have the highest specific energy, though they may have cycle life issues, depending on the depth of discharge and specific manufacturer. Other chemistries, such as LFP, have the highly desirable characteristic of thermal stability, which increases system reliability and improves TigerSat’s chances of winning a CSLI award. Many of these chemistries do not exist in commercially available CubeSat battery modules, however,

so the final selection of battery chemistry is dependent on specific battery modules.

5.3.2 Battery Module

The vast majority of off-the-shelf CubeSat battery modules use Li-Ion batteries because of their experienced flight heritage and high specific energy. An OTS CubeSat battery module was chosen instead of a custom-built module because Princeton lacks significant institutional knowledge of satellite battery systems. Without past CubeSat experience, an OTS module provides far more reliability for this vital component. Few manufacturers provide CubeSat battery modules with a large enough capacity to meet thrusting time requirements, so the available OTS battery modules were traded, as seen in Table 5.3.

The PumpkinSpace BM2 was chosen as the battery module because it had the highest capacity of any of the systems. In order to maintain cycle life, the batteries cannot be discharged to more than 65% state-of-charge. With 100 Wh of energy and 35% DOD, the 200 W CHT can fire for only 10.2 minutes, just meeting the firing time requirement (see Section 5.4). Also note that the factory-supplied connections are limited to 10 A discharge current, which limits power output of this pack to around 150 W. To meet the 200 W requirement of the CHT, the option to use a custom wiring harness will be executed, allowing the LG 18650 HG2 battery cell limits of 20 A discharge current to be achieved (see [36]). With this wiring harness, the battery module can output up to 300 W, more than enough to deliver the required power to the CHT, even taking into account efficiency losses from wiring and boost converters.

Furthermore, the BM2 meets, without exceeding, Requirement C5 of the CDS, which limits total stored chemical energy to 100 Wh. The BM2 control circuitry also helps in meeting requirements C1, C3, C4, and C6 by including pins for an RBF pin, multiple software-enabled inhibits controlling power release, and voltage and current monitoring sensors to determine power usage. Finally, BM2 can operate fully in the required thermal environment. Should battery temperature drop below 0°C, software-enabled built-in heaters can run for short periods of time to maintain battery temperature and prevent degradation of cell life.

5.3.3 Solar Panels

Table 5.4 compares multiple off-the-shelf 3U CubeSat solar panels for TigerSat. Because many off-the-shelf panels, including the four compared, are made of Triple Junction GaAs Solar Cells, the specifications varied minimally in terms of power, efficiency, operating

	Pumpkinspace BM2	GOMSpace BPX	ClydeSpace 40Whr
Price	\$11,500	\$8,250	\$3,900 (savings for using EPS bundle)
Cell Type	Li-Ion	Li-Ion	LiPo
Configuration	4S2P	4S2P	2S4P
Pack Voltage (V)	10.4-16.8	10.4-16.8	6.0-8.4
Charge (Ah); Energy Capacity (Wh)	7; 100	5.2; 77	5.2; 40
Mass (g)	692 (542 without mounting brackets)	500	335
Dimensions (cm)	10 x 10 x 4.84 (w/ mounting brackets)	9.3 x 8.6 x 4.1	9.5 x 9.0 x 3.6
Other Notes	Software-enabled battery heaters (10-15W power usage)	Software-enabled battery heaters (6W power usage)	Overcharge, undercharge, over voltage, over current protections
	User-provided captive harness allows for “Higher discharge currents (well in excess of 10A)”	Short circuit protection 10A current max (can use PBAT2 for raw power)	Includes solid state high-side, low-side launch inhibits
	Fully integrated telemetry, programming	Pay extra for ISS acceptance test for NASA requirements (vibration, vacuum, battery)	Has CAD model
	Has CAD model		

Table 5.3: Comparison of high-capacity OTS CubeSat battery modules. Information from component datasheets, [33], [34], and [35].

temperatures, among others. Thus, the main parameters for comparison were cost and compatibility with other CubeSat launch systems. For this reason, the Clyde Space Solar Panels were the optimal choice due to the combination of a relatively lower price and compatibility with the mechanisms components of the TigerSat.

Panel	Endurosat 3U Solar Panel [37]	Clyde Space Triple Deployable Solar Panels [38]	Pumpkinspace PMDSAS 7 Panel, 56 Cell "Turkey Tail" [39]	CubeSatShop CubeSat Solar Panels [40]
Type	Triple Junction GaAs Solar Cells	Triple Junction GaAs Solar Cells	Triple Junction GaAs Solar Cells	Triple Junction GaAs Solar Cells
Max Power (W)	59	55	56	48.3
Specified Operating Temperature (degrees Celsius)	-55 to 125	-100 to 125	-40 to 85	-40 to 125
Efficiency	29.5%	29%	28%	30%
Price (Dollars USD)	25,200	32,500	95,000	70,000
Notes		Compatible module with many commercially available launch pods	Expensive (\$95,000)	Easily deployable with many off-the-shelf CubeSat products, but produces less power output

Table 5.4: A trade study for various CubeSat off-the-shelf solar panels.

5.3.4 CHT Control Electronics

A variable DC-DC boost converter will increase the battery voltage to the voltage required to the thruster, powering the thruster with around 200 W. There are few OTS DC-DC boost converters that can output 300 V at 200 W or more. One such example is the Advanced Energy 1/2 C series 250 W Boost Converter [41]. This boost converter increases and regulates a 23-30 V input to 0-500 V at up to 250 W via software control, allowing the Command and Data Handling system to easily issue control inputs to the payload. Unfortunately, this boost converter is packaged with a heavy case that brings the component mass to 1.18 kg, which would destroy the mass budget. Fortunately, the power electronics literature abounds with papers addressing the design of high-power, high-voltage DC-DC boost converters, including References [42] and [43]. These designs have not yet been produced on a commercial scale due to a lack of significant market demand, but the component could be manufactured in-house in accordance with the specifications laid out in past research. Once manufactured, extensive testing (including in vacuum) will prove the converters flight-worthiness.

5.3.5 Bill of Materials

Table 5.5 is a Bill of Materials for the Cubesat mission. While the other components are important for EPS, the largest sources of mass and cost are from the Clyde Space Solar panels and the Pumpkinspace BM2. Currently without boost converters in the budget, the total mass of the TigerSat is 1210 grams. The total mass of the electrical power system will be less than 1.5 kilograms in order to meet the mass requirements of the deployment. In order to meet this requirement new voltage converters, specified to be less than 290 grams, will be designed. It is important to note that to size the mass of wires, a conservative estimate of 25 feet of 20 gauge wires was used (while bigger wires may be used for the thruster, the length will likely be much shorter than that used in the estimate).

5.3.6 Power Budget

Table 5.6 shows the required budget to power each of the TigerSat subsystems, excluding operation of the Hall thruster. In the average case, the satellite will require roughly 3 Watts, and it will require 6 Watts in the max power case. These power requirements are less than the 55 Watts produced by the solar panels. Thus, the solar panels alone

Component	Mass (g)	Cost (Dollars USD)
Clyde Space Triple Deployable Solar Panels	370	32,500
Pumpkinspace BM2 Module	540	11,500
Clyde Space Motherboard	86	4400
Endurosat CPU	56	3625
Pumpkinspace Remove Before Flight Pin	20	50
Pumpkinspace Flight Switch Module	60	325
Wires	40	20
Fuses and Fuse Block	70	10
Boost Converter	*	*
Total	1210*	52420*

Table 5.5: A Bill of Materials for the Electrical Power System.

*No commercially available Boost Converter modules that fit both the voltage requirement of the thruster and within the total mass constraints. Thus, the team plans to develop its own converter, and make modifications to the battery module so that both requirements are satisfied.

Subsystem	Average Power per Orbit (W)	Max Power (W)	Operating Voltage (V)
CDH	0.8	4	3.3 (Transceiver), 5 (Antenna)
ACDS	1.5	2	12
Thermal	0	0	0 (no power from EPS)

Table 5.6: Required power for each TigerSat subsystem.

can sufficiently power all subsystems while concurrently charging the batteries while the TigerSat faces the Sun.

5.4 Analysis

Throughout all analysis, a worst-case approach is taken. Table 5.7 shows the basic inputs, intermediary outputs, and critical outputs. We assume a constant maximum spacecraft mass of 4.5 kg (maximizes number of thrust cycles required), an orbit altitude of 400 km (minimizes available solar power), a beta angle of zero, a 35% DOD on the batteries, a solar panel max output of 39.6 W due to .72 ratio inherent degradation (typical assembly and temperature losses), an average per orbit (APO) standby power of all non-payload subsystems of 5 W (3 W expected), a mission baseline success of 9 orbit changing cycles, and a required ΔV of 222 m/s. Payload thrust, Isp, and efficiency were parameterized from the payload characteristic charts as a function of input power, held to a maximum of 200 W here. Orbit period and sunlight time per orbit were calculated from the orbital altitude using standard orbital analysis equations, such as the ones given [44].

Under these worst-case scenarios, the EPS still meets the minimum thrusting time requirement and the duty cycle requirement. In addition, the battery cycle count indicates the total number of times the battery module will need to cycle to 35% DOD. While cycle life is a concern for many Li-Ion chemistries, recent research of Li[NiMnCo]O₂ (H-NMC) battery cells, of the same chemistry of the Pumpkin BM2's LG HG2 cells, shows that even at the maximum discharge rates, under high temperature, and with an excessive DOD, the cells can reach 3,000 cycles with only 20% loss of capacity [45]. Should the number of cycles exceed 3,000 (whether due to ground testing or an attempt to increase the number of orbit cycles), the cells can still provide an acceptable 70 Wh of capacity even after 5000 cycles. This is more than enough to power the thruster for the required minimum duration of 10 minutes.

Currently the solar panels are rated in the best case to produce 55 Watts of power for the system. However, the best case is not always available, as variations in temperature cause a loss in efficiency and the solar panels degrade over time. Figure 5.4 [46] illustrates the variations in efficiency relative to temperature. As temperature increases, efficiency of the solar panels decreases. Assuming a worst case scenario of 70 degree Celsius operating temperature provided from the thermal team, the largest efficiency drop will be around 10-15%. In addition, from Professor Gonzalez's lecture on Space Power Systems

Mass CubeSat (max.)	4	kg
Mass Fuel (max.)	0.5	kg
CHT Input Power	200	W
Orbit altitude	400	km
Battery Cycling Capacity	35.0	Wh
Solar Panel Max Output	39.6	W
Standby Power Usage (APO)	5	W
# Orbit Changing Cycles	9	cycles
DeltaV per Orbit Cycle	222.0	m/s
Thrust	7.14	mN
Isp	2000	s
Efficiency	0.35	
Orbital Period	92.6	min
Time in sun per orbit	56.5	min
Orbits to fill battery	1.83	orbits
Time to fill battery	169	min
Thrusting time on battery	10.2	min
Thrusting orbits/battery cycle	0.11	orbits
Total orbits per thrust cycle	1.94	orbits
DeltaV per thrust cycle	.98	m/s
Thrust Cycles per Orbit Cycle	228	cycles
Battery Cycle Count	2503	cycles
Duty Cycle	16.51	

Table 5.7: Orbit Power Calculations. First nine lines are inputs. Worst case analysis assumes beta is zero, solar panels have inherent degradation of .72, lowest orbit altitude, total mass is initial mass, and stand-by power usage (APO) exceeds baseline power budget. Key outputs are thrust duration, orbits needed to fill battery, battery cycle count, and thrusting duty cycle.

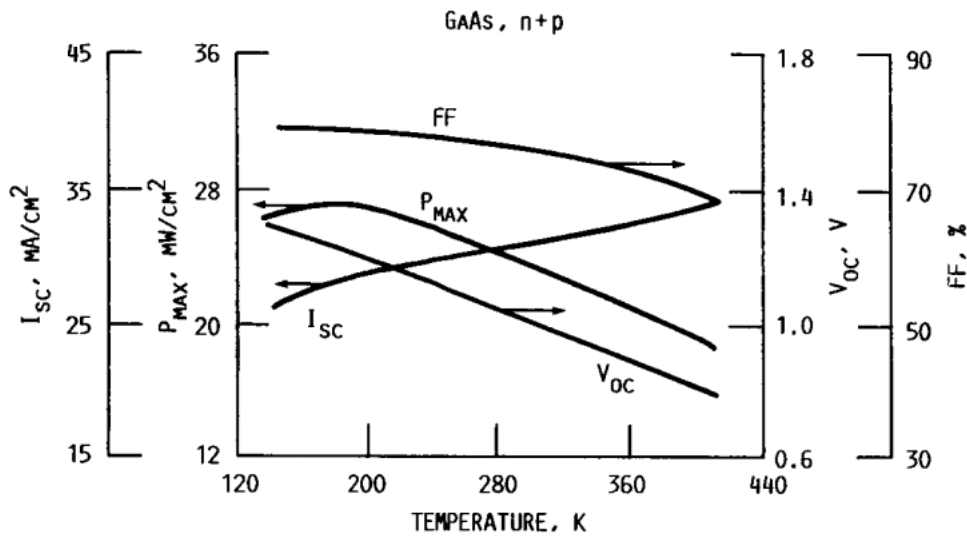


FIGURE 6. - VARIATION OF CELL PARAMETERS WITH TEMPERATURE FOR GaAs.

Figure 5.4: Variations in Triple Junction GaAs solar cell efficiency as a function of temperature

(slide 19), the solar panels will be expected to drop around 15% in efficiency over six years. Even though the mission is only planned for a fraction of this time, the 15% is used to measure a worst case scenario. In the least efficient temperature range at EOL, the solar panels will be expected to generate around 40-43 Watts, which is more than enough to power all of the subsystems and concurrently charge the batteries.

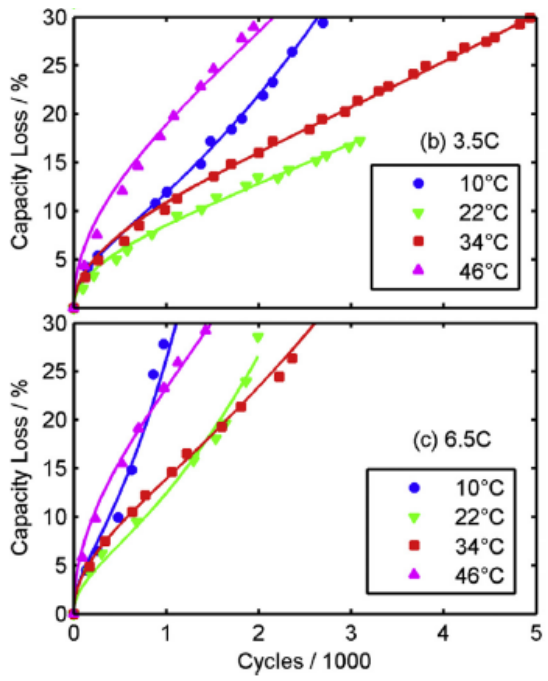


Figure 5.3: From [45]: “Capacity loss at four temperatures (10°C , 22°C , 34°C , 46°C). The panels each correspond to a single rate (3.5 C and 6.5 C, respectively). The depth of discharge is 50% for all data points in the figure. The x-axis scale is thousands of cycles.” 20 A discharge from the BM2 module corresponds to a 3.3C rate, and the “hot case” of 34°C is used.

Chapter 6

Mechanisms

6.1 Introduction

It was necessary to choose the method by which the solar panels would be deployed. As detailed in Chapter 5, TigerSat has a large power requirement, and the addition of solar panels will allow the satellite to generate the power that is needed to complete the mission. These panels are sufficiently large, however, such that they cannot simply be body mounted. Even with the most efficient solar panels, only having body-mounted panels would not provide enough surface area for the cells to produce the amount of power that is required. To reach the power requirement of 55W, a deployable solar array is needed.

In a deployable solar array, multiple panels are folded onto each other when the CubeSat is in its undeployed state, and are then released into their expanded form as a part of the start up sequence when the satellite begins orbiting the Earth.

When the solar panel array has been deployed, it can then either be fixed at a certain angle for the duration of the flight or it can be actuated to follow the sun to allow for maximum power production. Both options have pros and cons, and it was best to assess the different options available through a trade study. The trade study served as a means of identifying the deployment mechanism and solar panel array that would best meet all of the requirements of the system, which are outlined in the following section.

6.2 Requirements

The most important requirement of the solar array is that it be able to generate at least 55W of power. This will allow the system to provide sufficient power to each subsystem throughout the duration of the mission as was calculated in Chapter 5.

Since the duration of the mission is conservatively 2 years, as is designated in Chapter 2, the solar panels and any actuating mechanism they must be able to function for at least this time frame.

When the TigerSat is orbiting the Earth and cycling between altitudes of 400-600km, it will experience temperatures between $-30^{\circ}C$ and $30^{\circ}C$. The solar array must be tested to withstand temperatures at least within this range.

Another important factor in the mechanism selection is reliability. The more parts there are in the mechanism, the greater chance there is of failure. Having a simpler part will increase reliability and allow for more certainty that the deployment will go as planned. Additionally, a deployment mechanism that is at TRL 9 and is readily available on the market will have a greater chance of success due to thorough testing by the manufacturer and other consumers.

Because the entire TigerSat must weigh less than 4.8kg, weight was a concern for the deployment subsystem. A system that was too heavy could make it difficult to stay within the weight requirements as imposed by NanoRacks.

Finally, while the cost of the total system is not a limiting factor, the cost should be competitive for the features that the system offers.

The system requirements are summarized in Table 6.1.

System Requirements
The system must produce at least 55W
The system must be operational for at least 2 years
The system must be operational between at least $-30^{\circ}C - 30^{\circ}C$
The deployment mechanism must be reliable and at TRL 9
The system should have minimal weight
The system should have a competitive cost

Table 6.1: Requirements for the solar panel deployment mechanism that dictated the necessary factors in the trade study.

6.3 Component Selection

In order to determine which option to choose as the deployable solar panel array, a trade study was conducted. Using the requirements outlined above as a guideline, six options were judged against each other. Figures 6.1 and 6.2 show the six options and their design specs in the Raw Values column. Any values highlighted in yellow were ones that were not found directly from the company's website, but rather were conservatively estimated based on communication with the manufacturer or other comparable products with available details.

	Category Weights	Clyde Space Triple Deployable Solar Panels			CubeSatShop Deployable solar panels DSA/1A			Endurosat 3U Solar Panel X/Y MTQ		
		Raw Values	Category Comparison	Score	Raw Values	Category Comparison	Score	Raw Values	Category Comparison	Score
Cost	1.25%	\$32,500.00	0.687	0.009	\$16,600.00	0.859	0.011	\$3,575.00	1.000	0.013
Reliability	11.72%	99.90%	1.000	0.117	99.90%	1.000	0.117	99.90%	1.000	0.117
Weight	14.75%	0.37 kg	0.813	0.120	0.14 kg	0.990	0.146	0.13 kg	1.000	0.148
Power	37.50%	55.00W	0.833	0.313	12.00W	-6.333	-2.375	8.43W	-6.928	-2.598
Lifetime	16.61%	5 years	1.000	0.166	2 years	0.000	0.000	2 years	0.000	0.000
Temperature Maximum	9.08%	80.00 °C	0.500	0.045	130.00 °C	1.000	0.091	70.00 °C	0.400	0.036
Temperature Minimum	9.08%	-40.00 °C	0.200	0.018	-80.00 °C	1.000	0.091	-30.00 °C	0.000	0.000
Totals	100.00%			0.788			-1.920			-2.285
Sources	-	https://www.clyde.space/products/76-triple-deployable-solar-panels			https://www.cubesatshop.com/product/solar-panels/			https://www.endurosat.com/products/cubesat-3u-solar-panel-x-y-mtq/		

Figure 6.1: Solar array deployment mechanism trade study with Clyde Space Panels [47], CubeSatShop Panels [48], and Endurosat Panels [49].

	Category Weights	University of Michigan eXtendable Solar Array System			Pumpkin Space PMDSAS 7-panel, 56-cell Solar Array			CTD Deployable Articulating Array		
		Raw Values	Category Comparison	Score	Raw Values	Category Comparison	Score	Raw Values	Category Comparison	Score
Cost	1.25%	\$20,000.00	0.822	0.010	\$96,000.00	0.000	0.000	\$50,000.00	0.498	0.004
Reliability	11.72%	99%	0.000	0.000	99.90%	1.000	0.117	99.90%	0.000	0.000
Weight	14.75%	1.40 kg	0.000	0.000	0.40 kg	0.786	0.116	0.60 kg	0.630	0.076
Power	37.50%	23.00W	-4.500	-1.688	56.00W	1.000	0.375	50.00W	0.000	0.000
Lifetime	16.61%	2 years	0.000	0.000	3 years	0.333	0.055	2 years	0.000	0.000
Temperature Maximum	9.08%	70.00 °C	0.400	0.036	85.00 °C	0.550	0.050	70.00 °C	0.400	0.018
Temperature Minimum	9.08%	-30.00 °C	0.000	0.000	-40.00 °C	0.200	0.018	-30.00 °C	0.000	0.000
Totals	100.00%			-1.641			0.732			0.098
Sources	-	https://deepblue.lib.umich.edu/bitstream/handle/2027.42/83836/AIAA%20quend			http://www.pumpkininc.com/content/doc/forms/pricelist.pdf			http://calpoly.edu/~bklofas/Presentations/SummerWorkshop2013/Turbo_Deploy/		

Figure 6.2: Solar array deployment mechanism trade study with University of Michigan Panels [50], Pumpkin Space Panels [51], and CTD Panels [52].

After collecting the raw data for each of the products, the most important decision was how heavily to weight each criterion. After choosing the requirements that were most important, an algorithm was put in place to determine how well each of the six options met the requirements and how the options fared against each other.

To weight the requirement categories, a pairwise weighting system was implemented, as is shown in Figure 6.3 [53]. All requirements are judged against each other and

rated from 1-9, with 1 meaning that the requirements are of equal importance and 9 meaning that the task is much more important. The relative importances are averaged and normalized for each criterion, resulting in a percentage weight. As is seen in Figure 6.3, the most important requirement was power with 37.5%, and the least important requirement was cost with 1.25%.

A	B	C	D	E	F	G	H	I	J	K	L	M	N	O
	Cost	Reliability	Weight	Power	Lifetime	Maximum Temperature	Minimum Temperature			Geometric Mean	Normalized Weight		Value	Description
Cost	1	0.11	0.11	0.11	0.11	0.11	0.11			0.2380952381	1.25%		1	Equal importance
Reliability	9	1.00	1.00	0.13	0.50	2.00	2.00			2.232142857	11.72%		3	Moderately more important
Weight	9	1.00	1.00	0.17	0.50	4.00	4.00			2.80952381	14.75%		5	Strongly more important
Power	9	7.00	8.00	1.00	7.00	9.00	9.00			7.142857143	37.50%		7	Very strongly more important
Lifetime	9	2.00	2.00	0.14	1.00	4.00	4.00			3.163265306	16.61%		9	Extremely strongly more important
Maximum Temperature	9	0.50	0.25	0.11	0.25	1.00	1.00			1.73015873	9.08%			
Minimum Temperature	9	0.50	0.25	0.11	0.25	1.00	1.00			1.73015873	9.08%			
										Sum	19.04620181	100.00%		

Figure 6.3: Solar array deployment mechanism trade study, weighting analysis.

The next step was to determine how well each of the options met each individual requirement. In some cases, like when judging the options for power generation, there was a reference value to judge against (55W in the case of power). Options failing to meet the reference value were given a negative value based on how much they were short by. Options that met the reference value were given a positive value, which was higher depending on how easily the reference value was met. In the case that there was no reference value, as in the instance of weight or reliability, the options were rated on how well they either minimized or maximized the criterion (it was necessary to minimize weight and maximize reliability, for example).

After these Category Comparison scores were computed, they were then multiplied by the Category Weights that were previously found. Finally, the Scores were summed to find the option that would best fit for TigerSat's needs.

The option that came out with the highest result in the trade study was the Clyde Space Triple Deployable Solar Panel Array. This choice also the winner of the trade study that was done in Chapter 5 to determine the solar panels that would work best for the system. After seeing that this trade study result agreed with the power trade study result, it was confirmed that this product would be best for the system.

The Clyde Space Triple Deployable Solar Panels are compatible with the existing 3U structure and meet each of the requirements that were imposed. The details of the system are outlined in the following section.

6.4 Mechanism Characteristics

As discussed above, the Clyde Space Triple Deployable Solar Panels are not actuated during the flight, so mechanisms for actuation are not necessary. The panels are, however, deployed once at the beginning of the mission. This deployment is made possible by a system of mechanisms that include a hold down and release mechanism (HDRM) a thermal knife driver (TKD) circuit, and a set of spring-loaded hinge mechanisms [38]. While the exact details of all of the components and their operation are not available, due to their proprietary nature, it has been possible to collect partial documentation through both Clyde Space and other sources.

At the highest level, the system operates by firing the TKD to sever the space-qualified Dyneema cord that holds the HDRM in tension against the spring-loaded hinge mechanisms. This then releases the solar panels to deploy via the force provided by the spring-loaded hinges and lock out at a 90 ° angle from its stowed position. This assembly is also re-settable by ground personal, which allow for it to be tested on the ground prior to deployment [38].

6.4.1 Hold Down and Release Mechanism (HDRM)

An HDRM (also known as a separation nut) operates by maintaining a pre-load tension on an attached rod until a bridge-wire is severed [54]. This current severs the wire and releases the tension. In the case of this Clyde Space solar panel array, the HDRM is made of two cylinder halves compressed tightly around a rod. These halves are held in place by a wrapping of Dyneema cord that ensure the mechanism does not deploy prematurely. Once this cord is cut, the cylinder halves separate enough to allow the rod to slide out from its locked position.

A HDRM has a few advantages over other options, such as pyrotechnic devices, which are often used in similar applications. The first is that it is lower shock than a typical pyrotechnic device that has an ignition explosion, the actuation of the pyrotechnic, and the shock of the device moving from its pre-loaded state. When it comes to an HDRM, it only has the third type of shock, which is less significant when considering it in combination with the other two. The second advantage of an HDRM is that it is reliable and low risk. The device's actuation has only a single potential point of failure, and two break-points can be put in the same cord to ensure redundancy. Additionally, this device has a long heritage and has been successfully deployed on many missions [38]. Finally, since the area of the cord that is cut is relatively small, it also has a low thermal



Figure 6.4: A hold down and release mechanism consists of two half-cylinders that are tightened around a rod using cord [54]

mass, which makes it much more tolerant to temperature changes when compared to other options.

6.4.2 Thermal Knife Driver (TKD) Circuit

While the HDRM restrains the solar panels from deploying, it is the TKD that is needed to cut the Dynema cord that keeps the HDRM together. Unlike most HDRMS, which release their cord by causing a bridge wire to fail under a given current, the Clyde Space system uses a thermal knife [38]. The TKD is able to break through the cord quickly due to the chord's small size. It uses current to heat a thermal knife to burn through and gradually weaken the wire, rather than sever it through the use of a bridge-wire. This means the release is even less of a shock to the solar panel system during release.

6.4.3 Spring-Loaded Release Mechanism

The final component of the solar panel deployment assembly is the spring-loaded release mechanism. This mechanism is housed in the deployment hinges of the solar panel array and it causes the pre-load that the HDRMs resist while they are in use. Once the cord

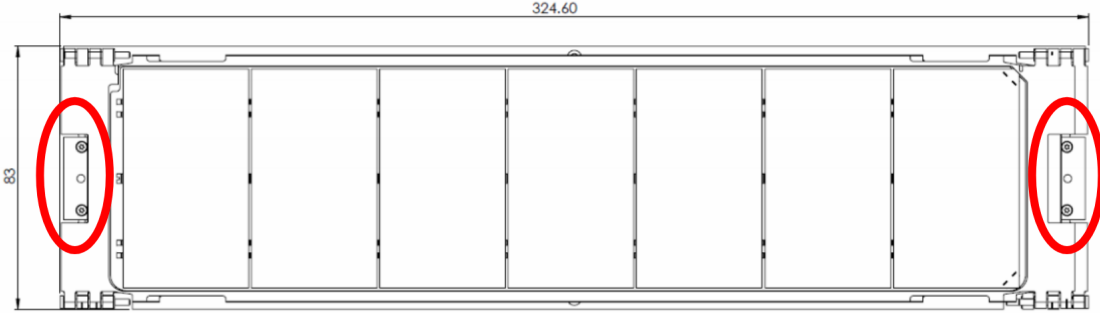


Figure 6.5: The locations of the HDRMs on the Clyde Space array [38]

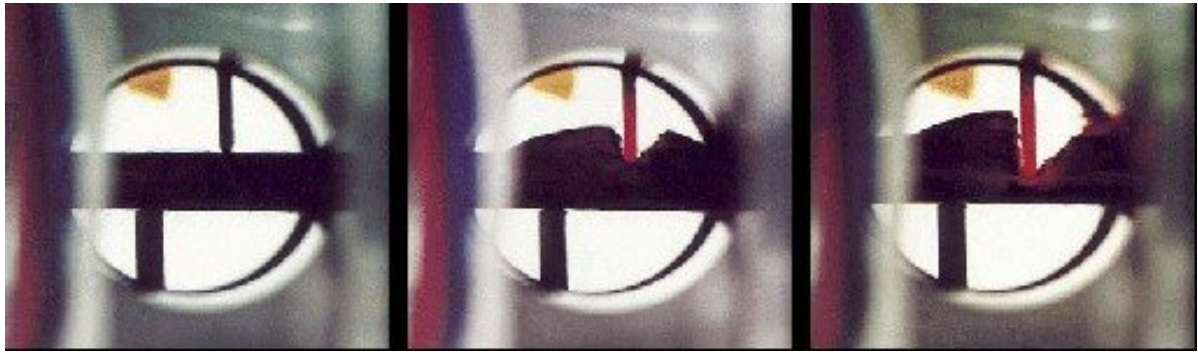


Figure 6.6: A thermal knife driver cutting through a cord in an HDRM [55]

is severed by the TKD, the HDRM releases and the spring-loaded release mechanisms cause the solar panels to snap to their intended positions [38].

The deployment hinges consist of not only the springs that drive the panels into position, but also the lock-out mechanism that holds them in place and transitions the array from a moving mechanism to a static structure. The exact method that is used to lock out the hinges is not available from Clyde Space, but many similar hinges deploy pins or lenticular struts to lock the assembly into position [56].

6.5 Testing

While most testing, analysis and qualification would be done by Clyde Space - the component manufacturer, it would still be recommended for the TigerSat team to do some level of lot acceptance testing in order ensure the provided device meets mission standards for the team and has acceptable levels of workmanship. Based on industry standards outlined in The New SMAD, this level of acceptance would require the tests

to be completed with the test factors and durations outlined in Table 6.2.

Test	Acceptance Factors (and Duration)
Structural Loads	$1.00 \times$ Limit Load
Centrifuge/Static Load Sine Burst	5 cycles @full level per axis (30 seconds)
Acoustics	Limit Level (1 minute)
Random Vibration	Limit Level (1 minute/axis)
Sine Vibration	Limit Level (4 oct/min)
Mechanical Shock	1 actuation Limit Level
Thermal-Vacuum	Max./min. predict $\pm 5C$
Thermal Cycling	Max./min. predict $\pm 20C$

Table 6.2: Tests and test acceptance factors and durations [2]

Alternatively, if standards for acceptance and reliability can be agreed upon with the vendor, testing the assembly using a simple "pop and hold" test would suffice to ensure the device is operating as expected, without needing to subject it to additional testing [57]. This is likely a preferable option, if possible, due to the possibility of not being able to access the proper equipment to do such tests at Princeton.

6.6 Conclusion

In conclusion, it was found that the Clyde Space Triple Deployable Solar Panel Array was the best option for this mission given our requirements. It was also found that using a deployed and then fixed solar panel array was the best course of action, as it eliminated unnecessary risk that would have resulted in only limited gain in terms of additional power generation. It was also confirmed that the components of the deploying system not only individually made sense in their selection, but could also be tested by the TigerSat team in addition to the testing done by Clyde Space.

Chapter 7

Structures and Configuration

7.1 Configuration Overview

Both a 3U and a 3U+ CubeSat were considered for this mission. The 3U+ allows for an extra cylindrical space aligned axially with a diameter of 6.4cm that juts out 3.6cm from the rear of CubeSat. [58] Ultimately, because the CHT has a diameter slightly larger than this (the diameter is 7.3cm), it could not easily fit in this extra "tuna can" space. The final chassis size was fixed at 10cm by 10cm by 34.05cm to conform with standard NanoRacks 3U CubeSat dimensions.

While determining the location of components inside the chassis, the center of mass (COM) requirements, thermal properties, and physical dimensions were taken into account. By CubeSat standards, no components are allowed to jut out more than 6.5 mm normal to the side of the CubeSat during launch to fit in the dispenser envelope (B.2).

The NanoRacks deployer, who's specifications can be found in section B.2, also specifies the COM must be within 2mm of the geometric center in the lateral directions and within 8mm of geometric center in the axial direction. While fully fueled and ready for launch, the CubeSat is within these specifications as seen in table 7.1.

Finally, it was important to keep sensitive components such as the radio electronics and battery far from the CHT in order to avoid unnecessary heat fluxes near the sensitive electronics and potentially volatile lithium ion battery. The CHT is fixed to one end of the CubeSat and sits in a small cylindrical housing bracket. On the opposite end of the CubeSat, the deployable antenna has room to expand beyond the standard 10cm by 10cm dimensions for communication with Earth. The battery was placed next to the antenna, far from the CHT.

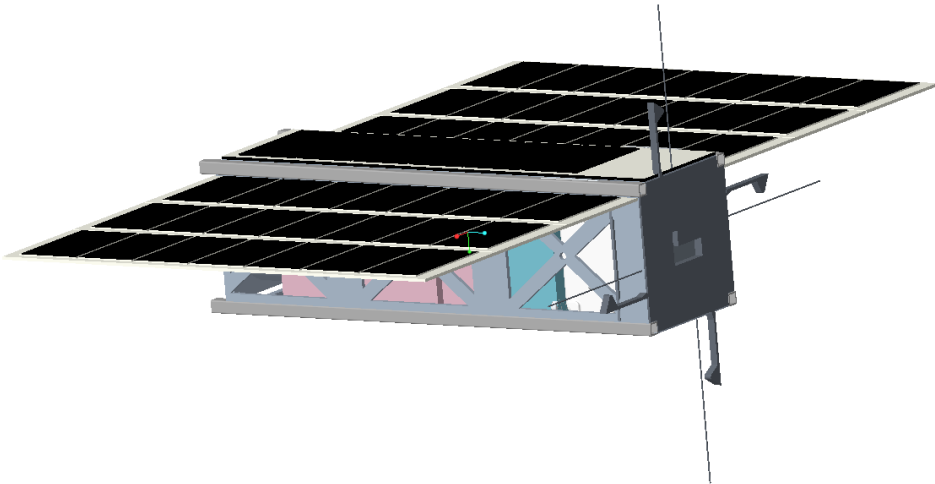
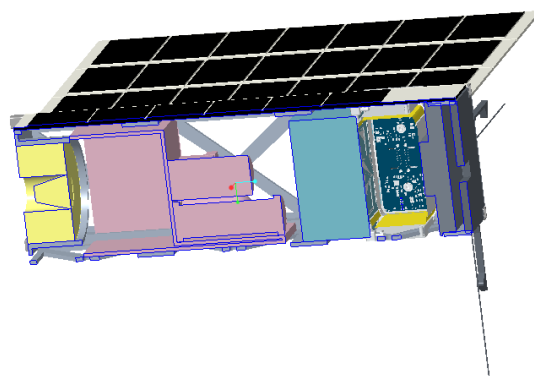


Figure 7.1: The full TigerSat assembly with solar panels and antenna fully deployed.



Clipping State:XSEC0002

Figure 7.2: An internal view of the TigerSat. The CHT is in yellow, fuel management system is in red, the ADCS system is in blue, the battery is dark blue and yellow, and the antenna and radio electronics are in dark gray opposite the CHT.

The final components inside the CubeSat are the ADCS and fuel management system. It was found that placing the fuel management system nearest the CHT while configuring the ADCS next to the battery kept COM constraints within the limits determined by the NanoRack deployer. The final COM, with respect to the geometric center, was:

Axis	With Fuel (mm)	Without Fuel (mm)
X	-1.33	-1.33
Y	-1.77	-3.28
Z	7.02	12.15

Table 7.1: The COM listed as a distance from geometric center of a 3U CubeSat. The axes are shown in Figure 8.3.

For absolute reference, the COM with respect to the coordinate system shown in figure 7.3 is shown in table 7.2.

Axis	With Fuel (cm)	Without Fuel (cm)
X	4.89	4.82
Y	18.23	18.79
Z	5.14	5.33

Table 7.2: The COM listed with respect to the coordinate system in figure 7.3.

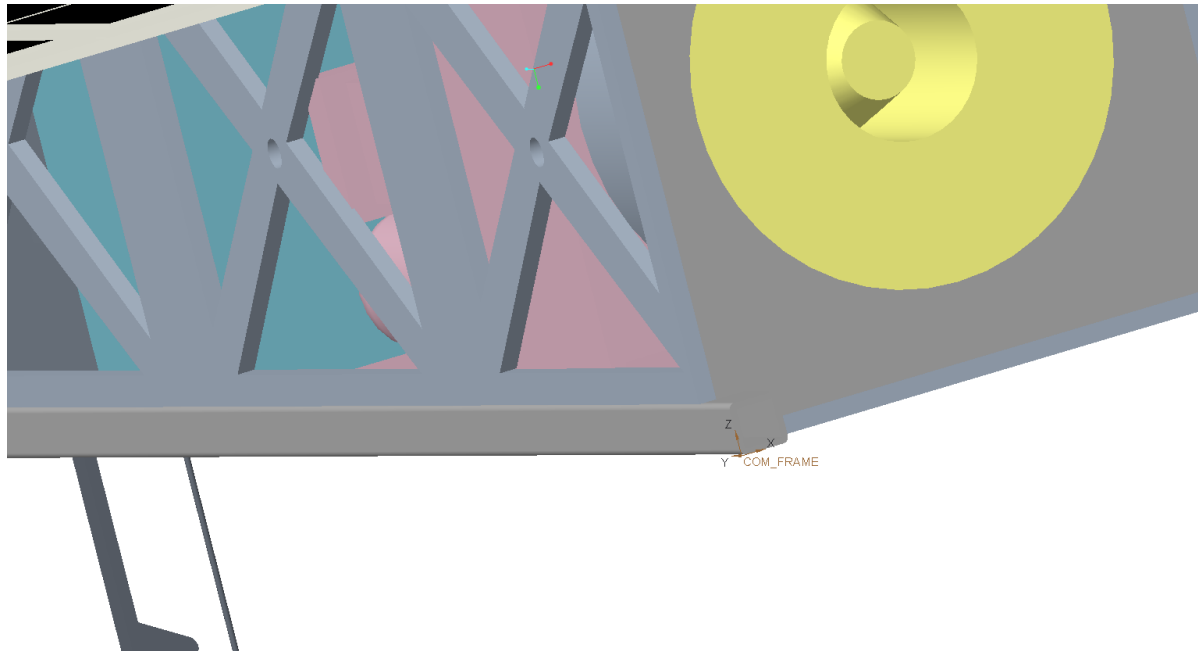
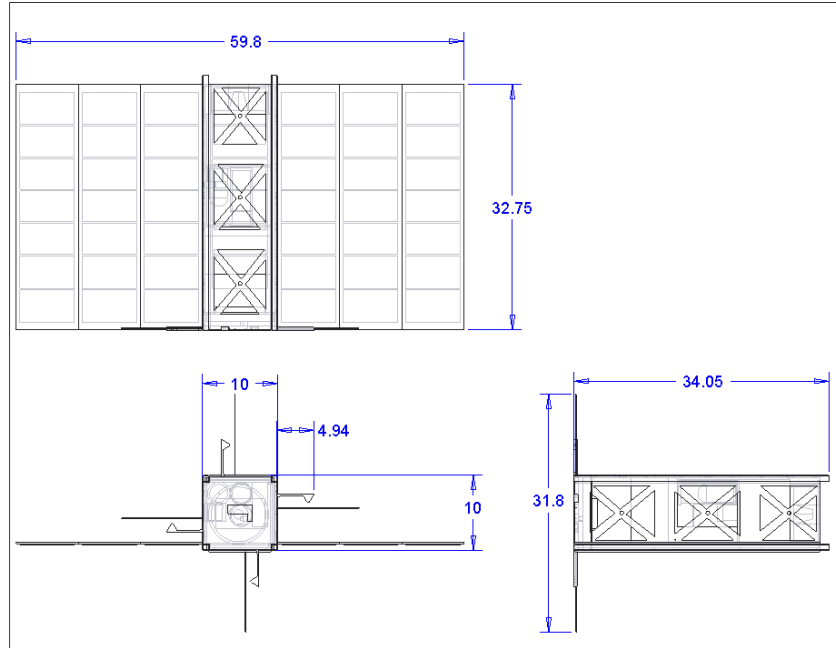


Figure 7.3: The coordinate system, applied to the back left corner of the CubeSat by the CHT, used as reference for the absolute COM coordinates in table 7.2.

Three solar panels are stowed in a "w" shape, folded against each side of the CubeSat during launch. After deployment, they extend in a plane 24.9cm away from the chassis on both sides, as in figure 7.1. The top panel of the CubeSat is covered by a 7th solar panel. The full primary outer dimensions are shown in figure 7.4. Because the solar panels are 1.05 mm thick, when stowed their thickness of 3.15 mm will not exceed the maximum allowable distance normal to the CubeSat chassis of 6.5mm.



SCALE : 0.250 TYPE : ASSEM NAME : FULL_CUBESATASSEM SIZE : A

Figure 7.4: The primary outer dimensions of the 3U CubeSat. All dimensions are in centimeters.

Because the solar panels and antenna extend out so far, the satellite's primary moments of inertia are not insignificant. Once the solar panels and antenna are deployed, they cannot be retracted, so throughout the mission the moment of inertia (MoI) of the satellite are as follows:

Axis	With Fuel (g/cm^2)	Without Fuel (g/cm^2)
I1	1.6388251e+05	1.6437869e+05
I2	5.2786206e+05	5.2099169e+05
I3	6.4360266e+05	6.3620099e+05

Table 7.3: The MoI of the satellite with deployed panels and antenna, with and without fuel. The axes are shown in figure 8.3.

7.2 Structural Analysis

7.2.1 Requirements

As specified in the NASA LSP requirements document (Appendix B.1), the CubeSat must meet certain structural analysis and testing requirements. The requirements that are relevant in this scope are the structural analysis requirements, since prototype testing is not yet possible at this stage. For quasi-static loads, the structural analysis qualification safety factor requirements are as follows:

- 1.6 x Limit load with respect to material yield strength
- 2.0 x Limit load with respect to material ultimate strength

The CubeSat must also withstand quasi-static load and random vibration testing, at limits specified more thoroughly in Appendix B.1 and B.2.

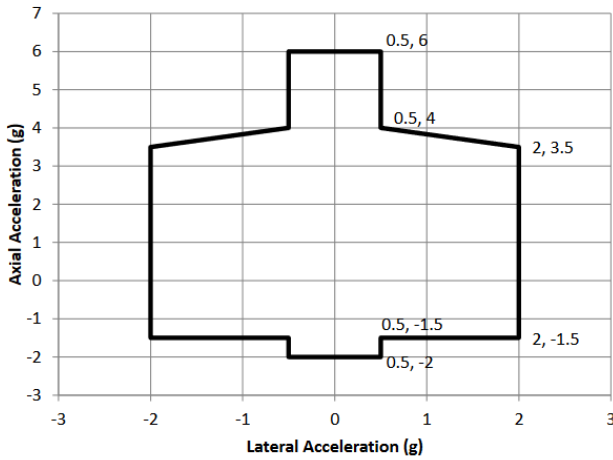
7.2.2 Loads

The primary loads that the CubeSat will experience are internal loads on the chassis structure by the components. These loads will peak during launch. Since TigerSat Blue will be delivered to the ISS on a resupply mission, the exact design load factors cannot be specified without a guaranteed specific launch vehicle. The design load factors for TigerSat Blue were estimated with the Falcon 9 as a baseline. The Falcon 9 design load factors appear in figure 7.5a.

Additionally, the CubeSat and dispenser system will experience vibrational loads during the launch phase. NanoRacks provides a standard random vibration testing profile. The vibrational load profile is shown in figure 7.5b.

7.2.3 Quasi-Static Analysis

In order to ensure the chassis can withstand the full load the structure will experience during launch, 10 times standard Earth's gravitational acceleration was applied to all three axes of the satellite chassis simultaneously. This worse case scenario assumes more than 1.6 x the largest load factor on the Falcon 9. During the simulation, the satellite was secured by all 4 rails, as it would be while stowed inside the NanoRacks deployer. The resulting von Mises stresses inside the aluminum chassis reached a maximum of 1.412 MPa, as shown in Figure 7.6.



(a) Falcon 9 design load factors.

Table 2 Random Vibration Test Profile	
Frequency (Hz)	Maximum Flight Envelope (g^2/Hz)
20	0.057 (g^2/Hz)
20-153	0 (dB/oct)
153	0.057 (g^2/Hz)
153-190	+7.67 (dB/oct)
190	0.099 (g^2/Hz)
190-250	0 (dB/oct)
250	0.099 (g^2/Hz)
250-750	-1.61 (dB/oct)
750	0.055 (g^2/Hz)
750-2000	-3.43 (dB/oct)
2000	0.018 (g^2/Hz)
OA (grms)	9.47

(b) NanoRacks random vibration testing profile.

Figure 7.5: Launch loads that TigerSat Blue will experience [59].

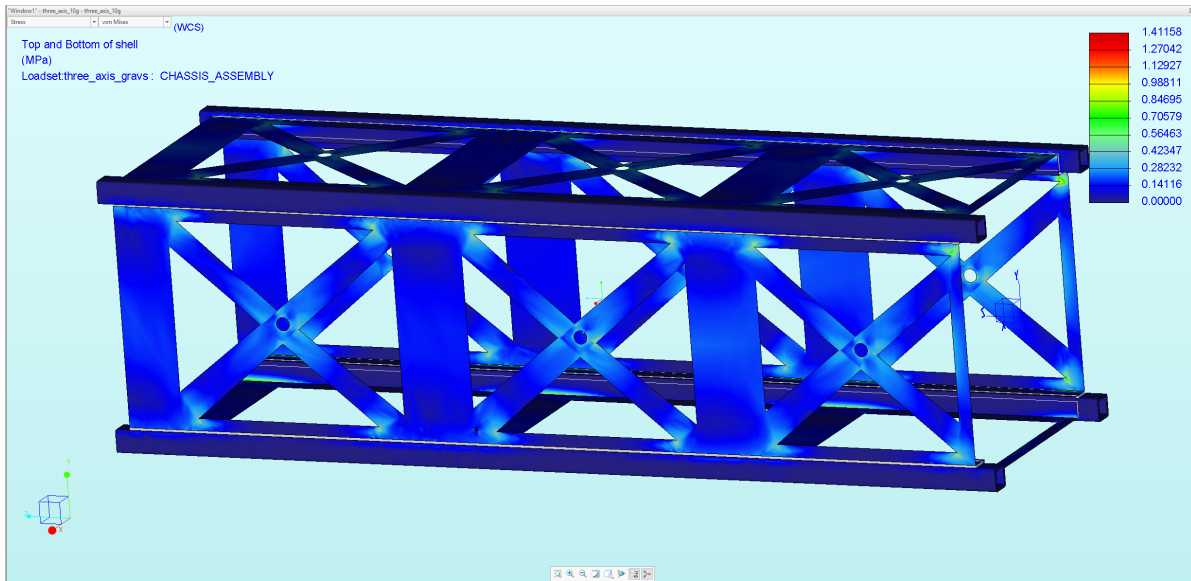


Figure 7.6: 1.67 x maximum load factor the chassis will experience during launch, applied along all axes at once to account for potential non-static loads. Units are in MPa.

Because aluminum 6061 does not yield until it reaches 276 MPa, the structure is in no danger of yielding or failing during launch. [60]

7.2.4 Modal Analysis

A modal analysis was also performed to ensure the structure would survive the random vibrations during launch. Although this analysis is sensitive to internal components and would likely change as the design was manufactured and iterated upon, it is important to prove the survival of the structure at every stage of the design process.

This analysis was conducted with all 4 rails again constrained as they would be inside the NanoRacks deployer.

Mode	Frequency (Hz)
1	1,241
2	1,272
3	1,307
4	1,324

Table 7.4: The four modes closest to vibration frequencies experienced during launch.

Table 7.4 shows the results of the analyses up to 2000hz. The structure does not have any modes until at least 1,241hz. At this frequency, the amplitude is $0.02 g^2/hz$. This is a safety factor of almost 5 before the structure is at any risk of damage (see figure 7.5b).

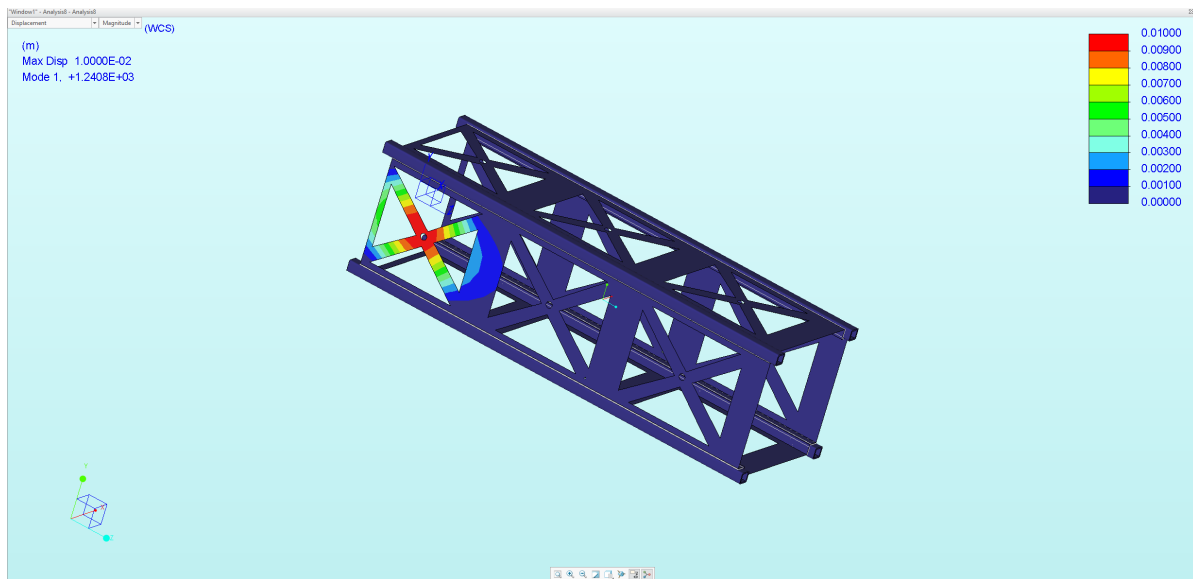


Figure 7.7: The deflection anticipated if the structure were to reach its first mode.

If the structure were to reach a frequency of 1,241hz, parts of it would deflect as much as 0.01m, as in figure 7.7.

7.3 Mass Budget

The TigerSat Blue mass budget appears in Table 7.5. As shown in the table, the mass margin is tight. In the best-case the total mass will be just under the requirement, and in mass-adjusted case the mass will exceed the requirement by about 400 g. To remedy this, excess weight will be removed from the satellite by custom building components to save mass and by modifying off-the-shelf components to be lighter and more design specific. This is true of the power subsystem, which provides the most significant contribution to mass with the battery, panels, boost converter, and other electronics. The fuel management system and thruster provide the next largest mass, but as this is the payload system, the mass will be accommodated to meet the mission goals. Mass may also be removed from the chassis upon further structural analysis.

The mass requirement is also not necessarily a hard requirement. According to the NanoRacks guidelines, in Appendix B.2, the mass limits are set by NASA requirements on ballistic properties of the CubeSat to ensure the CubeSat will naturally de-orbit within a reasonable time limit. Since the CubeSat will have a significantly larger cross-sectional area than a standard 3U CubeSat, due to the large fixed deployable solar panels, TigerSat Blue will not be in danger of becoming too dense to be affected by atmospheric drag. As stated in the guidelines, larger masses than specified in the limits may be approved on a case-by-case basis by NanoRacks. As shown in Chapter 3, care is taken with the TigerSat Blue mission so that it will de-orbit within 25 years. Even if over-weight by a small margin, TigerSat Blue will still be fit for approval by these constraints and standards.

TigerSat Blue Mass Margin			
Component	Mass (g)	Factor	Adj. Mass (g)
Battery	540	1.15	621
Solar Panels	370	1.05	388.5
ADCS Kit	910	1.05	955.5
CPU	94	1.05	98.7
Radio	60	1.05	63
Antenna	85	1.05	89.25
Thruster	546	1.2	655.2
Electronics	964	1.1	1060.4
Chassis	505	1.1	555.5
MLI Blankets	7	1.2	8.4
Fuel	500	1	500
Fuel Management System	167	1.15	192
Mass Requirement (g)	4800		
Total Mass (g)	4748		
Total Adj. Mass (g)	5187.45		
Mass Margin (g)	-387.45		

Table 7.5: TigerSat Blue mass budget. The mass requirement is set by the NanoRacks Interface Control Document which appears in appendix B.2. Masses are adjusted by a growth factor based on relative confidence in the mass estimate.

Chapter 8

Attitude Determination and Control System

8.1 Requirements and Modes

When the CubeSat is ejected from the NanoRacks CubeSat Deployer, it will first deploy solar panels and antennas. It will then begin the process of detumbling. Once steady, it will slew to attain an earth pointing position, to orient the antenna and start communication. After these initial modes [61], it will begin a steady alternating pattern of sun pointing for power collection, thruster pointing for burns during the eclipse, and earth pointing slews to communicate with the ground station. These slews will require a 1-5 degree pointing accuracy [61], which played a role in package determination. Along with these mission modes, attitude control will take into account the effect of environmental torques and off-center thruster torques and apply reaction wheels accordingly. Every few orbits, the system will perform momentum dumping and desaturate the reaction wheels with the help of magnetorquers. It is important to recognize that slews are saturation neutral maneuvers, and thus do not contribute to the saturation of the reaction wheels.

8.2 ADCS Package Selection and Specifications

Three off-the-shelf ADCS packages were considered and compared. The trade study for these packages is shown in Figure 8.1.

It was determined that the XACT package by Blue Canyon Technologies was the best choice [62] [63]. It has the following specifications (Figure 8.2). The package includes

Trade Selection of ACDS package		Models		
Requirements	Requirement Explanation	MAI-100	IMI-200	XACT
Max Voltage Usage	Minimize system drain on power	16 V	28 V	12 V
Torque Capability (per wheel)	How flexible and fast can the sat change orientation	0.635 mNm	0.466 mNm	4.00 mNm
Spacecraft Pointing Accuracy	How efficiently can we find the sun	0.0008 degree	-	0.0003
Enclosed Volume	Minimizes space that system needs	0.1mx0.1mx0.078m	0.07mx0.07mx0.07m	0.1mx0.1mx0.05m
Mass	Minimize mass of system	0.865 kg	0.915 kg	0.910 kg
Momentum Storage (per wheel)	Flexibility of sat in changing orientation	1.1 mNms	3.6 mNms	15 mNms
Slew Rate	Efficiency of manoeuvre	8.4 degree/s	-	10 deg/s
Max radiation intake	Minimize damage to hardware	30 krad	30 krad	-
Selection		9	8	13

Figure 8.1: Trade studies comparing different ADCS packages. Green boxes are awarded 3 points, yellow boxes are 2 points, and red boxes are 1 point.

a star tracker, a sun sensor, a magnetometer, magnetorquers, reaction wheels, and rate sensing gyroscopes. The GPS that will be used is not included in the XACT package, but is instead integrated in the flight computer [64].

Specifications	XACT Parameters
Max Voltage Usage	12 V
Torque Capability (per wheel)	4.00 mNm
Spacecraft Pointing Accuracy	0.0003
Enclosed Volume	0.1mx0.1mx0.05m
Mass	0.910 kg
Momentum Storage (per wheel)	15 mNms
Slew Rate	10 deg/s
Reaction Wheel Dimensions	42x42x19 mm
Reaction Wheel Mass	0.130 kg

Figure 8.2: XACT Package Specifications.

Integrated testing of ADCS will be done through Day in the Life Testing in conjunc-

tion with the communication and data handling subsystem.

8.3 Cubesat Coordinate System

Attitude control of the CubeSat is dependent on its center of mass and its principal axes. To gain a complete understanding of the variation in control needed as the CubeSat's fuel is depleted, calculations are focused on the CubeSat at full tank and at empty tank. This will allow a full range of possible torques to be calculated.

The moment of inertia of a body is a tensor. This tensor is useful in determining how much torque to apply about each axis to obtain the angular acceleration value for that axis. In 3D space it is given by a 3 x 3 matrix about three linearly independent axes, 1, 2, and 3:

$$I = \begin{bmatrix} I_{11} & I_{12} & I_{13} \\ I_{21} & I_{22} & I_{23} \\ I_{31} & I_{32} & I_{33} \end{bmatrix}$$

The eigenvalues of this matrix are the principal axes, three orthogonal axes that make the inertia matrix diagonal, with the corresponding eigenvectors pointing in the direction of the principal axes [65]. The principal moments of inertia for a full tank at the start of the mission, I_{full} , and for an empty tank, I_{empty} are given in kg-m² as:

$$I_{full} = \begin{bmatrix} 1.644 \times 10^{-2} & 0 & 0 \\ 0 & 5.209 \times 10^{-2} & 0 \\ 0 & 0 & 6.362 \times 10^{-2} \end{bmatrix}$$

$$I_{empty} = \begin{bmatrix} 1.638 \times 10^{-2} & 0 & 0 \\ 0 & 5.278 \times 10^{-2} & 0 \\ 0 & 0 & 6.436 \times 10^{-2} \end{bmatrix}$$

The orientation of the principal axes are as follows: Axis 1, or the positive z-axis, points in the opposite direction of the thruster. Axis 2, or the positive x-axis, also lies in the plane of the thruster exhaust and is oriented 90° clockwise of the z-axis. Axis 3, or the positive y-axis points is defined by the cross product of axes 1 and 2, as we are in a right-handed coordinate system.. These are shown in Figure 8.3.

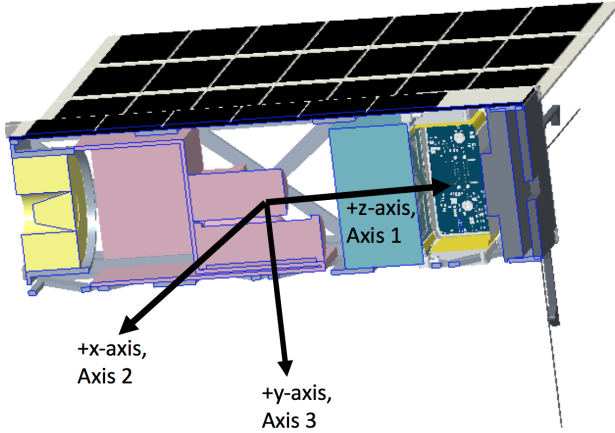


Figure 8.3: Principal axes of the CubeSat.

8.4 Detumbling

After on-orbit deployment and the subsequent deployment of solar panels and antennas, detumbling will be initialized to stabilize the CubeSat and to minimize the high angular velocity spinning that results from ejection from the NanoRacks deployer on the ISS [66]. This detumbling involves use of B-dot control laws and magnetorquers in the CubeSat ADCS package as the actuators to generate magnetic moments. These magnetic moments interact with the Earth's magnetic field and then produce external torques that act on the CubeSat.

The control law is given as follows [67]:

$$M_i = -k\dot{B}_i \quad (8.1)$$

where M_i is the commanded magnetic dipole moment about the i^{th} axis, and k is the positive gain constant of the controller. The general principle behind B-dot control is to generate a magnetic field that is opposite in sign to the rate at which the magnetic field measured by the magnetometer is changing. If the spin of the CubeSat about the z-axis is considered, the torque about any axis is the cross product of the magnetic dipole and the magnetic field in that direction. About the z-axis this can be stated as

$$T_z = M_x B_y + M_y B_x \quad (8.2)$$

where the first term is the magnetic dipole moment applied across the x-axis and the second is applied about the y axis, both of which create torques in the z-direction. B_x

and B_y reference the Earth's magnetic field in the x-y plane with respect to the x or y-axis. This can be represented depending on the orientation as follows [67]:

$$B_x = B_o \cos (\omega_z t) \quad (8.3)$$

$$B_y = -B_o \sin (\omega_z t) \quad (8.4)$$

From our control law in Equation 8.1 we see that

$$M_x = k B_o \omega_z \sin (\omega_z t) \quad (8.5)$$

$$M_y = k B_o \omega_z \cos (\omega_z t) \quad (8.6)$$

Combining eqn 8.2 with these, we obtain:

$$T_z = (k B_o \omega_z \sin(\omega_z t))(-B_o \sin(\omega_z t)) - (k B_o \omega_z \cos(\omega_z t))(B_o \cos(\omega_z t)) \quad (8.7)$$

Which reduces to:

$$T_z = -k B_o^2 \omega_z = \dot{H}_z = I_z \dot{\omega}_z \quad (8.8)$$

$$\dot{\omega}_z + \frac{k B_o^2 \omega_z}{I_z} = 0 \quad (8.9)$$

$$\dot{\omega}_z = \omega_{zo} e^{-1/T} \quad (8.10)$$

$$T = \frac{I_z}{k B_o^2} \quad (8.11)$$

T gives the time decay constant of the spin about each axis, or the time taken for the angular velocity about each axis to completely decay given that two magnetorquers act about that axis to produce perpendicular torques [67]. These control laws are used by the B-dot controllers on the on-board computer to calculate torques required by each magnetorquer. The torque value calculated by the B-dot controller is sent to the magnetorquers as pulse width modulation (PWM) signals.

The following formulas were used to calculate the time taken to detumble for each

axis of the CubeSat:

$$\tau = \mu \times B \quad (8.12)$$

$$\tau = I \frac{d\omega}{dt} \quad (8.13)$$

$$\text{Time}_{\text{axis}} = \frac{I_{\text{axis}} \omega}{\tau} \quad (8.14)$$

where μ is the magnetic moment of the magnetorquer for an axis, B is the strength of the Earth's magnetic field at the location, and ω and I_{axis} are respectively the angular velocity and moment of inertia about that axis.

An initial angular velocity of 6 revolutions per minute (RPM), or 36 degrees per second per axis was assumed. The XACT ADCS datasheet specified a maximum magnetic moment of 0.1 Am^2 , and the Earth magnetic field at 400 km has field strength of $30,000 \mu\text{T}$. For detumbling, all the magnetorquers of perpendicular axes are used; for instance, to detumble the CubeSat about the x-axis, magnetorquers controlling the y- and z-axis would be used. From this concept, the time taken to detumble along each axis was calculated to be: $\text{Time}_x = 5.0726 \text{ min}$, $\text{Time}_y = 6.2262 \text{ min}$, and $\text{Time}_z = 1.6586 \text{ min}$. Considering the non-parallel detumbling case, in which each axis is detumbled successively, and not simultaneously, a conservative total time of **12.9574** minutes, or approximately 13 minutes, for all three axes to detumble.

8.5 Initial Location and Orientation Acquisition

A GPS carried on the CubeSat will be used for initial location acquisition. The procedure behind this is as follows: 4 GPS satellites that have known trajectories with respect to the earth will communicate their distances to the CubeSat after detumbling. These distances will be communicated as time ranges accompanied by a bias, denoted b , in measurement due to the imprecision in the time measured by the clock on the CubeSat. Thus the coordinates of the CubeSat can be determined as so:

$$d_i = \sqrt{(x_c - x_i)^2 + (y_c - y_i)^2 + (z_c - z_i)^2 + bt_i} \quad (8.15)$$

where x_c , y_c , and z_c denote the x , y , and z coordinates of the CubeSat, x_i , y_i , and z_i with i from 1 to 4 refer to the coordinate locations of the GPS satellites, d_i refers to the distance from the CubeSat to each satellite and t_i is the range from the CubeSat to

the satellite measured as time. The four unknowns comprising the spatial coordinates of the CubeSat and the bias in the measurements are determined from the use of the four GPS satellites. Figure 8.4 shows the coordinate locations of the satellites and the CubeSat.

The initial attitude of the satellite is obtained through the use of the TRIAD or QUEST algorithm [66]. Under the worst case scenario, the orbital insertion of the CubeSat from the NanoRacks deployer occurs in the eclipse portion of the orbit. In this case, the star sensor and the magnetometers will be used to determine the initial attitude of the CubeSat. Two vectors f_1 and f_2 are linearly independent unit vectors from the magnetometer and star sensor on the CubeSat. Two reference vectors r_1 and r_2 will denote the vectors from the same stars and the magnetic field from a point in inertial space. The TRIAD algorithm involves constructing two orthonormal bases of reference, r , and attitude vectors, f , from these initial four vectors and deriving a direction cosine matrix (DCM), denoted $\overset{\leftrightarrow}{A}$, that allows the conversion from the inertial location coordinate system to the attitude of the CubeSat. The DCM contains three angle values that pertain to the angle of rotation, denoted θ_1 , θ_2 , and θ_3 , about the three principal axes. The QUEST method performs a similar function as the TRIAD algorithm, however, it works with quaternions, which specify positions in inertial space, rather than reference and direction vectors [66].

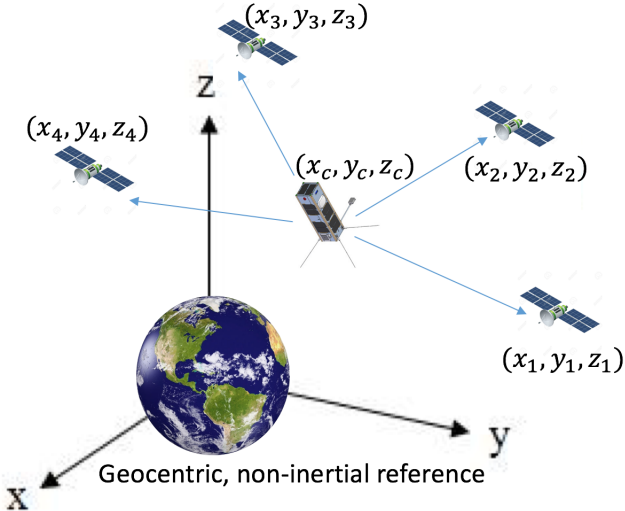


Figure 8.4: GPS location determination. The four GPS satellites will use Equation 8.15 for determining the location of the CubeSat with respect to the earth.

8.6 Orbit Maintenance

A Kalman filter detects errors in trajectories. This filter uses a state vector (provided by the sensors) and dynamics vector, which is calculated using input from magnetometers, the moments of inert of the CubeSat, and the rate sensing gyroscope, among other means, to compute a new state vector after a given time increment. In order to linearize the information provided and compensate for discrete sensor measurements, additional algorithms incorporated in an extended Kalman Filter will be used [66]. A Proportional Derivative (PD) controller controls the errors detected by the extended Kalman Filter, in the state vector and the rate of change of the state vector error, given by the state dynamics vector [66].

8.7 Slews

Slews were calculated by considering the case in which the greatest attitude change would be required, which comprised the maximum angle about which to rotate the CubeSat, 180 degrees, and about the axis with the greatest moment of inertia (highest magnitude principal axis, which would require the greatest amount of torque [68].

These slew calculations were performed by considering physical principles of torque and angular momentum. Torque, τ , is defined as the rate of change of angular momentum, H :

$$\tau = \frac{dH}{dt} \quad (8.16)$$

$$\tau dt = dH \quad (8.17)$$

This can be integrated to yield:

$$\tau t = H \quad (8.18)$$

H is the product between the moment of inertia about a given axis, denoted I_i , and the angular velocity:

$$H = I_i \omega \quad (8.19)$$

$$\tau t = I_i \omega \quad (8.20)$$

ω is the change in angular distance, $\Delta\theta$, with time, so the above becomes:

$$\tau t = I_i \frac{\Delta\theta}{t} \quad (8.21)$$

From which we can calculate the time taken to slew for about a certain angle is:

$$t = \sqrt{\frac{I_i \Delta\theta}{\tau}} \quad (8.22)$$

The τ values used for this calculation would ideally be the maximum torque that can be produced by the reaction wheels of the XACT ADCS package, 0.004 Nm, but for a conservative torque estimate these calculations utilized half of the available maximum torque (0.002 Nm). Further calculations show that increasing the torque applied by the reaction wheels (denoted RWA in Figure 8.5) increases the slew rate and decreases time taken to slew.

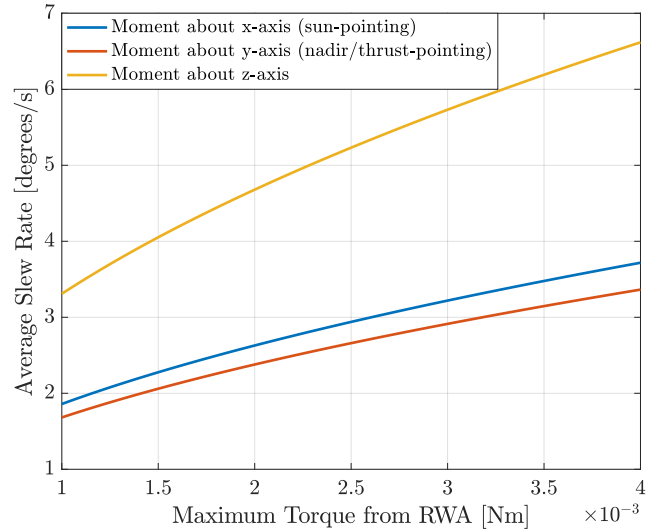


Figure 8.5: Relationship between the amount of torque applied by the reaction wheels and the slew rate. As the torque applied increases about any axis, the slew rate increases. Full tank conditions are shown here.

8.7.1 Nadir-pointing

The nadir-pointing orientation is defined as the attitude when the positive z-axis of the CubeSat, which contains the antennas used for ground communication, is pointing to the earth. The most conservative slew estimate for this case will arise from a slew about

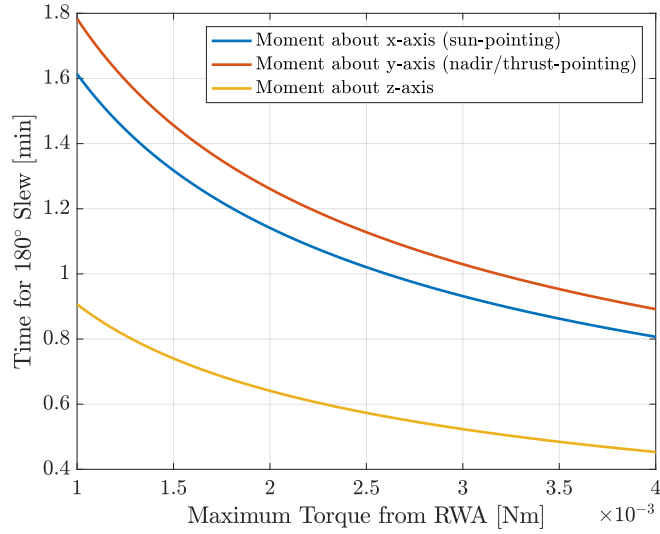


Figure 8.6: Relationship between the amount of torque applied by the reaction wheels and the time of slew. As the torque applied increases about any axis, the time of slew decreases. Full tank conditions are shown here.

the y-axis. For a full tank this results in a total of **1.261** minutes to slew, at a rate of **2.378** degrees per second. For an empty tank the values are: **1.268** minutes slew with **2.365** degrees per second slew rate.

The rate at which reaction wheels in the XACT ADCS package were also computed using the concept of conservation of angular momentum. Given the mass of one reaction wheel, 0.130 kg, radius, 2.1 cm, the moment of inertia of the reaction wheel, I_{rw} was determined:

$$I_{rw} = \frac{1}{2} m_{rw} r_{rw}^2 \quad (8.23)$$

and the rotation rate of the wheel for a specific axis i , is determined through the conservation of angular momentum, in terms of rotations per minute (RPM):

$$H = I_i \omega_s = I_{rw,i} \omega_{rw,i} \quad (8.24)$$

$$\omega_{rw} = \frac{I_i \omega_s}{I_{rw}} \times \frac{60}{360} \quad (8.25)$$

where the i indicates the axis of focus and ω_s is the slew rate about the i^{th} axis. These calculations were done to check if the resulting values were reasonable. Nadir-pointing slews with a full and empty tank resulted in the y-direction reaction wheel rotation rates of **879** and **885** RPM respectively.

8.7.2 Sun-pointing

Solar pointing of the CubeSat is done by defining two primary unit vectors \mathbf{Y}_s and \mathbf{S}_n where the former is the y-axis, and the latter is the vector from the sun that is optimally perpendicular to the face of the solar panels [69].

$$\mathbf{Y}_s = [y_1 \ y_2 \ y_3] \quad (8.26)$$

$$\mathbf{S}_n = [s_1 \ s_2 \ s_3] \quad (8.27)$$

The sun-pointing slew will allow \mathbf{Y}_s and \mathbf{S}_n to have a 180 degree angle between them, or \mathbf{Y}_s must point away from the sun vector by exactly 180 degrees. The angle of the sun on the solar panels initially prior to the slew will be measured by the sun sensor and presented to the on board computer [68].

For sun-pointing, the most conservative slew involves rotating the CubeSat, whose solar panels are pointed 180 degrees away from the sun, about its x-axis. Similar calculations as performed for nadir-pointing reveal the following values: time to slew of **1.141** minutes with a slew rate of **2.628** degrees per second and the x-axis reaction wheel rotating at **796** RPM for the full tank and time to slew of **1.148** minutes with a slew rate of **2.611** degrees per second and the reaction wheel rotating at **801** RPM for the empty tank.

8.7.3 Thrust-pointing

Because thrust-pointing involves CubeSat orientation about the same axis as the nadir-pointing slew, about the z-axis, the most conservative slew estimate is about the y-axis, yielding the same values as for the nadir-pointing case. For the full tank, the time of slew was **1.261** minutes, slew rate of **2.378** degrees per second, and y-axis reaction wheel rotation rate: **879** RPM; empty tank time of slew: **1.268** minutes, **2.365** degrees per second slew rate, and **885** RPM reaction wheel rotation rate.

The slew rates for all of these slews are high rate slews, defined as any slew rate greater than 0.5 degrees per second [61]. These higher slew rates played a role in ADCS package determination, and made it necessary to have gyroscopes and reaction wheels in the package [61].

8.8 Environmental Disturbance Torques

Given the moment of inertia matrices of the full and empty CubeSat, we can calculate the torques each environmental factor will exert [61]. Some factors are cyclical or constant, and do not create saturation. These are solar radiation pressure (cyclical), magnetic field torques (cyclical), and aerodynamic drag (constant).

Solar radiation pressure torque can be calculated using the following formula [61]:

$$T_s = \frac{\phi}{c} * As * (1 + q) * (cp - cm) * \cos(\phi) \quad (8.28)$$

$$T_s = 1.02 \times 10^{-7} \text{Nm} \quad (8.29)$$

Magnetic Field torque can be calculated using the following formula [61]:

$$T_m = \frac{M}{R^3} \lambda h B \quad (8.30)$$

$$T_m = 2.18 \times 10^{-5} \text{Nm} \quad (8.31)$$

Aerodynamic drag torque can be calculated using the following formula [61]:

$$T_a = 0.5\rho C_d A V^2 (c_p a - c_m p) \quad (8.32)$$

$$T_a = 3.99 \times 10^{-8} \text{Nm} \quad (8.33)$$

Some factors are secular, and do create saturation, such as the gravity gradient torque, which arises due to earth's gravity decreasing with distance, resulting in torques on the CubeSat depending on how far each component is from the earth. It can be calculated using the following formula [61]:

$$T_g = \frac{3\mu}{2 * R^3} |I_z - I_y| \sin(2\theta) \quad (8.34)$$

$$(8.35)$$

The magnitude of these torques will vary as each burn decreases our fuel mass, and thus the mass of the CubeSat. Let us consider the two extreme possibilities - one

where the fuel tank is full and one where it is completely empty. If we calculate the environmental torques of both these conditions, we will know the entire range of torques possible. For a full tank, the torque evaluates to $T_g = 2.20031$ Nm, and for an empty tank this torque is 2.21753 Nm.

8.8.1 Desaturation of Environmental Torques

The gravity gradient torque will accumulate momentum and cause saturation of the reaction wheels [70]. The momentum capability per wheel is known to be 0.015 mNms. Since the torques are equivalent within the uncertainty, let us take the example of the full tank.

The time it will take for the gravity gradient torque to completely saturate the wheel can be found by

$$\text{Saturation Time} = \frac{\text{Momentum Capability}}{\text{Torque}} \quad (8.36)$$

$$\text{Saturation Time} = 171,644.35 \text{ s} = 2,860.73 \text{ min} \quad (8.37)$$

For an initial orbital period of 92 minutes, this is equivalent to approximately 30 orbits. After 30 orbits, we will employ the magnetorquers to desaturate the reaction wheels.

The torque thus generated can be given by Equation 8.13, given earlier, and with the definition of the magnetic moment μ :

$$\mu = iA \quad (8.38)$$

where i is the current going through the wire and A is the area of the coil. The specific magnetorquer in this package has a coil area of 0.0025 m². A rough estimate of the magnetic field, B at this altitude orbit is 3.0×10^{-2} Tesla.

Magnetorquers are best equipped to create a small torque for a sustained period of time. If we assume that the wheels will desaturate at a 100th of the max Torque capability (0.00004 Nm), we can calculate the amount of current needed to oppose a reaction wheel in a particular axis to be 0.53 Amps. Further, it would need to be applied for 375 seconds, or approximately 6.25 minutes, which is a reasonable fraction of the

orbit.

8.9 Torques from Error in Thruster Placement

Another aspect of attitude control is accounting for rotational torques caused by thruster misalignment, either in a distance offset or in an angle offset.

A range of distance offsets are assumed and the torques caused by each of these offsets are calculated. The thrust maximum is 12 mN. As before, we will consider the worst case scenario. The rotational torque will be maximum at max thrust. Figure 8.7 shows the relationship of increasing rotational torque with increasing distance offset. The distance offset range considered here is 0-2 cm.

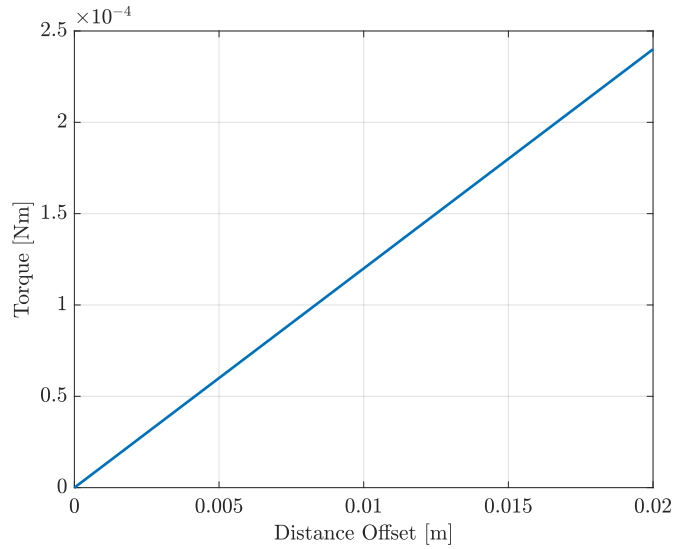


Figure 8.7: Torque created by various distance offsets of the thruster.

Given that the burn time for a single firing is 10 minutes or 600 seconds and the maximum momentum storage capacity of the wheel about the axis of the thruster, the z-axis, is 0.015 Nms, we can calculate the maximum offset torque tolerable before the wheel becomes saturated in a single burn. This can be computed by dividing total momentum of the reaction wheel, H_{rw} by burn time, t_{burn} (a rearrangement of Equation 8.36), shown here:

$$\tau_{max} = \frac{H_{rw}}{t_{burn}} \quad (8.39)$$

which is 2.5×10^{-5} Nm. This is the maximum torque the distance offset can be allowed

to cause, considering momentum saturation due to misalignment in isolation. Dividing this maximum torque by the thrust of the CubeSat, T , which is 12 N, provides the length of the moment arm, L :

$$L = \frac{\tau_{max}}{T} \quad (8.40)$$

This is the maximum offset of the thruster on the CubeSat which will result in the complete saturation of the reaction wheel during a single burn because it will consume maximum torque. L is 0.001667 m or 0.167 cm.

Thruster misalignment can also occur in the form of an angle offset. This is shown in Figure 8.8, where d is the length of the moment arm, a is the distance from the center of mass to the end of the thruster, and α is the angle offset. The maximum angle offset can be determined through simple trigonometry, using Figure 8.8 and Equation 8.41

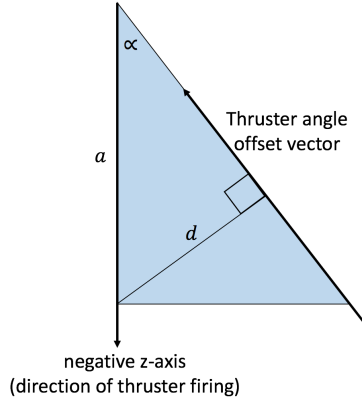


Figure 8.8: Trigonometry to find moment arm of angle offset.

$$\sin(\alpha) = \frac{d}{a} \quad (8.41)$$

For the range of alpha of 0-10 degrees, the torque created is shown in Figure 8.9:

The distance from the center of mass to the thruster along the axis of the thruster is 0.177 m. The moment arm maximum is still at 0.001667 m. The center of mass in which translates to an angle offset of 0.54 degrees.

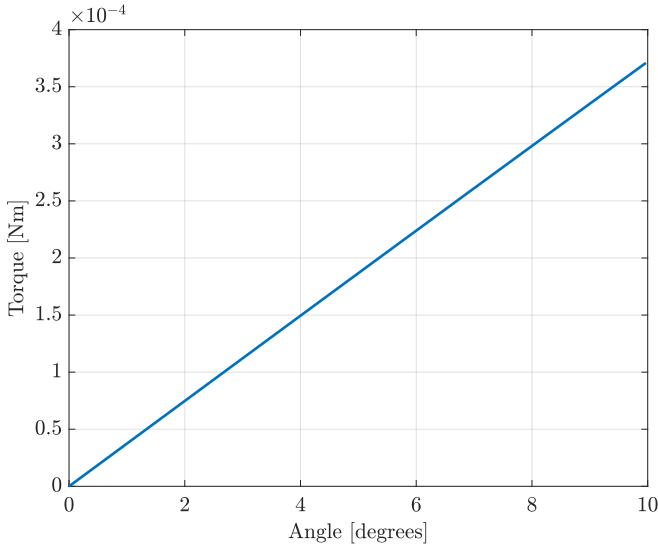


Figure 8.9: Torque created by a range of thruster angle offsets.

8.10 Conclusion

The ADCS system of the CubeSat is the XACT ADCS package, containing a star tracker, sun sensor, magnetometers, rate sensing gyroscope, and reaction wheels. Magnetorquers and B-dot controllers will allow the CubeSat to detumble completely after ejection from the NanoRacks deployer, after which its initial acquisitions will begin. Initial location is given by the GPS on the flight computer. Initial attitude will be provided by the sensors working in conjunction with the TRIAD algorithm on the on board computer. If the CubeSat is released in eclipse, magnetometers and the star tracker will be used. If released in the sunlit orbit, magnetometers and the sun sensor will be used. Upon acquisition, the CubeSat will begin nadir-pointing slews, to point antennas at the earth for ground communication, sun-pointing slews to charge batteries, and thrust-pointing slews during eclipse to raise orbit. During this process, algorithms on the on board computer and controllers will be used to detect and correct errors in trajectory. The effect of environmental disturbances such as solar radiation pressure, magnetic field torques, atmospheric drag, and gravity gradient torques were quantified. Due to its secular nature only gravity gradient torques will lead to reaction wheel saturation. The time taken to desaturate the reaction wheel using magnetorquers was determined. Further, manufacturing errors, such as thruster misplacement or angle offset, can also lead to reaction wheel saturation during thruster firing. The maximum angle offset and thruster displacement were calculated given the maximum torque and momentum capacity of the

reaction wheels.

Chapter 9

Communications and Data Handling

9.1 Introduction

The communications and data handling subsystem is responsible for the transmission of all commands and telemetry sent to and from the satellite. This requires selection of spacecraft and ground station communications hardware (including a radio and antenna), selection of spacecraft computational hardware (a processor), design of an overall software architecture, and development of a test plan for hardware and software. This section details the trade studies conducted and components selected for the subsystem.

9.2 Requirements

The requirements that must be satisfied by this subsystem are detailed in Table 9.1.

Table 9.1: Communications and Data Handling Requirements

Top-Level Requirement	Derived Requirements	Verification Method
Spacecraft Communications		
Communications system shall have uplink and downlink capability		Datasheet, software/hardware test protocol
Continued on next page		

Table 9.1 – continued from previous page

Top-Level Requirement	Derived Requirements	Verification Method
Communications system shall have sufficient link margin to ensure stable communications at all orbital altitudes		Verification of derived requirements
	Uplink BER shall be no less than 10^{-6}	Link budget
	Downlink BER shall be no less than 10^{-6}	Link budget
	Link margin shall be no less than 3 dB	Link budget
Communications system shall transmit telemetry detailing the CubeSat's position, velocity, orientation, fuel usage, relevant thruster usage data, and spacecraft health data		Software/hardware test plan, verification of derived requirements
	Communications system shall support a minimum total downlink quantity of 4 mB/day	Datasheet, link budget, orbit analysis
The communications sub-system shall be compliant with FCC and ITU regulations		Verification of derived requirements
	Downlink packets shall contain a unique satellite ID	Software test protocol
	Communications system shall be inhibited for at least 45 minutes after on-orbit deployment	Software/hardware test protocol
Continued on next page		

Table 9.1 – continued from previous page

Top-Level Requirement	Derived Requirements	Verification Method
	Spacecraft shall have one RF inhibit and RF power output of no greater than 1.5 W at the transmitting antenna's RF input OR The spacecraft shall have two independent RF inhibits	Review of electrical design
Communications system shall be able to control transmitter activation by software command		Software test protocol
Communication system shall be mechanically compatible with the spacecraft		Review of mechanical design
Communications system's power consumption shall be within EPS capabilities		Review of power budget
Spacecraft Computer Hardware		
The spacecraft shall have sufficient computational resources to run flight software		Software test protocol
	The spacecraft shall have at least 10 MB of flash memory for software	Component datasheet
	The spacecraft shall have at least 32 MB of data memory	Component datasheet
	The spacecraft shall have at least 1 MB of RAM	Component datasheet
	The processor shall run at at least 40 MHz	Component datasheet
Computational hardware shall be capable of operation in the space environment for a mission duration of two years		Verification of derived requirements
Continued on next page		

Table 9.1 – continued from previous page

Top-Level Requirement	Derived Requirements	Verification Method
	Computational hardware shall function at temperatures from 0°C to +65°C	Thermal/vacuum test
	Computational hardware shall be radiation tolerant at expected dosages	Datasheet, simulated analysis
Processor shall have sufficient number of interfaces to hardware components in the satellite		Component datasheet, review of C&DH system design
Computational hardware shall be mechanically compatible with the spacecraft		Review of mechanical design
Computational hardware's power consumption shall be within EPS capabilities		Review of Power Budget
Ground Station Hardware		
Ground station shall have sufficient link margin to transmit and receive data from CubeSat		Link budget
Uplink commands shall be encrypted		Software test plan
Ground station shall meet all FCC/ITU licensing requirements		C&DH system review
Spacecraft Software		
Spacecraft software shall support BOL functions		Verification of derived requirements
	Spacecraft software shall enforce 30-minute passive period after deployment	Software test protocol
	Spacecraft software shall command mechanism deployment	Software/hardware test protocol
Spacecraft software shall support operational mission functions		Verification of derived requirements
Continued on next page		

Table 9.1 – continued from previous page

Top-Level Requirement	Derived Requirements	Verification Method
	Spacecraft software shall be capable of processing and storing all sensor data	Software test protocol
	Spacecraft software shall be capable of transmitting stored data during communications windows	Software test protocol, link budget analysis, orbit analysis
	Spacecraft software shall command engine firing at times scheduled by ground station command	Software/hardware test protocol
Spacecraft software shall support EOL functions		Verification of derived requirements
	Spacecraft software shall initiate de-orbit in response to ground station command	Software/hardware test protocol
Spacecraft software shall be capable of running autonomously during periods of no contact with ground station		Verification of derived requirements
	Spacecraft software shall include on-board orbit and attitude determination	Software test protocol
	Spacecraft operation shall be separated into modes. Software shall have the capability to operate and switch between these modes automatically	Software test protocol
	Spacecraft software shall include autonomous health monitoring and transition into a "safe mode" in the event of a failure	Software test protocol
Ground Station Software		
Continued on next page		

Table 9.1 – continued from previous page

Top-Level Requirement	Derived Requirements	Verification Method
Ground station software shall store all received spacecraft telemetry		Software test protocol
Ground station software shall be capable of commanding all spacecraft functions		Software test protocol
Ground station software shall display spacecraft health and status information		Software test protocol

9.3 Data Budget

In order to determine the required data transmission rate for the communication link, it was necessary to estimate the amount of data that would be generated by the spacecraft. A packet size for data from each subsystem was selected based on estimates of sensor precision and the number of sensors that would be generating data. For example, it was estimated that the thermal subsystem could use 16-bit integers to record temperature readings from any thermocouples used, and that no more than 8 temperature sensors would be needed, so a 128-bit data packet would suffice for the thermal system. For a given sensor in the “on” state, it was determined that data would be stored at a sample rate of 0.1 Hz for all cases except that of the thruster, which samples data at a rate of 132 Hz. Duty cycles of 1 were assumed for all components except the thruster, which has a duty cycle of 0.016. All of this information was used to estimate the total amount of data generated by each subsystem per day, which is given in Table 9.2. The total data generated was estimated at 2.68 mB/day (where a day is a 24-hour period). Initial orbital trajectory simulations showed that approximately 1600 seconds per day would be available for communications, which meant that the minimum transmission rate for any transceiver would need to be approximately 13 kb/s.

Source	Packet Size (b)	Data Generated (mB/day)
Thruster	48	1.09
Thermal	128	0.14
ADCS	640	0.69
Orbit	192	0.21
Power	256	0.28
Other system data	256	0.28

Table 9.2: Data rate estimates.

9.4 Communications

There were two driving questions to be considered in the design of the overall approach to communications:

- I. Is it necessary to communicate with the satellite in both directions? That is, can the satellite self-sustain operations without commands from the ground?
- II. Is it necessary to have frequent access to the satellite or will several daily ground station flyovers be sufficient?

To address the first question, it was decided that two-way communication would be desirable to allow for flexibility in scheduling burns and debugging should any part of the satellite fail. For this reason, it was necessary to use a duplex transceiver (which can both transmit and receive data) instead of a simplex transmitter. The answer to the second question was less clear, but would determine whether a conventional ground station-spacecraft link should be developed, or an existing satellite constellation should be used. Some CubeSats communicate with the Iridium or GlobalStar satellite networks to allow near-real-time data transmission [71]. Since it was not certain whether use such a network would represent an improvement over the traditional ground station method, both options were traded.

For the option of using an existing satellite constellation, both the Iridium and GlobalStar networks were considered. An integrated system for CubeSats to communicate with the GlobalStar network was readily available and use of this network by other CubeSat programs is documented [72]. No commercially-available system could be located for communicating with the Iridium network, so the GlobalStar system was selected for trading with the traditional communication methodology. Specifically, the EyeStar D2E system was used in the trade study [73].

In addition to the constellation communication method, a variety of UHF, VHF, and S-band transceivers were considered. Of the initial group, several were immediately

discarded because their data rates would not support transmission of the estimated data quantities necessary over the estimated flyover time that would be available for transmission. The options were narrowed to two produced by the company GOMSpace: an S-band transceiver-antenna package and a UHF/VHF transceiver combined with an antenna produced by EnduroSat. Details are given in the trade study in Figure 9.1, and datasheets can be found in references [74], [75], [76], and [77].

The non-constellation-based communication method requires a ground station. The physics department at Princeton has access to a ground station with a 60-ft dish (the refurbished TIROS station) that would likely provide more than enough capability for this application. This ground station was selected for the traditional communication systems in the trade study because it would be readily available for use with this mission. The specifications of the ground station, which were provided by Professor Daniel Marlow, are given in Table 9.3.

Frequency	1296 MHz with 432 MHz upgrade pending
Beam width	+/- 0.5° @ 1296 MHz, +/- 1.5° @ 432 MHz
Aperture efficiency	50%
Transmit power	250 W @ 1296 MHz, 1000 W @ 432 MHz
Diameter	18.29 m
Reflector shape	parabolic
Gimbal accuracy	0.1°

Table 9.3: Ground station specifications

The link budget for each transceiver-antenna combination was computed from the following equation from Prof. Kasdin's lecture notes, where all parameters are in decibels:

$$\frac{E_b}{N_o} = P + L_l + G_t + L_s + L_a + G_r - k - T_s - R. \quad (9.1)$$

P denotes transmitter power, L_l denotes line loss, G_t denotes transmitting antenna gain, L_s denotes space loss, L_a denotes atmospheric loss, G_r denotes receiving antenna gain, k denotes Boltzmann's constant, T_s denotes the system noise temperature, and R denotes the data rate [78].

For each spacecraft radio and antenna combination, P , G_t , G_r , and R were obtained from the component datasheets [74, 75, 76, 77]. P and R for the ground station were provided by Professor Marlow, as shown in Table 9.3. The ground station antenna gain

Requirement	EyeStar D2E	GOMSpace S-Band Transceiver (SR2000) with ANT2150-DUP Antenna	GOMSpace NanoCom AX100 with EnduroSat UHF Antenna
Type	duplex w/ Globalstar satellite constellation	S-band transceiver capable of full and half duplex configurations	UHF/VHF transceiver configurable as full-duplex or half-duplex (full-duplex has not yet been tested in operation)
Cost	\$7,499 + \$4,800 for 2-year data plan	\$23,300 + ?? antenna	\$10,000 transceiver + \$3,750 antenna
Accessibility	near-constant	~6 times per day	~6 times per day
Input voltage	range 7-20 V, nominal 10 V	5 V	3.3-3.4 V transceiver, 5 V antenna
Max. power consumption	500 mA @ 10 V power-up (5 W)	transceiver w/ 1 modem: 4.13 W; antenna 11 W (TX active)	4.08 W
Standard power consumption	0.5 W receiving, 4.5 W transmitting	transceiver w/ 1 modem: TX: 4.10 W, RX: 3.88 W; antenna RX: 0.8 W, TX: 10.7 W	2.8 W TX; 0.4W RX
Data rate	50Mb/day @ 50%; 700 Bytes/sec	500-2000 kbit/s TX	0.1-115.2 kbps (selectable)
Frequency	TX: 1610-1625 MHz downlink; RX: 2484-2499 MHz uplink	RX 2025-2100 MHz; TX 2200-2290 MHz	435 +/- 5 MHz
Rad hardening	Al and Ta spot shielding	shielded	unlisted, but has operated successfully on multiple spacecraft
Operating temperature range	antenna: -50 to 85°C; radio -40 to 60°C; non-operational -60 to 100°C	-40 to 85°C	transceiver: -30 to 85°C; antenna: -40 to 85°C
Dimensions	transceiver: 61x119x22 mm; antenna: 60 mm dia x 10 mm high	transceiver: 92.0x88.9x13.8 mm; antenna: 100.5x82.6x20.1	transceiver: 65x40x6.5 mm; antenna: 98x98x12 mm
Mass	138 g	transceiver: 201.3 g; antenna: 110 g	transceiver: 24.5 g; antenna: 85 g
Total energy usage in 24 hours (W-hr)	16.2	112.4	9.7
Link budget: uplink (dB)	N/A	23.6	59.33
Link budget: downlink (dB)	N/A	31.1	32.45
Score:	26	18	30

Figure 9.1: Trade study for radio and antenna. Red denotes 0 points, orange denotes 1 point, and green denotes 2 points.

was computed via the standard gain formula for a parabolic antenna [78]:

$$G = \left(\frac{\pi d}{\lambda}\right)^2 e_A, \quad (9.2)$$

where d denotes the antenna diameter, λ denotes the wavelength, and e_A denotes the aperture efficiency. Based on the Princeton ground station's parameters, its gain was computed to be 35.4 dB. However, the gain in practice may be lower, since the spacecraft may not be at the center of the beam. The estimated tracking error is the sum of the error due to inaccuracy in the antenna gimbal and the error due to inaccuracy propagating the spacecraft's orbit. By combining two-line element (TLE) data from NORAD with a modern propagator, it is possible to know the position of a spacecraft in LEO to within approximately two kilometers [79]. At an altitude of 400 km, this corresponds to an error of approximately 0.28° , and thus the maximum total tracking error is approximately 0.38° . Because this is well within the half-power beamwidth of the ground station in both the S-band and the UHF band, the half-power gain of 32.4 dB was used as a conservative estimate of the ground station antenna gain.

L_l , the line loss, was estimated to be 0.9 dB based the standard value provided in

[78]. The concept of operations does not require the ability to make ground station contact during times of severe weather; there is sufficient ground station contact time per week to allow for missed passes. Therefore, a 0 dB atmospheric loss was assumed in the link budget computation. This is the standard clear weather approximation for communications frequencies below 10 GHz [78].

System noise temperatures were computed based on standard conservative estimates for spacecraft uplink and downlink. The spacecraft uplink noise temperature was estimated to be 290K [78], and the spacecraft downlink noise temperature was estimated to be 490K [80].

The maximum required $\frac{E_b}{N_o}$ was estimated to be 10.5 dB based on the chart shown in Figure 9.2 and the use of BPSK with bit error probability estimated at 10^{-6} . The other parameters used for each of the two transceiver-antenna combinations are given in Figure 9.3.

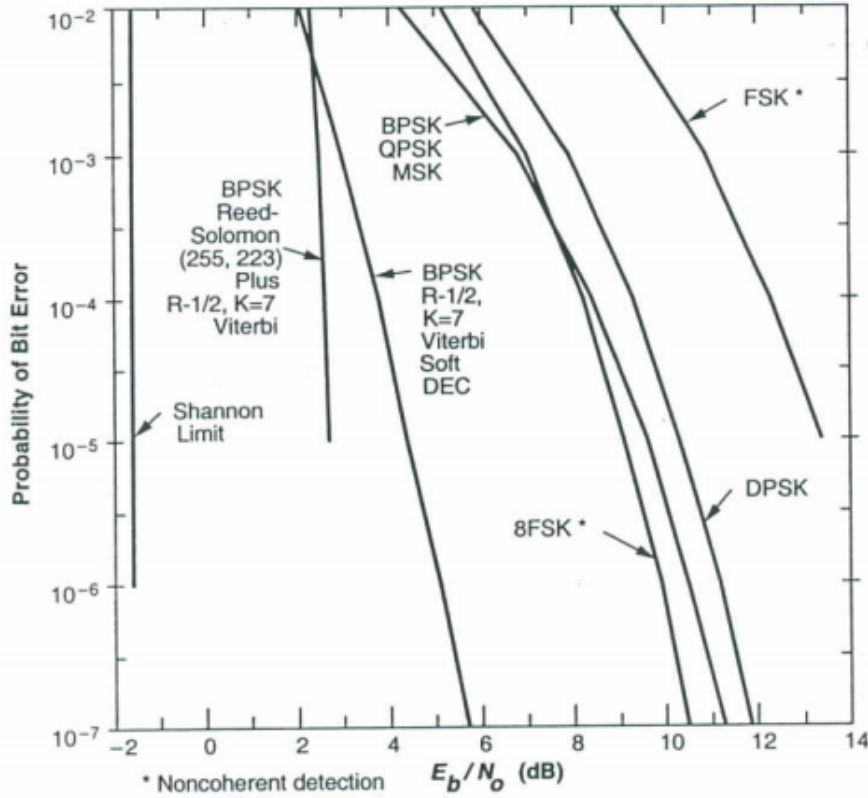


Figure 9.2: Required $\frac{E_b}{N_o}$ based on estimated bit error rate.

The trade study led to the selection of the GOMSpace NanoCom AX100 with the EnduroSat UHF antenna. The GOMSpace S-band antenna was clearly undesirable

Parameter (all in dB except where noted)	GOMSpace S-Band Transceiver (SR2000) with ANT2150-DUP Antenna	GOMSpace NanoCom AX100 with EnduroSat UHF Antenna
Antenna gain	5	0
Transmit power (W)	33	35.4
Data rate	57	50.6
Space loss	167.4	152.6
Boltzmann's constant	-198.6	
Ground station antenna gain		32.4
System noise temperature - uplink		24.6
System noise temperature - downlink		26.9
Atmospheric loss		0
Line loss		-0.9
Computed Eb/No - uplink	23.6	59.33
Computed Eb/No - downlink	31.1	32.45
Max. required Eb/No (estimated)		10.5
Margin - uplink	13.1	48.83
Margin - downlink	20.6	22.45

Figure 9.3: Parameters of the link budget.

because of its high mass and power usage as well as incompatibility with the ground station in terms of frequency. The GOMSpace UHF/VHF system was selected over the EyeStar system because it was physically smaller, significantly lighter, and consumed less power.

9.5 Processing

The on-board computer (OBC) will be responsible for all on-board actions that require computer processing, except for those handled by the attitude determination and control system's processor. These actions include orbit determination, system health data collection, command execution, and communications management. Selection of the OBC was based on which OBC best met the C&DH system requirements. The key areas that particularly drove the selection were:

- I. **Data interfaces:** Because the components selected for other subsystems used a variety of data interfaces, it was critical that the OBC have enough ports to interface with the rest of the system.
- II. **Radiation tolerance:** Because the spacecraft must survive a 3-year mission, and because the OBC is typically the component of a spacecraft that is most susceptible to radiation damage, it was also critical that the OBC have significant radiation hardening.
- III. **Processing power:** Because the OBC must handle high-speed data collection and communications, it must have sufficient computational resources (processing speed and RAM) to handle the data collection process.

Based on the overall system requirements, as well as these particular areas of concern, a trade study was conducted to select an OBC. The three OBCs included in the trade study were chosen based on a survey of COTS CubeSat OBCs that had flight heritage and were readily available for purchase. These options were CubeSpace Cube Computer [81], the Innovative Solutions in Space (ISIS) OBC [82], and the Clyde Space OBC [83]. The Clyde Space OBC can optionally be purchased with an integrated GPS, which is a component that will be needed for on-board orbit determination. Therefore, the Clyde Space OBC + GPS bundle was used in the flight computer trade study. Figure 9.4 shows the trade study and selection for the OBC.

Based on this trade study, the Clyde Space OBC + GPS bundle was selected. The Clyde Space OBC meets all requirements, and was particularly strong in both having sufficient connectors to interface with other subsystems and in radiation hardening. Each of the other options was inferior in one of these areas: the ISIS OBC had relatively little protection against latch-up and single event upsets due to radiation, and the CubeSpace Cube Computer did not have sufficient connectors to interface with other subsystems.

Four key features of the Clyde Space OBC provide radiation hardness. These are:

- I. Latch-up current limiting, which safely shuts off the processor in the event of a

Requirement	Cubespace Cube Computer	ISIS On board computer	Clyde Space OBC + GPS Bundle (SELECTED)
Cost	\$4,500	\$9,850	\$11,000
Flight heritage	ADCS Processor on 2 spacecraft	Main OBC on 2 spacecraft	Main OBC on multiple spacecraft
Average power consumption	310 mW	400 mW	400 mW
Processor speed	48MHz	400 MHz	50 MHz
Software flash memory	4 MB	1 MB	8 MB
RAM	2 MB	64 MB	8 MB
Data memory	1 GB redundant microSD	8 GB redundant microSD	4 GB Flash
Radiation hardening	Internal & external watchdog, tested to TID of 20 krad, SEE @ 60 MeV	On-board watchdog, hardened code memory	Latch-up current monitoring and limiter, Hardened code memory, SEC-DED code to safeguard against SEU bit flips, watchdog timer
Operating temperature range	-10°C to 70°C	-25°C to 65°C	-40°C to 80°C
Dimensions	90x96x10 mm	96x90x12.4 mm	90x96x10.2 mm
Mass	70 g	94 g	62 g
Connectors	2 I2C, 1 Debug UART, 1 CAN	1 I2C, 1 SPI, 2 UART, 8 ADC, 6 PWM, 27 GPIO, 1 USB, 1 Image sensor interface, JTAG for programming, UART debug	2 I2C, 2 UART, 1 Debug UART, 1 SPI, 17 GPIO, 1 JTAG, 1 ETM
Operating system compatibility	KubOS	FreeRTOS, KubOS	KubOS or Proprietary option
Score:	20	23	24

Figure 9.4: Trade study for on-board computer. Red denotes 0 points, orange denotes 1 point, and green denotes 2 points.

power surge.

- II. A hardware watchdog, which monitors program execution and resets the processor if an abnormality is detected.
- III. Hardened memory with error detection and correction (EDAC) monitoring.
- IV. Single error correct, double error detect (SEC-DED) code to protect against bit flips in program RAM.

These features provide sufficient protection to ensure reliability throughout the mission lifetime.

The overall C&DH system architecture is a hybrid of a bus architecture and a central processor architecture. Most components interface with the central processor directly via a dedicated data interface, as in a central processor architecture. However, for those components that are designed to use the standardized I²C bus, a bus architecture is used. These components all share the same I²C lines, and the OBC acts as a master component, commanding which component sends or receives data at any time. Table 9.4 contains a summary of the data protocols used, and figure 9.5 shows the overall system architecture.

9.6 Software

The spacecraft software is designed to meet all mission requirements with minimal complexity. Because the spacecraft will only communicate with the ground station for a small period during each orbit, the spacecraft is designed to operate with significant

Protocol	Pins	Type	Maximum Data Rate (Mb/s)
I ² C [84]	2	Half-duplex data bus [85]	5
RS-232 [85]	9	UART	10
RS-442 [85]	12	UART	10
GPIO	1	Single-pin analog or digital	.256

Table 9.4: Data Protocols Employed on Spacecraft. UART stands for universal asynchronous receiver-transmitter, a type of serial communications protocol.

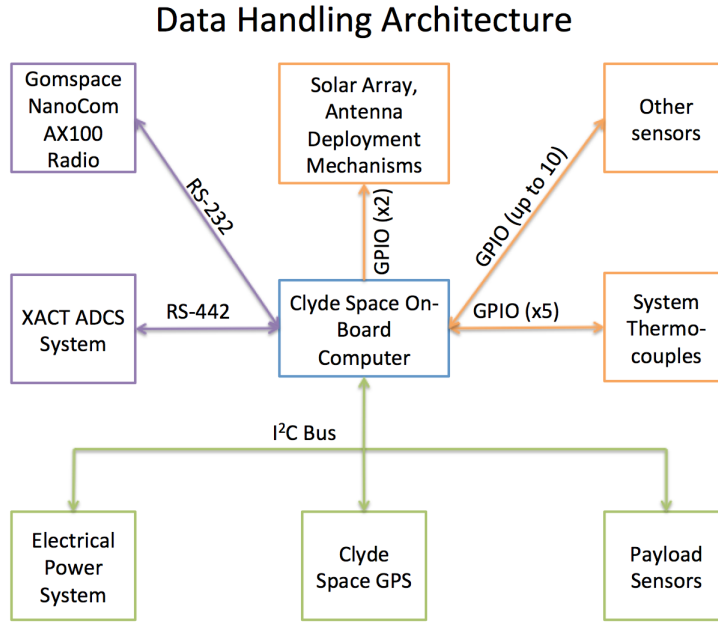


Figure 9.5: Spacecraft C&DH system architecture with communications protocols labeled.

autonomy. The software will be developed in C++, and will be based on KubOS, an open-source Linux distribution for cubesats with significant flight heritage [86].

Figures 9.6 and 9.7 show the full software state diagrams. Figure 9.6 covers beginning-of-life operations. The spacecraft software will be initialized as soon as the spacecraft is released from the deployer. It will then enter a 30 minute wait before deploying the solar array and antenna mechanisms, in order to meet NASA requirements. Once the mechanisms have deployed, the spacecraft will determine its attitude and orbit, detumble, and begin sun pointing. After mechanism deployment, an additional 15 minute timer will enforce the NASA requirement prohibiting RF emission until 45 minutes after leaving the deployer.

Throughout all software modes, the spacecraft will collect data about its position, attitude, and health. Position data will be provided by the Clyde Space GPS, and an orbit will be computed by an orbit determination algorithm on the processor, as was discussed in section 3.1.3. Attitude data will be provided by the XACT attitude determination and control system. Spacecraft health data will include thermocouple readings throughout the spacecraft, voltage data from the EPS, and data on CPU and memory usage from the processor.

Once the spacecraft has completed these steps, it will begin a pre-operations loop. During this period, the spacecraft will stay in sun-pointing mode unless it is over the ground station, in which case it will point at the ground station and transmit data. Orbit data based on GPS measurements will be used to compute when the spacecraft is in range of the ground station. During the “standby for contact” mode, the spacecraft will check whether it needs to begin a slew towards ground station pointing every 10 seconds, based on the time until the next ground station contact window and estimated time required to slew to ground station pointing. During the pre-operations period, ground station operators will verify that the spacecraft is functioning properly. Once this verification has been completed, they will command the spacecraft to transition to an operational mode. At this point, the spacecraft will set a flag in its non-volatile memory to prevent it from repeating its beginning-of-life operations if the processor ever reboots. It will then transition into the operations detailed in figure 9.7.

During mission operations, the spacecraft will spend most of its time in the operational standby loop. In this loop, the spacecraft will sun point, except when it is in range of the ground station, in which case it will point its antenna at the ground station and communicate data. Thruster firings will be scheduled by ground station commands, and scheduled firings will take priority over ground station communications or sun pointing. Similarly to the pre-operations loop, the spacecraft will check every 10 seconds whether it needs to slew toward its attitude for thruster firing or ground station communication, based on orbit and attitude data. During thruster firings, the spacecraft will activate both the thruster itself and the sensors on the payload.

The spacecraft will use the system and payload data it collects to monitor its health. In the event that health data strays outside its nominal range, the spacecraft will enter a safe mode. Safe mode may be triggered from any state by a dangerously low battery charge, a processor latch-up, or any abnormal voltage readings in the EPS. Additionally, during thruster firings, any abnormal data readings from the thruster sensors will lead to a switch to safe mode. In safe mode, the spacecraft will shut down its thruster,

set its radio to receive mode, and sun point. It will also cancel all currently scheduled thruster firings, so that ground station operators have a chance to review data before subsequent firings. Safe mode will be exited either when all system health data is in its nominal range, or when the spacecraft is commanded to return to normal operations by the ground station.

The spacecraft's software is also designed to protect it against a sudden change in the attitude estimate, which may occur under conditions such as stray light entering the star camera. In these situations the spacecraft will enter an attitude error wait, in which thruster firing and radio transmission will be stopped (if applicable), and the spacecraft will not attempt to control its attitude (because the data this would be based upon may be faulty). Once the attitude estimate shows a continuous trajectory, the spacecraft will enter safe mode.

Spacecraft Software State Diagram (1 of 2)

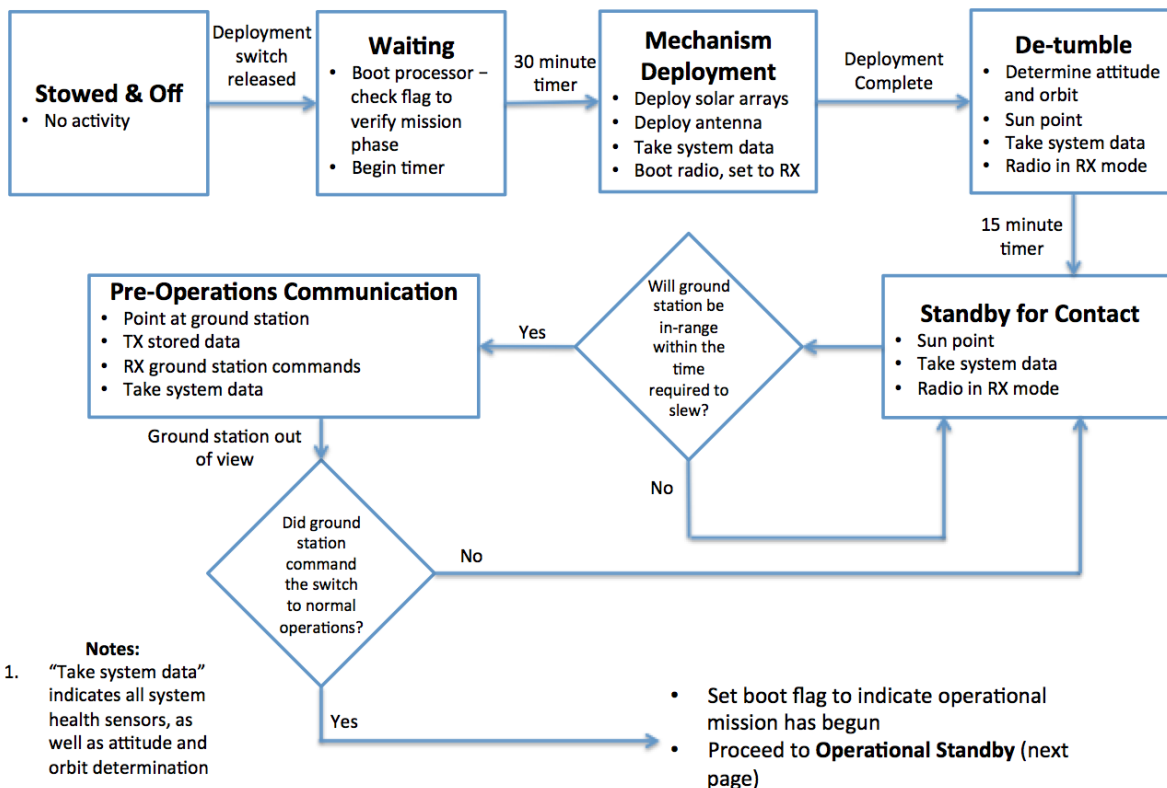


Figure 9.6: Spacecraft software state table (1 of 2). Shows beginning-of-life.

The ground station software is significantly simpler than that for the spacecraft. Its purpose is to handle communications during passes. It will be developed in ruby, and

Spacecraft Software State Diagram (2 of 2)

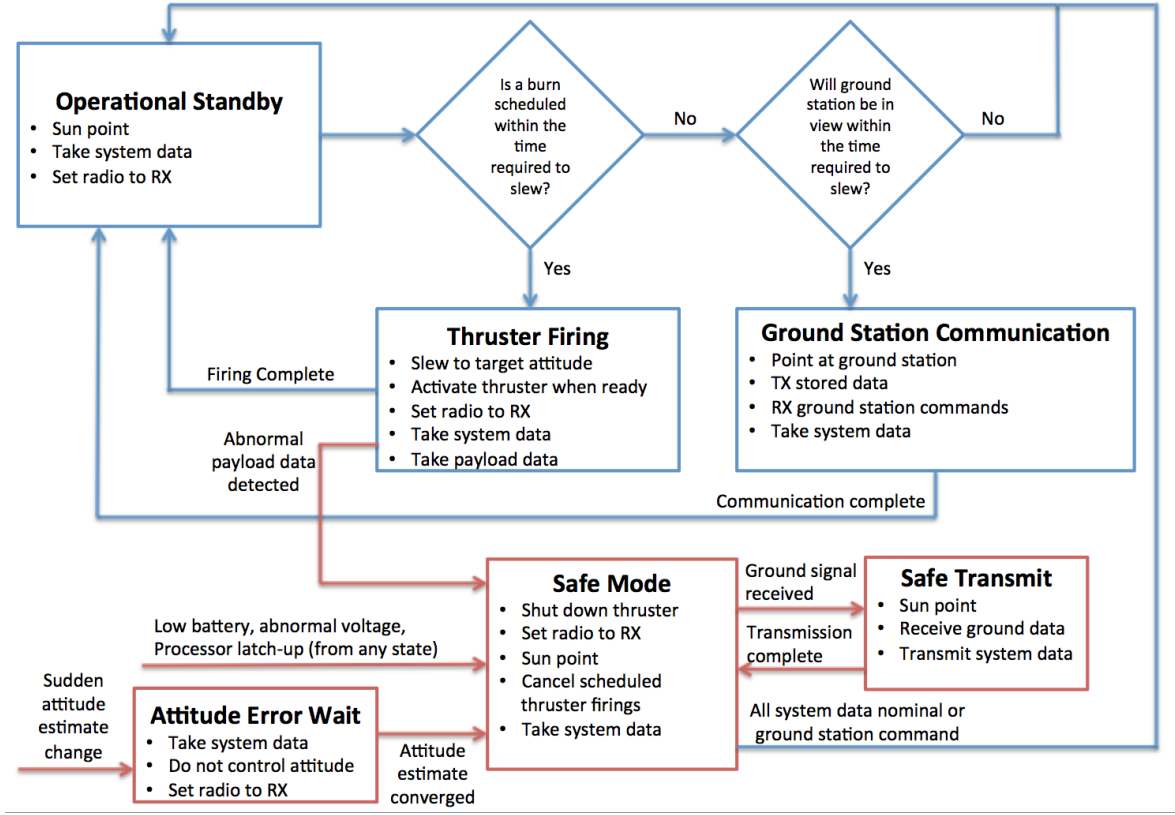


Figure 9.7: Spacecraft software state table (2 of 2). Shows operational mission.

based on Ball Aerospace's COSMOS, a free and open-source spacecraft ground station software [87].

Figure 9.8 shows the ground station software state diagram. During standby mode, the ground station software will monitor the orbital position of the spacecraft, based on the two line element (TLE) provided by NORAD [88]. When the spacecraft is predicted to be above the horizon, the software will command the ground station antenna to track its position. It will then receive and record any transmitted data from the spacecraft, and transmit any scheduled command uploads.

Because TigerSat has propulsion capabilities, ground control system will be designed to meet standard best practices for spacecraft cybersecurity [89]. These measures will include encrypting uplink commands, ensuring proper security on all ground station computers, and controlling physical access to the ground station terminals.

Ground Station Software State Diagram

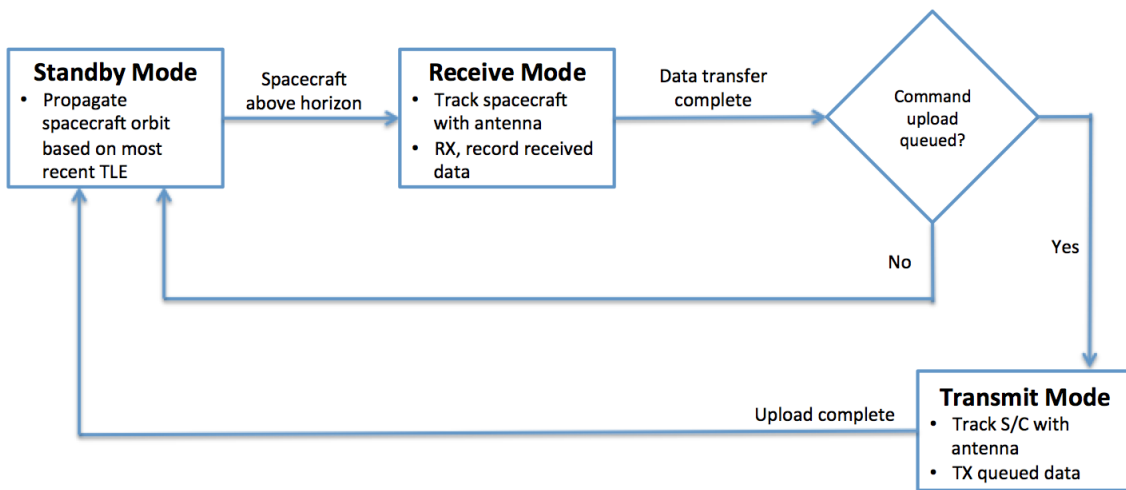


Figure 9.8: Ground station software state table.

9.7 Testing

In addition to the integrated system testing that will be done for the spacecraft, subsystem-level testing will be conducted on the telecommunications equipment. Component-level testing for the processor, transceiver, and antenna is conducted by the vendors and so will not be repeated. The main hardware test will be a line-of-sight radio test to ensure robust communication between the ground station and the transceiver from as great a distance as possible. Software tests run will be as follows:

- Command execution: receive commands from ground station using umbilical connectors and execute appropriately.
- “Day-in-the-life” test: step through mission operations using simulated sensor data.
 - Verify system operation timeline after deployment (no RF transmission for 45 minutes, etc.).
 - Generate abnormal sensor data and ensure appropriate aborts and safe mode are triggered and data is recorded accurately.
 - Test data dump to ground station.
 - Test transmission activation during flyovers based on simulated GPS data.

9.8 Conclusion

The communications and data handling subsystem will consist of a ground station operated by the Princeton Physics Department, a duplex UHF/VHF transceiver and antenna on-board the spacecraft, and an integrated on-board-computer and GPS bundle that will also assist in orbit determination. The selected on-board components are summarized in Table 9.5. The spacecraft software, the architecture of which has been described above, will be developed in C++ and be based on KubOS. All aspects of the system have been designed to minimize complexity and integrate as many parts as possible while meeting mission requirements.

Transceiver	GOMSpace NanoCom AX100
Antenna	EnduroSat UHF Antenna
Computer	Clyde Space OBC + GPS Bundle

Table 9.5: Summary of on-board C&DH components.

Chapter 10

Thermal

10.1 Overview

The main role of the thermal team is managing the temperatures of critical components within the satellite such that they lie within their operating range. Thermal control is critical to the survival of the mission since the space environment in which the CubeSat lies is extremely harsh and extreme. Due to its low orbit, the CubeSat will experience a wide range of temperature swings throughout its orbit as it travels between direct sunlight and the Earth's eclipse, all of which must be managed either through passive or active means. After extensive thermal analysis and weighing in factors such as mass, power consumption, and complexity, a completely passive thermal management system was designed for the CubeSat mission. This passive thermal control consists of an array of different surface finish patterns to provide effective thermal properties necessary to keep the sensitive CubeSat components within their operating temperature range.

10.2 Design Assumptions

Design assumptions govern the geometry of the CubeSat, its orbit, material composition, the surrounding space environment, and power transfer calculations. Specifically, the CubeSat is assumed to be manufactured to industry specifications without substantial geometric flaws. Furthermore, thermal analyses require that accurate thermal capacities and masses of materials comprising the CubeSat are known. To this end, each subsystem was assumed to be represented completely by the predominant material of which it is comprised. The CubeSat was also assumed to radiate to 0 K, which is very near the

cosmic background radiation temperature.

The CubeSat is assumed to revolve about the Earth between orbit altitudes of 400 km and 600 km, and with some arbitrary beta angle, defined as the angle which exists between the solar vector and the orbit plane. By considering these extreme conditions, which encompass all possible orbit characteristics of the CubeSat, the following thermal analyses are therefore ensured to yield results which include all possible thermal conditions of the CubeSat.

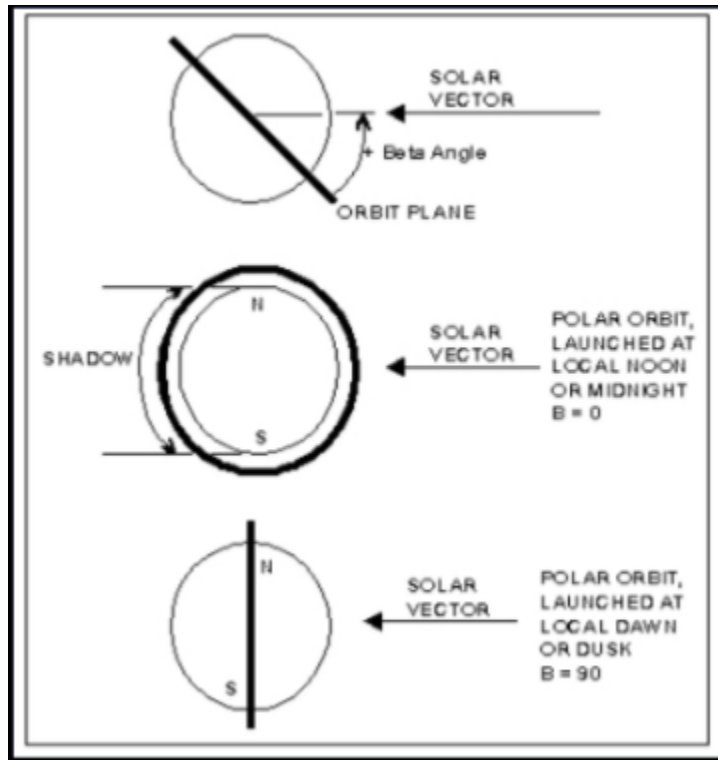


Figure 10.1: Visualization of Beta Angle

Another assumption made was that the chassis acts as a sufficient heat sink for all of the components mounted to it. Thus, a thermal model considering the various components in the chassis separately can model the temperature of the entire chassis as one value, as the chassis will effectively facilitate any thermal discrepancies such that they are negligible.

A further assumption which was made is that the thruster should not be treated as a separate node in energy transfer calculations due to its low duty cycle, which has an irregular impact on temperature. This assumption will be further discussed and validated in sections below.

10.3 Design Requirements

The temperature of each separate component of the CubeSat must stay within its individual operating temperatures during normal operation to ensure peak performance, and must stay within survival temperatures even when not powered to prevent damage or degraded performance. The figure below shows the operating and survival temperatures of each major component of the satellite. These numbers were sourced directly from the specifications sheet provided by the manufacturer of each component. In the event that this information was not available, a temperature range was referenced from SMAD as an effective approximation.

	Operating Min	Operating Max	Survival Min	Survival Max
Batteries	-15 °C	30 °C	-20°C	50°C
Solar Arrays	-85°C	100°C	-200°C	115°C
Electronics	-20°C	60°C	-20°C	60°C
ACS	-40°C	85°C	-50°C	100°C
Antenna	-100°C	100°C	-120°C	120°C

Operating Range : -15°C to 30°C

Survival Range : -20°C to 50°C

Figure 10.2: Temperature Requirements of Various Components

Due to the wide operating temperature range of the solar panels compared to the rest of the components, the thermal requirements of the CubeSat were divided into two sections, one comprising only the solar panels, and the other comprising all other components collectively housed in the chassis. From the figure above, one can see that the solar panels have an operating temperature range of -85 - 100 °, and that the chassis must collectively be kept within -15 - 30 ° to satisfy the narrower operating temperature range of its subsidiary components.

10.4 Heat Sources

The environmental factors which influence the thermal power balance of the CubeSat include solar flux, Earth IR flux, and the energy flux from the Sun reflected off of the Earth. For each of these environmental sources, a corresponding minimum and maximum case exists for each given instantaneous orbit altitude, beta angle, and position of the CubeSat along its orbit.

	Min	Max
Environmental		
Solar Heat Flux [W/m]	1,323	1,414
Earth IR Flux [W/m]	218	257
Earth Albedo at 0 Beta []	0.23	0.3
Earth Albedo at 90 Beta []	0.5	0.57
Internal		
Electronics [W]	3	3
Heater [W]	0	0

Figure 10.3: Heat Sources

Ignoring the condition for which the satellite passes through the eclipse of the Earth (and therefore receives no direct or reflected solar flux), the minimum and maximum solar heat flux impeding the CubeSat are 1,323 W/m and 1,414 W/m, respectively, for orbit heights ranging from 400 k to 600 km. Given the same constraints, the minimum and maximum Earth IR flux impeding the CubeSat are 218 W/m and 257 W/m, respectively. Further, the Earth albedo, a measure of surface reflectivity, for a zero beta angle orbit between an orbit height of 400 km and 600 km ranges from 0.23 to 0.3, and from 0.5 to 0.57 for a 90° beta angle orbit.

Internal sources of heat include general electronics, which produce approximately 3 W of power within the chassis. A heater would also contribute to this number if an active thermal management system was necessary to ensure component survivability and op-

eration, however thermal analyses to be discussed in subsequent sections confirmed that a heater is not necessary. As always, the best form of thermal management system is a passive thermal management system, as no further data or communication requirements are necessary to monitor the transient implementation of such a device. Additionally, greater CubeSat weight savings are realized by not utilizing a heater. Finally, any energy flux emanating from the thruster while in operation would also contribute to internal sources of heat. This metric is discussed in greater detail in the following sections.

10.5 Orbit Analysis

10.5.1 Single-Nodal Steady-State

A single-nodal steady-state analysis was performed to provide a greater preliminary understanding of the influence environmental and internal energy sources had on the thermal management needs of the CubeSat. This level of analysis assumed the entire spacecraft as a single node in space where the total power entering the spacecraft (sourced from its environment plus the power generated by the spacecraft internally, as described above) was balanced by the total power leaving the spacecraft via radiation. More specifically, the energy radiated by a surface depends on its temperature and emissivity. Rearranging this expression to solve for temperature, a steady state temperature for the overall spacecraft can be calculated. The relevant equations governing this equilibrium are presented below:

$$Q - W = \Delta U \quad (10.1)$$

$$Q_{env} + Q_{int} = Q_{out} \quad (10.2)$$

$$Q_{out} = \sigma T^4 \sum_{i=1}^n \epsilon_n A_n \quad (10.3)$$

$$T = \sqrt[4]{\frac{\alpha S [A_p + R A_R] + \epsilon I R A_{IR} + Q_{int}}{\sigma T^4 \sum_{i=1}^n \epsilon_n A_n}} \quad (10.4)$$

where Q is the net heat entering the CubeSat, W is the net work done by the CubeSat, U is the internal energy of the CubeSat, Q_{env} is the net heat from environmental sources, Q_{int} is the net heat from internal sources, Q_{out} is the net heat radiating out to space, σ is the Stephen-Boltzmann constant, T is temperature, ϵ is surface emissivity, α is surface absorption, S is solar flux, A_p is surface area receiving solar flux, R is albedo, A_R is

surface area receiving reflected solar flux, IR is infrared energy flux, and A_{IR} is surface area receiving IR.

Since the temperature of the spacecraft depends highly on the orbit path, a "hottest case" and "coldest case" analysis were each conducted to ensure that all possible thermal management scenarios of the CubeSat are enveloped by the analysis. The CubeSat reaches the greatest temperatures when in an orbit with a beta angle of 90 degrees, as the CubeSat is in direct sunlight for the full orbit, and the coldest temperatures when in a 0 beta angle orbit, which spends maximal time in the eclipse of the Earth.

Once scripts of the steady state temperature calculations were utilized to evaluate both of these extreme cases, different thermal control methods were implemented to attempt to align the resulting equilibrium temperatures within the operating temperature range of the components on board the CubeSat. One main thermal control parameter which was investigated was the surface finish of the satellite, which alters the absorptivity and emissivity of the surface and subsequently the final steady-state temperature. Surface absorptivity determines the fraction of impeding energy flux that is absorbed by a surface. Surface emissivity determines the fraction of thermal radiation energy leaving a surface. Both of these metrics greatly impact the hot and cold case calculations, as the total CubeSat energy balance depends significantly on these values. Despite this effort, the operating temperature ranges of the components were still not satisfied, so internal heating was considered to rectify the issue. However, the required power necessary to sufficiently operate the heater and satisfy the thermal requirements could not be realized due to demanding power budget constraints. Thus, the conclusion was made that a single-nodal steady-state analysis is insufficient in providing an optimal thermal control method and further analysis must be conducted.

10.5.2 Multi-Nodal Steady-State

The subsequent thermal analysis iteration conducted was a multi-nodal steady-state condition. For this investigation, the chassis and solar arrays were treated as the only two subsections of the CubeSat. They would each be at their individual uniform temperature throughout, and interact with one another via radiation and conduction means only (convection does not play a substantial role in vacuum). Conduction calculations between the chassis and solar arrays follow from the governing equation:

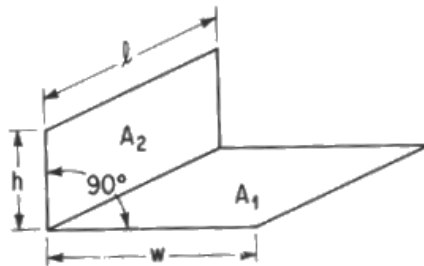
$$Q = k \frac{\Delta T}{\Delta x} \quad (10.5)$$

where k is the material thermal conductivity, T is temperature, and x is the distance over which the conduction acts.

However, accurately determining the influence of radiative energy transfer requires the utilization of view factors. View factors are numbers ranging from zero to one which scale the total power transfer to reflect the fraction of radiation leaving one surface which impedes a different surface of interest. In the case of this specific analysis, the solar arrays and chassis represent two finite rectangles of the same length, having one common edge and an interior angle of 90 degrees between each other. Thus, the relevant equation for the view factor calculation governing this geometry is:

C-14: Two finite rectangles of same length, having one common edge, and at an angle of 90° to each other.

Reference: [Hottel, 1931](#); [Hamilton and Morgan](#); [Byun, 1999](#).



Definitions: $H=h/l$ $W=w/l$

Governing equation:

$$F_{1-2} = \frac{1}{W\pi} \left(W \tan^{-1} \frac{1}{W} + H \tan^{-1} \frac{1}{H} - \sqrt{H^2 + W^2} \tan^{-1} \sqrt{\frac{1}{H^2 + W^2}} \right. \\ \left. + \frac{1}{4} \ln \left[\frac{(1+W^2)(1+H^2)}{1+W^2+H^2} \left(\frac{W^2(1+W^2+H^2)}{(1+W^2)(W^2+H^2)} \right)^{W^2} \left(\frac{H^2(1+H^2+W^2)}{(1+H^2)(H^2+W^2)} \right)^{H^2} \right] \right)$$

Figure 10.4: View factor between solar panels and chassis

This view factor expression evaluates to 0.265 for the dimensions of the CubeSat introduced above, when considering that the solar arrays extend from two sides of the chassis. Thus, 26.5% of the radiation emanating from the chassis impedes the solar arrays and vice versa.

Given the power balance between the chassis and solar arrays governed by conduction and radiation, plus environmental and internal heat fluxes as introduced in the Heat Sources section above, the multi-nodal steady-state analysis can now be fully investigated. The results yielded from this analysis highlight the significance of considering the chassis and solar arrays as separate components, as the two components resolved to drastically different steady-state temperatures. This is critical when one recognizes that the operating temperature range of the chassis is significantly disparate from that of the solar arrays. However, the hot and cold case steady-state temperatures of the chassis yielded from this analysis did not lie within its operating temperatures. Because passive thermal management systems are preferred to active ones, it was concluded that a transient, multi-nodal analysis would be necessary to further investigate this finding with the goal of not requiring a heater to satisfy operating temperature range requirements. The relatively short period of the CubeSat's orbit (< 2 hours), and the thermal capacity of the materials which comprise the chassis and solar arrays may help the CubeSat from reaching the unacceptable steady-state conditions calculated, thereby saving the mission the expense of leveraging a heater for an active thermal management system.

10.5.3 Multi-nodal transient analysis

The multi-nodal transient analysis operates similarly to the multi-nodal steady-state analysis, while also accounting for the amount of time it takes for components to heat up and cool down as the CubeSat transitions between the different thermal environments. Specifically, the thermal capacity of materials on-board the CubeSat determined how much the temperature of the chassis and solar arrays changed over a designated period of time and measured energy flux.

Part	Material	Thermal Conductivity [W/(m K)]	Specific Heat Capacity [J/(kg K)]
Chassis	Aluminum	204	921
Thruster	Steel	43	500
Electronics	Copper	401	385
Solar Panel	Gallium Arsenide	52	350
ACS	Polyurethanes	0.02	1450
Battery	Lithium	301	960

Figure 10.5: Thermal properties of various on-board materials

The governing equation for this analysis is as follows:

$$\frac{\delta Q}{\delta t} = mc \frac{\delta \Delta T}{\delta t} \quad (10.6)$$

where Q is heat, m is mass, c is specific heat, T is temperature, and t is time.

The orbit was divided into multiple segments, of which each had different environmental thermal heat fluxes based on the position of the satellite relative to the Earth and the Sun. Namely, the orbit consisted of segments for which the CubeSat (a) was in sunlight and received Earth IR radiation from the warmer, sunlit portion of Earth, (b) was in sunlight and received Earth IR radiation from the cooler, non-sunlit portion of Earth, and (c) was in the eclipse of the Earth. The duration of time for which the CubeSat was in each of these orbital segments depends on the orbital beta angle as well as the orbit height, which were both accounted for in the overarching energy balance computation.

Namely, for each second of the orbit, the different power fluxes going into and out of the satellite were calculated and any power imbalance was realized as an appropriate temperature change. This calculation was conducted over a duration of multiple orbits and the results were used to fine-tune necessary surface absorptivities and emissivities to develop a passive thermal management system. Once the desired absorptivity and emissivity values were determined, a striping pattern surface finish was chosen to achieve those values. This strategy of producing a striping pattern surface finish allows for a combination of surface properties found in different materials to be achieved when no single surface finishing material has the desired absorptivity and emissivity metrics. The resulting temperature range can be seen in Figures 10.6 and 10.7 below.

The lowest min is -13.9215 C.
The highest max is 26.2945 C.

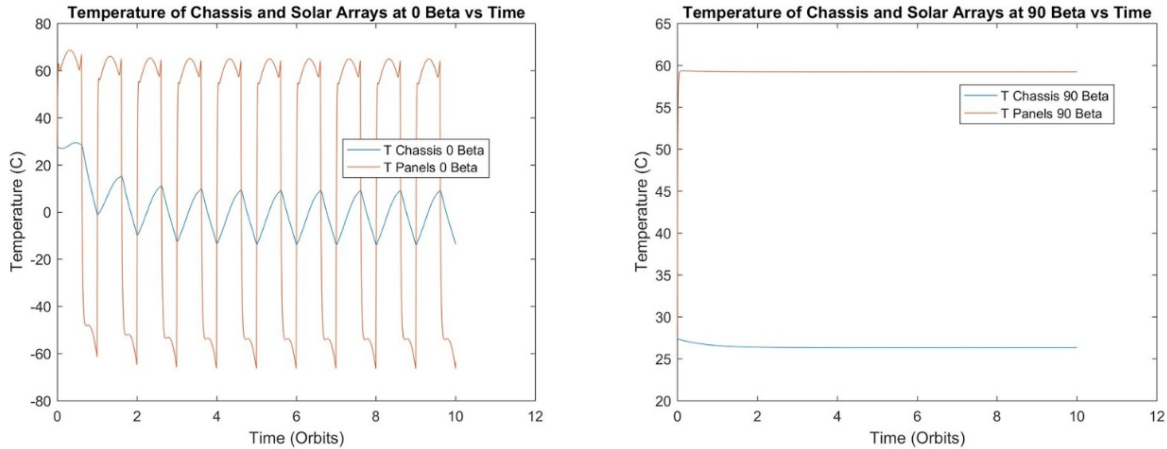


Figure 10.6: Multi-nodal Transient Analysis at 400km

The lowest min is -11.834 C.
The highest max is 26.2945 C.

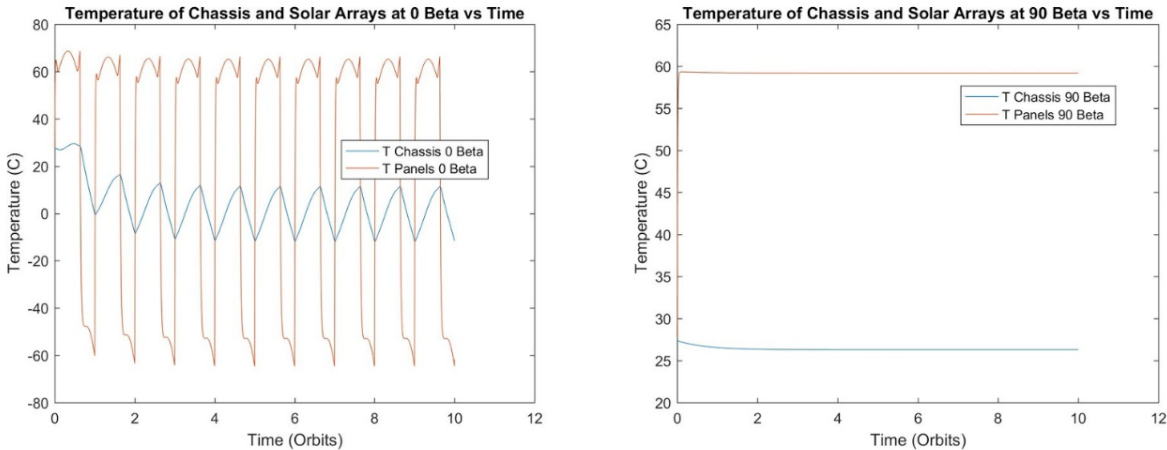


Figure 10.7: Multi-nodal Transient Analysis at 600km

10.6 Thruster Calculation

Recall that one of the assumptions made above is that the thruster will not be treated as a separate node in calculations due to its low duty cycle, resulting in irregular impacts on temperature. A more thorough analysis of the thruster is done to ensure that its ultimate thermal impact will not significantly affect the resulting temperature of the CubeSat.

Measures were taken to reduce the main two sources of heat transfer, radiation and conduction, between the thruster and surrounding chassis. A 30-layer multiple layer insulation (MLI) blanket composed of goldized Kapton will encapsulate the thruster to prevent radiative heat transfer. The MLI blanket will wrap around the thruster, with an open face extending to space at the rear of the chassis. The MLI blanket has an effective emittance of 0.5% due to its layer count, which implies that 99.5% of the impeding radiation is reflected back to the thruster. With this additional heat inflow, a subsequent power balance calculation was completed to determine the equilibrium temperature of the thruster during operation. This temperature was then utilized to determine how much energy propagates to the chassis via conduction. To minimize this conductive heat transfer, the material comprising the thruster-to-chassis connections was selected to be Garolite, which boasts an extremely low thermal conductance of 0.29 W / (m K). There will be a total of four cubic connections, with side faces measuring 1.25 cm².

Given these dimensions and relevant values, the amount of heat transferred from the thruster to the chassis totals approximately 4W during thruster operation. However, this quantity of energy transfer would consequently increase the hottest temperature case of the CubeSat chassis beyond the required operating temperature range of the batteries when the CubeSat is in view of the Sun. However, since this issue is only realized when the CubeSat is not in eclipse, it can be entirely avoided if the thruster is scheduled to fire only when it is within the shadow of the Earth.

Given that the CubeSat will only experience time in eclipse for a specific range of beta angles, further research was conducted to ensure that the mission objectives were still feasible given thruster firing only while in eclipse. The following figure shows the fraction of orbit spent in sunlight and eclipse per orbital beta angle.

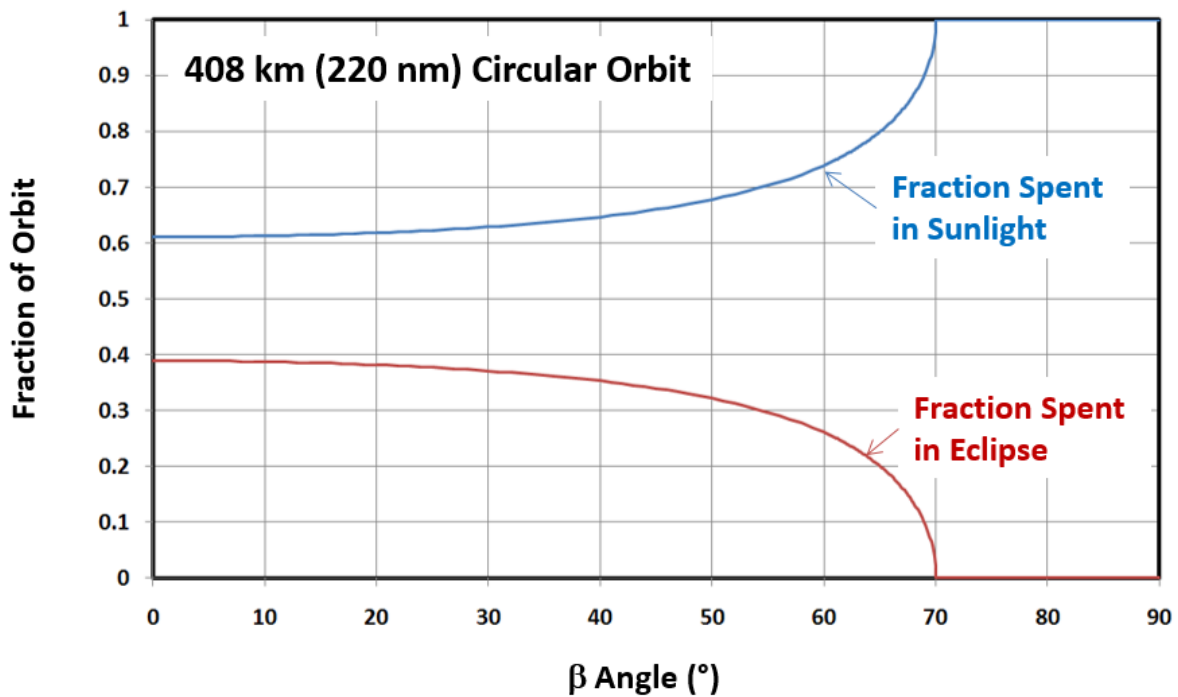


Figure 10.8: Effect of beta angle on eclipse shadow

Since an eclipse duration of longer than 10 minutes (the duration of thruster burn) is desired and the orbital period of the CubeSat is approximately 100 minutes, from Figure 10.8, it can be seen that the beta angle must be under 68° when firing. According to the following ISS data, this will only pose a problem for approximately six weeks over an arbitrary two year period, or about five percent of the time. Since the duty cycle of the thruster is sufficiently flexible, firing in only the eclipse should pose no issue for satisfying the mission objectives.

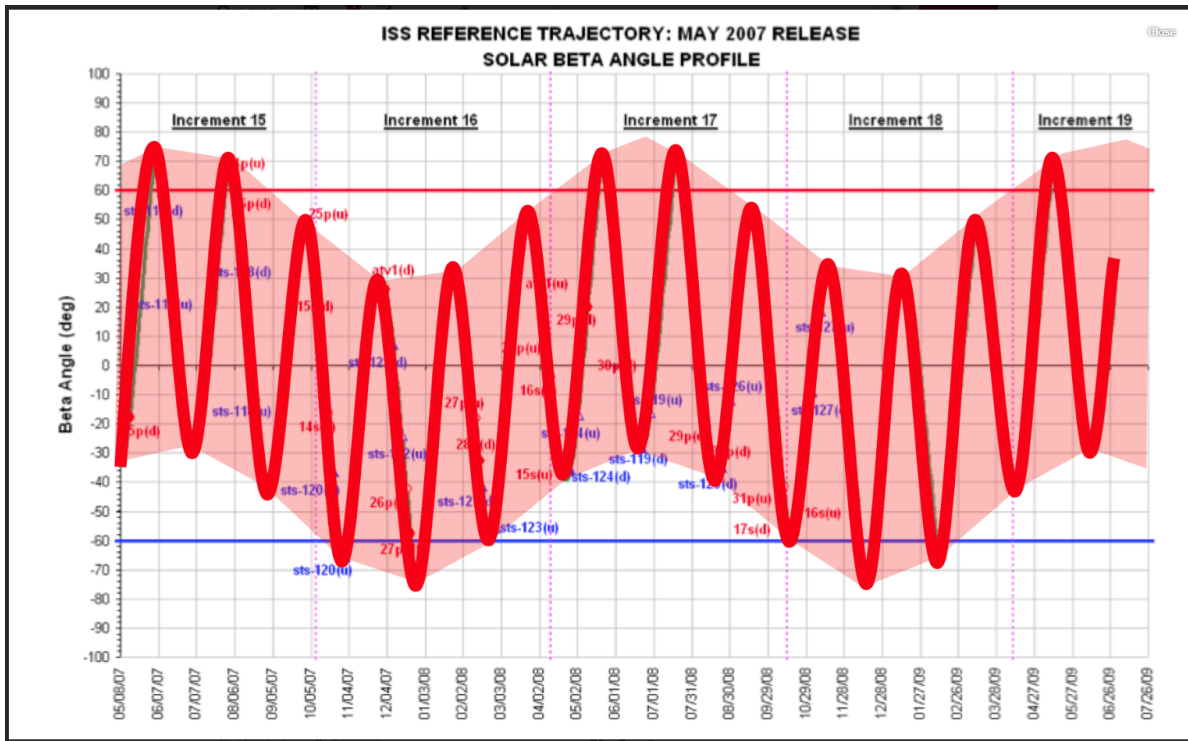


Figure 10.9: Beta angle as a function of time

10.7 Launch Temperature Transience

To determine the temperature of the CubeSat upon orbit injection, one must consider its chosen launch vehicle, any applicable climate control prior to launch, and the effects of radiation heating from the launch vehicle payload fairing to the payload for the duration of the launch.

The launch vehicle selected to deliver the CubeSat to space is the Falcon 9. Available data from prior Falcon 9 launches show that the Falcon 9 is air conditioned right until launch. This means that a steady state starting temperature of 21 °C can be assumed. A transient analysis was performed on the CubeSat while it is in transit, incorporating multiple worst-case assumptions, including a payload fairing temperature of 90 degrees Celsius (the highest temperature the payload fairing will reach throughout the entire flight) and direct radiative heating from the payload fairing to the CubeSat, which does not account for any insulating effects of the Nano Racks assembly. The result of this analysis can be seen in Figure 10.10 below:

The temperature of the CubeSat as it is ejected into orbit is 27.6498 C.

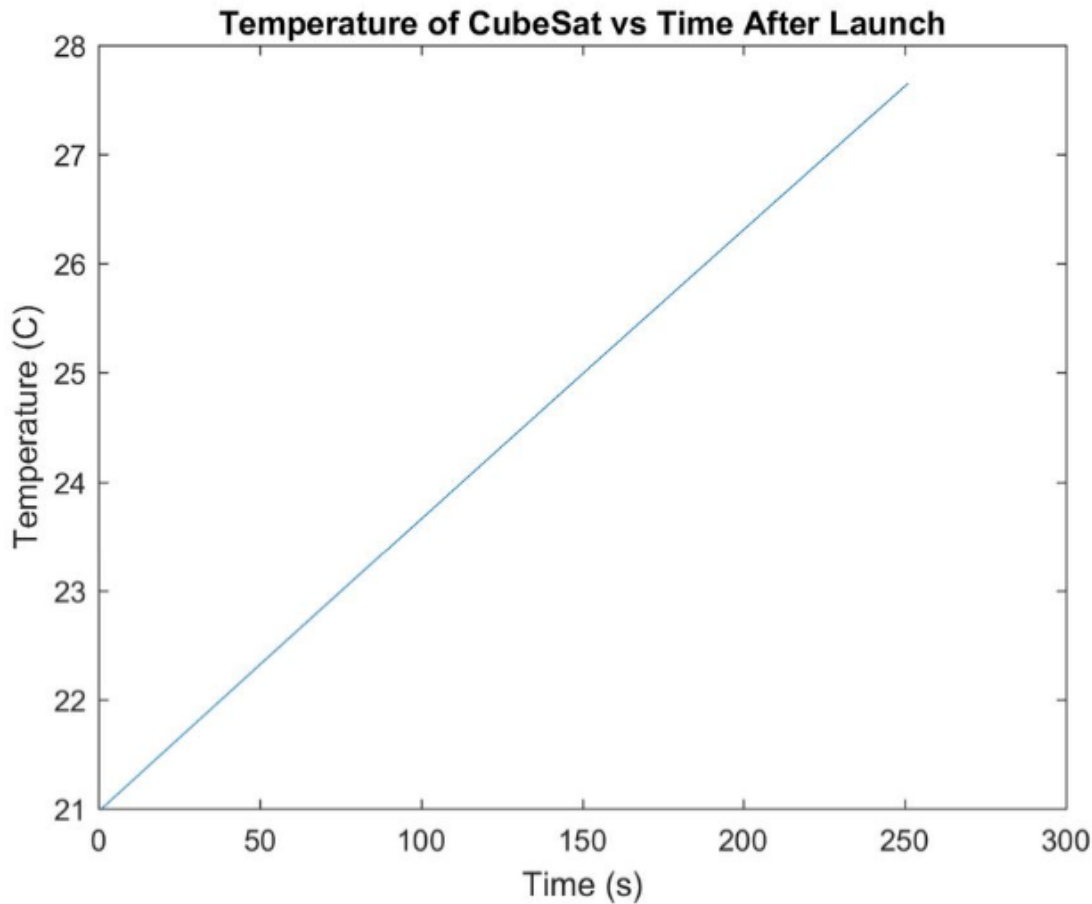


Figure 10.10: Beta angle as a function of time

10.8 Conclusion

The thermal management design of the CubeSat mission was successfully able to ensure that all components remain within their operating temperature range for the full lifetime of the mission. Further, this feat was able to be achieved while employing a strictly passive thermal management system, so no further data or communication requirements are necessary to monitor the transient implementation of an active system. Thruster operation must be restricted to when the CubeSat is in eclipse of the Earth, but this is a timing restriction which does not impact the feasibility of the mission objectives. The striping pattern surface finishes which satisfy all thermal requirements and will be

employed on the chassis and solar array surfaces are summarized neatly in the table below. Simply, the back of the solar arrays will be coated in magnesium/aluminum oxide paint, providing an area average absorptivity and emissivity of 0.505 and 0.885, respectively. All sides of the chassis will have an identical striping pattern comprised of approximately two-thirds 2 mm silver Teflon and approximately one-third vapor-deposited aluminum, providing an area average absorptivity and emissivity of 0.060 and 0.450, respectively.

Part	Material	Absorptivity	Emissivity	Area of Striping Pattern (%)	Area Avg. Absorptivity	Area Avg. Emissivity
Solar Array - Front	Gallium Arsenide	0.92	0.85	n/a		
Solar Array - Back	Magnesium/Aluminum Oxide Paint	0.09	0.92	n/a		
Solar Array					0.505	0.885
Chassis - Material 1	2 mm Silver Teflon	0.05	0.66	66.1		
Chassis - Material 2	Vapor-Deposited Aluminum	0.08	0.04	33.9		
Chassis					0.060	0.450

*Note: All sides of satellite chassis have an identical striping pattern.

Figure 10.11: Surface finish selection and striping pattern

Chapter 11

Bibliography

- [1] “Iss - orbit,” <http://www.heavens-above.com/orbit.aspx?satid=25544>. [Online]. Available: <http://www.heavens-above.com/orbit.aspx?satid=25544>
- [2] J. R. Wertz, D. F. Everett, and J. J. Puschell, *Space mission engineering: the new SMAD*. Microcosm Press, 2015.
- [3] “International reference ionosphere,” COSPAR, URSI, 2016. [Online]. Available: https://omniweb.gsfc.nasa.gov/vitmo/iri2016_vitmo.html
- [4] “Usa space debris environment, operations, and policy updates,” NASA, 2011. [Online]. Available: <http://www.unoosa.org/pdf/pres/stsc2011/tech-31.pdf>
- [5] W. J. Larson and J. R. Wertz, Eds., *Space Mission Analysis and Design*, 3rd ed. Microcosm, November 1999.
- [6] (2012, May) Process for limiting orbital debris. NASA. [Online]. Available: <https://standards.nasa.gov/file/2707/download?token=p6QZJZmj>
- [7] S. King, M. Walker, and C. Kluever, *Small Satellite LEO Maneuvers with Low-Power Electric Propulsion*. American Institute of Aeronautics and Astronautics, 2018/05/12 2008. [Online]. Available: <https://doi.org/10.2514/6.2008-4516>
- [8] (2018) State of the art small spacecraft propulsion. NASA. [Online]. Available: <https://sst-soa.arc.nasa.gov/04-propulsion>
- [9] (2015) Iodine hall thrusters. NASA. [Online]. Available: https://gameon.nasa.gov/gcd/files/2017/07/AISP_Hall-Thruster.pdf

- [10] (2008) The physics of spacecraft hall thrusters. University of Michigan. [Online]. Available: https://www.aps.org/units/dfd/meetings/upload/Gallimore_APSSDFD08.pdf
- [11] M. K. M. L. R. W. I. Joseph Homer Saleh, Fan Geng, “Electric propulsion reliability: statistical analysis of on-orbit anomalies and comparative analysis of electric versus chemical propulsion failure rates,” *arXiv:1706.10129 [physics.space-ph]*, June 2017. [Online]. Available: <https://arxiv.org/abs/1706.10129>
- [12] (2015) Iodine hall thruster. NASA. [Online]. Available: https://gameon.nasa.gov/gcd/files/2017/07/AISP_Hall-Thruster.pdf
- [13] (2015) Iodine hall thruster critical design review. NASA. [Online]. Available: <https://ntrs.nasa.gov/archive/nasa/casi.ntrs.nasa.gov/20150016535.pdf>
- [14] (2016) Busek bht-600 hall thruster. Busek. [Online]. Available: http://www.busek.com/index_htm_files/70000701%20BHT-600%20Data%20Sheet%20Rev-.pdf
- [15] (2015) Pressurized xenon propellant management system for the cubesat ambipolar thruster. NASA. [Online]. Available: <http://pepl.ingen.umich.edu/pdf/IEPC-2015-364.pdf>
- [16] S. Mauro. (2015) Thermal analysis of iodine satellite (isat) from preliminary design review (pdr) to critical design review (cdr). NASA. [Online]. Available: <https://ntrs.nasa.gov/archive/nasa/casi.ntrs.nasa.gov/20160009727.pdf>
- [17] (2000) Aliasing. Bruno A. Olshausen. [Online]. Available: <http://www.rctn.org/bruno/npb261/aliasing.pdf>
- [18] A. D. G. Brian E. Beal. (2002) Preliminary plume characterization of a low-power hall thruster cluster. University of Michigan. [Online]. Available: <https://ieeexplore.ieee.org/stamp/stamp.jsp?arnumber=25611>
- [19] (2018) Ammeter impact on measured circuit. All About Circuits. [Online]. Available: <http://www.dtic.mil/dtic/tr/fulltext/u2/a478729.pdf>
- [20] M. A. Noras. (2005) Ultra high impedance voltmeter for electrostatic applications. Industry Applications Conference. [Online]. Available: <https://ieeexplore.ieee.org/xpls/icp.jsp?arnumber=1518751&tag=1>

- [21] (2018) Low power consumption voltage monitor two wires digital volt meter. Wonmeter. [Online]. Available: http://www.wonmeter.com/036-dc-25032v-redbluegreen-led-digital-voltmeter-low-power-consumption-voltage-monitor-two-wires.html#.WvY_o2gvyU1
- [22] H. K. Alan R. Johnston. (1989) A miniaturized space-potential dc electric field meter. Jet Propulsion Laboratory. [Online]. Available: <https://ieeexplore.ieee.org/stamp/stamp.jsp?arnumber=25611&tag=1>
- [23] Temprel. (2018) How to choose a thermocouple. Temprel Sensors. [Online]. Available: <http://www.temprel.com/support/how-to-choose-thermocouple.aspx>
- [24] M. Mitchel. (2004) Implementing an ultra-low-power, single-chip thermocouple circuit with the msp430f423. Texas Instruments. [Online]. Available: <http://www.ti.com/lit/an/slaa218/slaa218.pdf>
- [25] (2008) Thermal characterization of a hall effect thruster. United States Air Force. [Online]. Available: <http://www.dtic.mil/dtic/tr/fulltext/u2/a478729.pdf>
- [26] (2010) Effect of anode temperature on hall thruster performance. Georgia Institute of Technology. [Online]. Available: <https://arc.aiaa.org/doi/pdf/10.2514/1.48028>
- [27] M. S. F. Center. (1992) Battery selection practice for aerospace power systems. NASA. [Online]. Available: http://www.klabs.org/DEI/References/design_guidelines/design_series/1221msfc.pdf
- [28] (2014) Lithium & solar power lifepo4. GWL Power. [Online]. Available: <http://gwl-power.tumblr.com/post/77599670684/faq-low-temperature-operation-what-is-the>
- [29] Pani. (2014) Silver zinc batteries. Electronics Tutorials. [Online]. Available: <https://electronicspani.com/silver-zinc-battery/>
- [30] W. S. Rosca, B., “Enhanced battery model including temperature effects,” *EVS27*, jan 2013. [Online]. Available: <https://www.narcis.nl/publication/RecordID/oai:tudelft.nl:uuid:21968309-2e90-4ee3-9b62-3fd178933fe9/uquery/Battery/id/20/Language/EN>
- [31] (2018) Eneloop battery lineup. Panasonic. [Online]. Available: <https://www.panasonic.com/global/consumer/battery/eneloop/lineup.html>

- [32] J. Salt. (2018) Understanding rc lipo batteries. RC Helicopter Fun. [Online]. Available: <https://www.rchelicopterfun.com/rc-lipo-batteries.html>
- [33] (2018) 40whr cubesat battery. ClydeSpace. [Online]. Available: <https://www.clydespace/products/49-40whr-cubesat-battery>
- [34] (2018) Nanopower. GOMSpace. [Online]. Available: <https://gomspace.com/Shop/subsystems/batteries/nanopower-bpx.aspx>
- [35] (2018) Intelligent protected lithium battery module with soc reporting (bm 2). Pumpkin Space Systems. [Online]. Available: http://www.pumpkinspace.com/store/p198/Intelligent_Protected_Lithium_Battery_Module_with_SoC_Reportin%28BM_2%29.html
- [36] (2014) Technical information of lg 18650hg2 (3.0ah). LG Chem: High Power Cell Development Team. [Online]. Available: <https://www.nkon.nl/sk/k/hg2.pdf>
- [37] (2018) Endurosat 3u solar panel. EnduroSat. [Online]. Available: https://endurosat-mxa7y13flfokttd.netdna-ssl.com/modules-datasheets/3U_Solar_Panel_User_Manual_Rev1.2.pdf
- [38] (2018) Clyde space triple deployable solar panels. Clyde Space. [Online]. Available: <https://www.clyde.space/products/76-triple-deployable-solar-panels>
- [39] (2017) Pumpkin price list. Pumpkin Space Systems. [Online]. Available: <http://www.pumpkininc.com/content/doc/forms/pricelist.pdf>
- [40] (2018) Deployable solar panels dsa/1a. CubeSat Shop. [Online]. Available: <https://www.cubesatshop.com/product/solar-panels/>
- [41] (2014) Ultravolt high-power c series datasheet. Advanced Energy. [Online]. Available: <https://www.advanced-energy.com/upload/File/UltraVolt/ENG-HPCSeriesDS-230-AA.PDF>
- [42] M. Nymand and M. Andersen, “High-efficiency isolated boost DC–DC converter for high-power low-voltage fuel-cell applications,” *IEEE Transactions on Industrial Electronics*, vol. 57, no. 2, pp. 505–514, feb 2010. [Online]. Available: <https://doi.org/10.1109/tie.2009.2036024>

- [43] S. Dwari and L. Parsa, “An efficient high-step-up interleaved DC–DC converter with a common active clamp,” *IEEE Transactions on Power Electronics*, vol. 26, no. 1, pp. 66–78, jan 2011. [Online]. Available: <https://doi.org/10.1109/tpel.2010.2051816>
- [44] R. N. Scott Sterling Arnold and A. Gordon-Ross. (2012) University of Florida, Gainsville. [Online]. Available: http://www.ann.ece.ufl.edu/pubs_and_talks/Aero12_arnold_ERB.pdf
- [45] P. L. J. H.-G. S. S. E. S. A. S. L. V. H. T. M. W. V. John Wang, Justin Purewal, “Degradation of lithium ion batteries employing graphite negatives and nickelecobaltemanganese oxide β -spinel manganese oxide positives: Part 1, aging mechanisms and life estimation,” *Journal of Power Sources*, vol. 269, no. 1, pp. 937–948, july 2014. [Online]. Available: <https://doi.org/10.1016/j.jpowsour.2014.07.030>
- [46] R. H. J. I. Weinberg, C.K. Swartz and R. Stater, “Radiation and temperature effects in gallium arsenide, indium phosphide, and silicon solar cells,” *Institute of Electrical and Electronics Engineers*, May 1987. [Online]. Available: <https://ntrs.nasa.gov/archive/nasa/casi.ntrs.nasa.gov/19870012665.pdf>
- [47] Triple Deployable Solar Panels. Clyde Space. [Online]. Available: <https://www.clyde.space/products/76-triple-deployable-solar-panels>
- [48] Deployable solar panels DSA/1A. CubeSatShop. [Online]. Available: <https://www.cubesatshop.com/product/solar-panels/>
- [49] 3U Solar Panel X/Y MTQ. Endurosat. [Online]. Available: <https://www.endurosat.com/products/cubesat-3u-solar-panel-x-y-mtq/>
- [50] eXtendable Solar Array System. University of Michigan. [Online]. Available: <https://deepblue.lib.umich.edu/bitstream/handle/2027.42/83636/AIAA?sequence=1>
- [51] PMDSAS 7-panel, 56 cell Solar Array. Pumpkin Space. [Online]. Available: <http://www.pumpkininc.com/content/doc/forms/pricelist.pdf>
- [52] Deployable Articulating Array. Composite Technologies Development, Inc. [Online]. Available: http://mstl.atl.calpoly.edu/~bklofas/Presentations/SummerWorkshop2013/Turse_Deployable_Array.pdf
- [53] Trade Study. MechaniCalc. [Online]. Available: <https://mechanicalc.com/reference/trade-study>

- [54] (2018) Hold down & release mechanisms. NEA Electronics, Inc. [Online]. Available: <http://www.neaelectronics.com/products/hold-down-and-release-mechanisms/>
- [55] (2014) Thermal knife cutting. European Space Agency. [Online]. Available: https://www.esa.int/spaceinimages/Images/2014/03/Thermal_knife_cutting
- [56] J. Munder, “Introduction to spacecraft mechanisms,” 2018.
- [57] T. P. Sarafin, Ed., *Spacecraft Structures and Mechanisms*. Microcosm, 2011.
- [58] J. Carnahan. (2013) Cubesat standard updates. California Polytechnic State University. [Online]. Available: http://mstl.atl.calpoly.edu/~bklofas/Presentations/SummerWorkshop2013/Carnahan_CubeSat_Standard_Update.pdf
- [59] “Falcon 9 user’s guide,” SpaceX, Oct. 2015. [Online]. Available: http://www.spacex.com/sites/spacex/files/falcon_9_users_guide_rev_2.0.pdf
- [60] (2018) Aluminum 6061-t6 specifications. Aerospace Secifications Metals Inc. [Online]. Available: <http://asm.matweb.com/search/SpecificMaterial.asp?baseNum=ma6061t6>
- [61] S. R. Staring and J. Eterno, *Attitude Determination and Control Systems*. Microcosm Press, 2011, pp. 1–33.
- [62] Mai-100 adacs miniature 3-axis reaction wheel & attitude determination and control system for cubesat kit nanosatellites. Pumpkin Inc. [Online]. Available: http://www.cubesatkit.com/docs/datasheet/DS_CSK_ADACS_634-00412-A.pdf
- [63] Imi-200 miniature 3-axis adacs product specification. IntelliTech Microsystems Inc. [Online]. Available: http://www.ati-space.com/ATI.files/11_index.files/IMI-20020Specification.pdf
- [64] Xact. Blue Canyon Technologiess. [Online]. Available: <http://bluecanyontech.com/xact/>
- [65] J. Peraire and S. Widnall. (2008) Lecture l26- 3d rigid body dynamics: The inertia tensor. [Online]. Available: <https://pdfs.semanticscholar.org/d2b5/e126c3d4bd54e39ee134b1cc28227b99a2b8.pdf>

- [66] J. Agolli, J. Gadoury, and A. Rathbun. (2017) Design and analysis of the sphinx-ng cubesat. [Online]. Available: <https://pdfs.semanticscholar.org/d2b5/e126c3d4bd54e39ee134b1cc28227b99a2b8.pdf>
- [67] T. Flatley, W. Morgenstern, A. Reth, and F. Bauer, “A b-dot acquisition controller for the radarsat spacecraft,” in *NASA conference publication*. NASA, 1997, pp. 79–90.
- [68] A. Cortiella, D. Vidal, J. Jane, E. Juan, R. Olive, A. Amézaga, J. F. Munoz, P. V. H. Carreno-Luengo, and A. Camps. (2017) Cat-2: Attitude determination and control system for a gnss-r earth observation 6u cubesat mission.
- [69] X. Xia, S. Wu, G. Sun, T. Wang, Z. Wu, Y. Bai, W. Chen, and Z. Mu, “Magnetic-based attitude control scheme for cubesat,” in *IEEE Chinese Guidance, Navigation and Control Conference*. IEEE, 2016, pp. 133–139.
- [70] J.-F. Tregouet, D. Arzelier, D. Peaucelle, and C. Pittet. (2015) Reaction wheels desaturation using magnetorquers and static input allocation. IEEE.
- [71] B. Klofas. (2018) CubeSat Communications System Table. [Online]. Available: <https://www.klofas.com/comm-table/>
- [72] Eyestar Comm Systems. Near Space Launch. [Online]. Available: <https://near-space-launch.myshopify.com/collections/comm-solutions>
- [73] (2018) Eyestar-d2e. Near Space Launch. [Online]. Available: <https://nearspacelaunch.com/product/eyestar-d2/>
- [74] NanoCom AX100. GOMSpace. [Online]. Available: <https://gomspace.com/Shop/subsystems/communication/nanocom-ax100.aspx>
- [75] UHF Antenna User Manual. EnduroSat. [Online]. Available: https://endurosat-mxa7y13fkfokttd.netdna-ssl.com/modules-datasheets/UHF_Antenna_User_Manual_Rev1.3.pdf
- [76] NanoCom ANT2000. GOMSpace. [Online]. Available: <https://gomspace.com/Shop/subsystems/communication/nanocom-ant2000.aspx>
- [77] NanoCom SR2000. GOMSpace. [Online]. Available: <https://gomspace.com/Shop/subsystems/communication/nanocom-sr2000.aspx>

- [78] P. Fortescue, G. Swinerd, and J. Stark, *Spacecraft Systems Engineering*. New York, NY: Wiley, 2011.
- [79] C. Levit and W. Marshall, “Improved orbit predictions using two-line elements,” *Advances in Space Research*, vol. 47, no. 7, pp. 1107 – 1115, 2011. [Online]. Available: <http://www.sciencedirect.com/science/article/pii/S0273117710006964>
- [80] B. E. Mendez, “Link budget for ntnu test satellite,” Master’s thesis, Norwegian University of Science and Technology - Trondheim, 2013.
- [81] (2018) Cubecomputer nanosatellite OBC. CubeSpace. [Online]. Available: <https://cubespace.co.za/cubecomputer/>
- [82] (2018) ISIS on board computer. Innovative Soltions in Space. [Online]. Available: <https://www.cubesatshop.com/product/on-board-computer/>
- [83] (2018) Clyde space on board computer + GPS bundle. Clyde Space. [Online]. Available: <https://www.clyde.space/products/7-nanosatellite-on-board-computer-gps-bundle>
- [84] J.-M. Irazabal and S. Blozis. (2003) I²C manual. Philips Semiconductors. [Online]. Available: <https://www.nxp.com/docs/en/application-note/AN10216.pdf>
- [85] G. Becke, C. Borgert, S. Corrigan, and F. Dehmelt. (2004) Comparing bus solutions. Texas Instruments. [Online]. Available: <https://www.lammertbies.nl/download/ti-appl-slla067a.pdf>
- [86] M. Culpepper, T. Browder, and J. Hamner. (2018) Kubos linux. KubOS. [Online]. Available: <http://www.kubos.com/kubos/>
- [87] R. Melton. (2018) Cosmos. Ball Aerospace. [Online]. Available: <http://cosmosrb.com/docs/home/>
- [88] T. S. Kelso. (2018) Norad two-line element sets. CelesTrak. [Online]. Available: <https://www.celestak.com/NORAD/elements/>
- [89] L. J. Cheney, “Development of safety standards for cubesat propulsion systems,” Master’s thesis, California Polytechnic State University San Luis Obispo, 2014.

Appendix A

Testing Procedures

A.1 Testing Procedure Overview

A.1.1 Subsystem Testing

- Mechanical
- Electrical Power Systems
- Communications and Data Handling
- Attitude Determination and Control System
- Propulsion/Payload

A.1.2 Integration Testing

- Fit check
- Satellite deployment test
- Mechanism deployment test
- Communication test
- ADCS test

A.1.3 Environmental Testing

- Vibration
- Shock
- Thermal Vacuum Bake Out

- Quasi-static Load
- Visual Inspection

A.2 Subsystem Testing Procedures

A.2.1 Mechanical

- Verify that structure is manufactured to specifications.
- Verify the function and reliability of deployable mechanisms individually

A.2.2 Electrical Power Systems

- Check all electrical connections.
- Verify proper function of all electronic components.
- Perform battery charging and discharging while testing thruster load.
- Verify proper function of solar panels by testing battery charging.

A.2.3 Communications and Data Handling

- Command execution: receive commands from ground station using umbilical connectors and execute appropriately.
- "Day-in-the-life" test: step through mission operations using simulated sensor data.
 - Verify system operation timeline after deployment (no RF transmission for 45 minutes, etc.).
 - Generate abnormal sensor data and ensure appropriate aborts and safe mode are triggered and data is recorded accurately.
 - Test data dump to ground station.
 - Test transmission activation during flyovers based on simulated GPS data.

A.2.4 Attitude Determination and Control System

- "Day-in-the-life" test: Ensure software performs proper mission operation based on simulated inputs.

- Verify system operation for initial detumbling and location acquisition.
- Test sun-pointing, thrust-pointing, and nadir-pointing operation.
- Verify proper slews and reaction wheel desaturation operation.

A.2.5 Propulsion/Payload

- Test proper function of thruster independent from satellite.
- Take thrust and sensor measurements for verification of physical relationships and verification of payload subsystem.

A.3 Integration Testing Procedures

A.3.1 Fit Check

- Verify assembly of all components inside chassis.
- Ensure proper connection of all components.
- Verify total mass and center of mass of assembled satellite.
- Check that assembled satellite fits inside the deployer.

A.3.2 Satellite Deployment Test

- Ensure satellite dispenses smoothly from the container.
- Ensure proper functions of all switches and deployer/CubeSat interfaces.

A.3.3 Mechanism Deployment Test

- Verify mission operations by simulated deployment.
 - Ensure reliable antenna deployment.
 - Ensure reliable solar panel deployment.

A.3.4 Communication Test

- Perform integrated line-of-sight radio test to ensure robust communication.
- Perform subsystem software tests again.

A.3.5 ADCS Test

- Perform subsystem software tests again.

A.4 Environmental Testing Procedures

Perform Prototypical Testing on Flight Unit per NASA LSP standards B.1 and per dispenser standards B.2.

A.4.1 Vibration

- Testing performed on CubeSat and Dispenser system.
- Qualify by application of random vibration at Max Predicted Environment (MPE) + 3 dB for 2 minutes on each of 3 axes.
- Qualify by application of sinusoidal vibration at 1.25 x MPE.

A.4.2 Shock

- Testing performed on CubeSat and Dispenser system.
- Qualify by application of MPE + 3 dB, 1 time in both directions of 3 axes.

A.4.3 Thermal Vacuum Bake Out

- Testing performed on CubeSat only.
- Dwell for minimum 3 hours at minimum temperature of 70°C and vacuum of 1×10^{-4} Torr.

A.4.4 Quasi-static Load

- 1.1 x Limit load with respect to material yield strength with no detrimental yielding of test article.
- 1.25 x Limit load with respect to material ultimate strength with no structural failure of test article.

A.4.5 Visual Inspection

- A final visual inspection will be performed to ensure no part of the CubeSat protrudes beyond limits or will interfere with mechanisms.

Appendix B

External Requirements

B.1 NASA-LSP-REQ-317



National Aeronautics and Space Administration
John F. Kennedy Space Center, Florida

LSP-REQ-317.01
Revision B

Launch Services Program

Launch Services Program Program Level Dispenser and CubeSat Requirements Document

Approved: C.P. Dool
Amanda M. Mitskevich
Manager, Launch Services Program

Date: 30 JAN 14

RECORD OF REVISIONS		
REV	DESCRIPTION	DATE
Basic	Basic Issue	July 24, 2009
A	ERB-09-102-2(7/7/2011): <ol style="list-style-type: none"> 1. Update 6.2.2 to remove CubeSat structural qualification requirement, 2. Update 6.2.3 and 6.3.3 to allow any sized CubeSats between 1U and 3U, 3. Update Table 1 for clarity, 4. Editorial corrections. 	October 13, 2011
B	PRCB 7/12/2013 <ol style="list-style-type: none"> 1. Update 5.1.12 to allow waivers per LSP-P-317.01 PRCB 11/15/2013 - ERB-09-102-3 (7/11/13) <ol style="list-style-type: none"> 1. Changed all instances of "PPOD" to "Dispenser" 2. Update 6.2.4 to allow CubeSat pressure containers 3. Update 6.2.9 to allow CubeSat real time clocks 4. Editorial Corrections PRCB 12/13/2013 – ERB-09-102-4 Reconvene <ol style="list-style-type: none"> 1. Update 6.2.3 to increase CubeSat upper size limit to 6U. 2. Update 6.2.1 CubeSat T-Vac not required if specified by LSP 3. Update 6.2.11 to 3 inhibits for RF Transmission. This change is effective for CubeSat Launch Initiative call 6 and subsequent calls. 4. Terminology Clarification pressurant to "contents" 	January 30, 2014

Table of Contents

1. Introduction.....	4
2. Applicable Documents.....	5
3. Definitions.....	6
4. Mission Objective.....	7
5. Programmatic Requirements.....	7
6. Program Technical Requirements.....	8

1. Introduction

1.1. Purpose

The purpose of this document is to define the Launch Services Program (LSP) program level and technical requirements placed on containerized CubeSat dispenser and Picosatellite (CubeSats) satellites for integration on NASA LSP ELV mission. These requirements are to ensure no increase in baseline risk to the Primary Mission. The requirements within this document are generic and independent of the Launch Vehicle (LV). The technical requirements contained in the document will be either implemented or flowed down to mission specific dispenser Interface Control Documents (ICDs) as well as dispenser and CubeSats specification documents.

It is the responsibility of the LSP to provide Certification of Flight Readiness (CoFR) statements for the integrated dispenser systems that fly on NASA ELV missions. LSP will perform verification of the LV to dispenser and the dispenser to CubeSat ICD requirements. LSP will have insight into all other CubeSat development activities such as design, development, testing and integration.

1.2. CubeSat Concept

The CubeSat Project was developed by California Polytechnic State University, San Luis Obispo (Cal Poly) and Stanford University's Space Systems Development Lab. The Project is an international collaboration of universities, high schools, and private firms developing picosatellites containing scientific, private, and government payloads. The primary mission of the CubeSat program is to provide access to space for small payloads. Cal Poly standardized the form factors for the CubeSat and the most common is a 1U, which is a approx. 10 cm cube. There are multiple CubeSat configurations based on the 1U form factor such as a 2U (22cm x 10cm x 10cm), 3U (34cm x 10cm x 10cm), 6U (34cm x 20cm x 10cm) etc.

1.3. Dispensers Description

The dispenser provides a standard interface between picosatellites class satellites and a launch vehicle. It also serves as a deployment system for the CubeSats.

The dispensers are a standard CubeSat deployment system, which ensures all CubeSat developers conform to a common CubeSat form factor 1U (10cm x 10cm x 10cm), which in turn reduces cost and development time. The most common dispenser has an internal volume of 34cm x 10cm x 10cm, and is called a 3U dispenser. There are other dispensers in industry using the CubeSat form factor of 6U which has an internal volume of 34cm x 20cm x 10cm. Other larger CubeSat dispensers are in development today that are consistent with the Cubesat form factor of 12U and 24U. The dispensers are versatile, with a small profile and the ability to mount to different launch vehicles in a variety of configurations and hold differing CubeSat form factors.

The design of the dispensers creates a predictable linear trajectory for the picosatellites resulting in a low spin rate upon deployment. The launch vehicle sends a signal to open a spring-loaded door, then the satellites are deployed from the dispenser by means of a spring and glide along smooth flat rails as they exit the dispenser.

2. Applicable Documents

All Compliance and Reference documents are compiled into this section. Documents listed herein are applicable to this document to the extent specified in the requirement.

2.1. Compliance Documents

- | | |
|----------------------------------|--|
| a. AFSPCMAN 91-710 | Range Safety User Requirements Manual Volume 3 – Launch Vehicle, Payloads, and Ground Support Systems Requirements |
| b. MIL-STD-1540C | Military Standard Test Requirements for Launch, Upper-Stage, and Space Vehicles |
| c. NASA-STD-6016 | Standard Materials and Processes Requirements for Spacecraft |
| d. NPR 8715.6 | NASA Procedural Requirements for Limiting Orbital Debris |

2.2. Reference Documents

- | | |
|----------------------------------|---|
| a. LSP-P-321.01 | Engineering Review Process (ERP) |
| b. LSP-P-317.01 | Dispenser and CubeSat Program Level Requirements Violation and Waiver Process |
| c. GSFC-STD-7000 | General Environmental Verification Standard (GEVS) for GSFC Flight Program and projects |
| d. JPL D-26086D | Environmental Requirements documents (ERD) |
| e. MMPDS | Metallic Materials Properties Development and Standardization |
| f. MIL-HDBK-5 | Military Handbook 5, Metallic Materials and Elements for Aerospace Vehicle Structures |

3. Definitions

Primary Mission: All hardware, software, systems, and analysis products pertaining to the manifested primary spacecraft customer (includes both primary and secondary payloads).

Auxiliary Payload: Are considered in this document as the picosatellites or CubeSats that have no interface (mechanical, electrical or RF) with the LV.

CubeSat(s): All hardware, software, systems, and analysis products pertaining to a Cube Satellite that is intended to be installed within a dispenser. This includes CubeSat mass simulators.

Dispenser(s): All hardware, software, systems, and analysis products pertaining to a CubeSat Deployer.

Dispenser System: An integrated system consisting of dispenser and installed CubeSats.

Launch Vehicle (LV): The selected Launch Vehicle for a specified CubeSat mission.

Launch Services Program (LSP): The NASA Launch Services Program.

Mandatory Compliance Requirements (MCRs): Are those requirements within the dispenser to CubeSat ICD, which LSP is required to verify to sign the CoFR.

Maximum Predicted Environment (MPE):

- Dynamic Environments MPE: Envelopes a P95/50 or mean + 5 dB of flight environments.
- Thermal MPE: Derived via simulation + 11° C for uncertainty

4. Mission Objective

The LSP desires to launch CubeSats utilizing containerized dispensers as an auxiliary payload.

5. Programmatic Requirements

Dispenser systems shall pose no increase to the baseline risk for the Primary Mission.

5.1. Program Requirements

- 5.1.1. LSP will procure integrated services and flight qualified dispensers per the requirement in this document and mission specific Dispenser to LV ICD.
- 5.1.2. LSP will apply best effort for the mission success of the individual CubeSats (LSP is not responsible for mission success of the CubeSats).
- 5.1.3. CubeSat mission will be approved by the Flight Planning Board before manifesting on NASA missions.
- 5.1.4. Flight Planning Board will inform the Primary Mission that CubeSats have been manifested on their mission.
- 5.1.5. LSP will provide resources to accommodate the integration of selected CubeSats mission.
- 5.1.6. LSP will not require attendance from the Primary Mission for Dispenser or CubeSat reviews and assessments; however, the Primary Mission will be informed and invited.
- 5.1.7. LSP will have approval authority for dispensers and CubeSat requirements and insight into all other dispenser and CubeSat development activities (e.g. design, development and test) as required.
- 5.1.8. CubeSats will be manifested per Manifesting Policy (TBD).
- 5.1.9. CubeSats will not interfere with the mission success of other CubeSats integrated in the same dispenser.
- 5.1.10. CubeSats shall be delivered to the integration contractor in a time frame that does not affect the dispenser integration-processing schedule.
- 5.1.11. Dispenser system shall be delivered to Launch Service Contractor in a time frame that does not affect the Primary Mission integration cycle or launch timeline.
- 5.1.12. All violations of the requirements listed in this document shall be reviewed and dispositioned per [LSP-P-317.01, Dispenser and CubeSat Program Level Requirement Violation and Waiver Process](#). All technical requirement changes shall be approved by LSP Engineering Review Board.

6. Program Technical Requirements

This section defines the technical requirements for LSP, CubeSats, dispensers and LV.

6.1. LSP Technical Requirements

- 6.1.1. LSP will conduct verifications for the Dispenser to LV ICD as well as the MCRs with the Dispenser to CubeSat ICD.
- 6.1.2. LSP will follow their standard review process for non-conformances, new flight items, changes in qualification status etc. per [LSP-P-321.01 Engineering Review Process \(ERP\)](#).

6.2. CubeSat Technical Requirements

- 6.2.1. CubeSats shall be designed, and verified to the environments defined in Table 1 - *Dispenser and CubeSat Test Environments Testing Table* and per Figure 1 - *Dispenser and CubeSat Qualification and Acceptance Test Flow Diagram*.
- 6.2.2. CubeSat Structural qualification is adequately achieved through environmental testing only. (PR 6.3.1, Table 1) During periods where all flight loads are applied, CubeSats are considered to be internal components of the dispenser assembly.
- 6.2.3. CubeSats shall be no smaller than a 1U (10x10x10cm) form factor and no larger than a 6U (30x20x10cm) form factor. (dimensions are nominal)
- 6.2.4. CubeSats shall not contain pressurized vessels. CubeSat containing non-ventable pressure containers are permitted if they satisfy the following requirements.
 - 6.2.4.1. Pressure shall be no more than 1 atmosphere while on Orbit.
 - 6.2.4.2. Pressure container contents shall be not endanger personnel or equipment or create a mishap (accident) if released.
 - 6.2.4.3. Pressure containers shall be structurally qualified in accordance with Table 2 - Strength Qualification Requirements
- 6.2.5. CubeSat shall not contain propulsion systems.
- 6.2.6. CubeSats shall not contain radioactive material.
- 6.2.7. CubeSats shall not contain any explosive devices
- 6.2.8. CubeSats hazardous material shall conform to AFSPCMAN 91-710, Range Safety User Requirements Manual Volume 3 – Launch Vehicles, Payloads, and Ground Support Systems Requirements.
- 6.2.9. CubeSats shall remain powered off from the time of delivery to LV through on orbit deployment. Real time clock circuits are permitted if they satisfy the following requirements. (Reference [ELVL-2013-0043486](#))

- 6.2.9.1. Real time clock circuits shall be isolated from the CubeSats main power system.
- 6.2.9.2. Real time clock frequencies shall be less than 320 kHz.
- 6.2.9.3. Real time clock circuits shall be current limited to less than 10 mA.
- 6.2.10. CubeSats shall not radiate RF from the time of delivery to LV through 45 minutes after on-orbit deployment.
- 6.2.11. CubeSats shall be designed with at least 3 independent inhibits to prevent inadvertent RF transmission.
- 6.2.12. CubeSats shall be self-contained, and provide their own power, sequencing, and wiring.
- 6.2.13. CubeSats shall be designed to accommodate ascent venting per Ventable Volume/Area < 2000 inches in accordance with accepted standards such as JPL D-26086, *Revision D, Environmental Requirements Document (ERD)*.
- 6.2.14. CubeSats mission design and hardware shall be in accordance with [NPR 8715.6 NASA Procedural Requirements for Limiting Orbital Debris](#).
- 6.2.15. CubeSats materials shall be selected in accordance with [NASA-STD-6016](#) (Section 4.2), *Standard Materials and Processes Requirements for Spacecraft*.

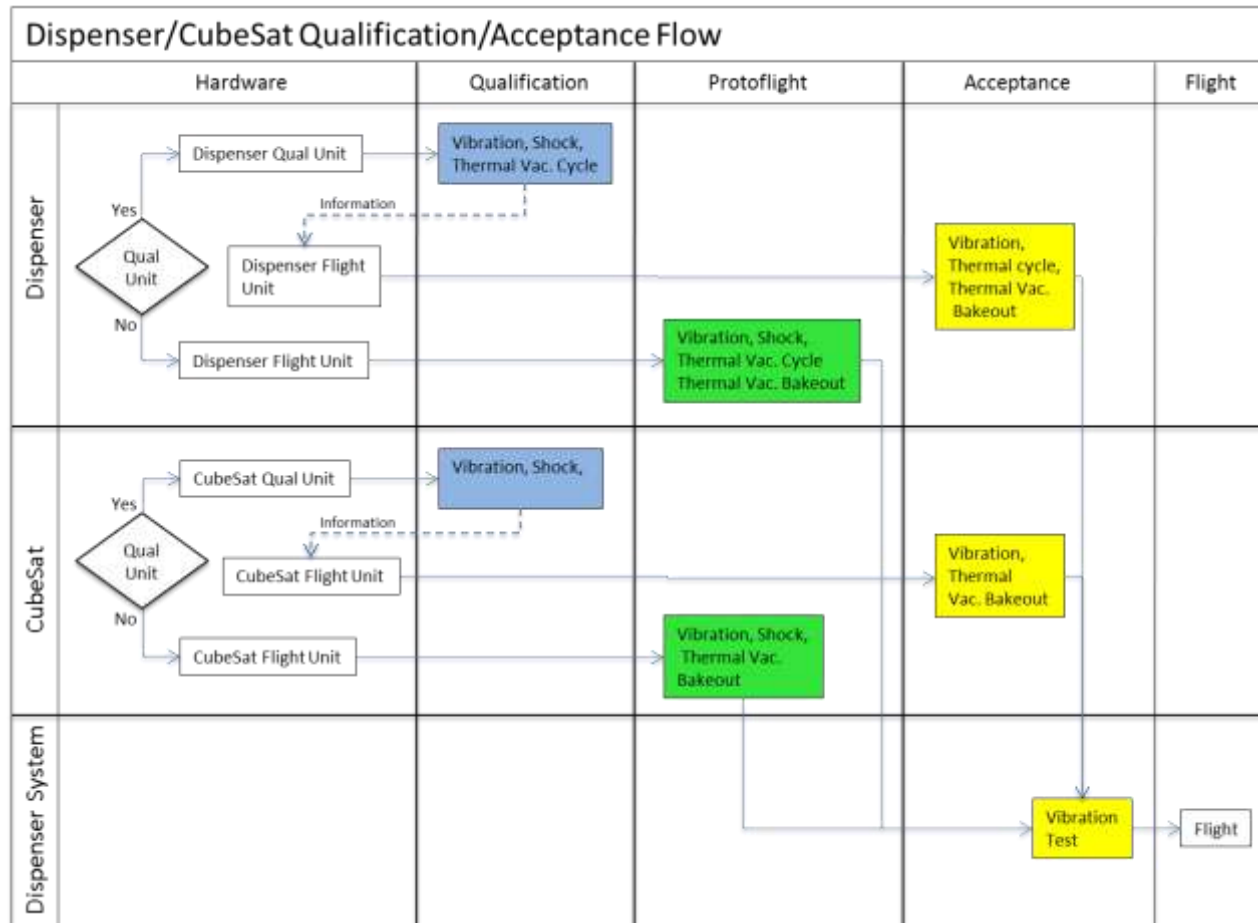
6.3. Dispenser Technical Requirements

- 6.3.1. Dispensers shall be designed, and verified to the environments defined in Table 1 - *PPOD and CubeSat Test Environments Testing Table* and per Figure 1 - *Dispenser and CubeSat Qualification and Acceptance Test Flow Diagram*.
- 6.3.2. Dispensers shall be structurally qualified in accordance with Table 2 - Strength Qualification Requirements.
- 6.3.3. CubeSat size limitations are established in 6.2.3 and occupy the full usable volume of a Dispenser.
- 6.3.4. Dispensers shall not violate the primary mission static and/or dynamic envelopes.
- 6.3.5. Dispensers shall not affect LV avionics qualification status or architecture.
- 6.3.6. Dispensers shall incorporate a sensor for door position (Open/Closed).
- 6.3.7. Dispensers' door release mechanism shall be designed to accept redundantly initiated signals.
- 6.3.8. Dispensers shall be designed to accommodate ascent venting per Ventable Volume/Area < 2000 inches in accordance with accepted standards such as JPL D-26086, *Revision D, Environmental Requirements Document (ERD)*.

- 6.3.9. Dispensers shall deploy CubeSats at a velocity sufficient to prevent re-contact with Primary Mission hardware.
- 6.3.10. Dispensers shall not deploy CubeSat mass simulator(s).
- 6.3.11. Dispensers shall utilize industry standards for locking methodologies on all fasteners consistent with [NASA-STD-6016](#).
- 6.3.12. Dispensers' material shall be in accordance with [NASA-STD-6016](#) (Section 4.2), *Standard Materials and Processes Requirements for Spacecraft*.
- 6.3.13. Dispensers shall conduct vehicle specific CubeSat separation analyses.
 - 6.3.13.1. The separation analysis shall determine the nominal and 3 sigma dispersion values of the impulse imparted to the LV for each CubeSat separation event to include consideration of separation system mechanism and CubeSat mass properties uncertainties.
 - 6.3.13.2. The separation analysis shall confirm that deploying CubeSat(s) during the CubeSat separation event(s) remain within the allowable separation cone(s) as specified by the LV contractor.
- 6.3.14. Dispenser System shall be designed to provide a minimum of 20 dB EMI Safety Margin (EMISM) for non-explosive actuator (NEA) circuits.
- 6.3.15. Dispenser System shall have a fixed base frequency greater than 120 Hz.

Table 1 – Dispenser and CubeSat Environments Test Table

Tests	Qualification by Test	Protoflight Test	Acceptance Test
Random vibration⁶ (CubeSat and Dispenser) Ref Mil-Std 1540C	MPE + 6 dB for (3) minutes, each of (3) axes ¹	MPE+3 dB for (2) minutes, each of (3) axes ¹	MPE for (1) minute, each of (3) axes ¹
Sinusoidal Vibration⁶ (CubeSat and Dispenser) Ref Mil-Std 1540C	MPE + 6 dB. Testing shall be performed for content that is not covered by random vibration testing	1.25 x MPE. Testing shall be performed for content that is not covered by random vibration testing	MPE. Testing shall be performed for content that is not covered by random vibration testing ¹
Shock⁶ (CubeSat and Dispenser) Ref Mil-Std 1540C	MPE + 6 dB, 3 times in both directions of 3 axes ^{1,3}	MPE + 3 dB, 1 times in both directions of 3 axes ^{1,3}	N/A
Thermal Vacuum Cycle (Dispenser Only) Ref.: MIL-STD 1540 B, GSFC-STD-7000	MPE ² +/- 10°C Minimum Range = -14 -3/+0°C to +71 -0/+3°C Cycles = 8 Dwell Time = 1 hour min. @ extreme Temp. after thermal stabilization Transition = < 5° C/minute Vacuum = 1x10 ⁻⁴ Torr	MPE ² +/- 10°C Minimum Range = -14 -3/+0°C to +71 -0/+3°C Cycles = 4 Dwell Time = 1 hour min. @ extreme Temp. after thermal stabilization Transition = < 5° C/minute Vacuum = 1x10 ⁻⁴ Torr	MPE ² +/- 5°C Minimum Range = -9 -3/+0°C to +66 -0/+3°C Cycles = 2 Dwell Time = 1 hour min. @ extreme Temp. after thermal stabilization Transition = < 5° C/minute Vacuum = 1x10 ⁻⁴ Torr
Thermal Vacuum Bake out (Dispenser Only) Ref.: MIL-STD 1540 B, GSFC-STD-7000	N/A	Min. Temp 70°C ^{4,7} Cycles = 1 Dwell Time = Min. 3 hour after thermal stabilization Transition = N/A Vacuum = 1x10 ⁻⁴ Torr	Min. Temp 70°C ^{4,7} Cycles = 1 Dwell Time = Min. 3 hour after thermal stabilization Transition = N/A Vacuum = 1x10 ⁻⁴ Torr
Thermal Vac Bake out (CubeSat Only) Ref.: MIL-STD 1540 B, GSFC-STD-7000	N/A	Min. Temp 70°C ^{5,8} Cycles = 1 Dwell Time = Min. 3 hour after thermal stabilization Transition = < 5° C/minute Vacuum = 1x10 ⁻⁴ Torr	Min. Temp 70°C ^{5,8} Cycles = 1 Dwell Time = Min. 3 hour after thermal stabilization Transition = < 5° C/minute Vacuum = 1x10 ⁻⁴ Torr
Hardware Configuration	Dispenser – Flight identical unit (includes NEA, cable and connector) CubeSat – Flight Identical unit	Dispenser – Flight unit (includes flight NEA, cable and connector) CubeSat – Flight unit	Dispenser – Flight unit (includes flight NEA, cable and connector) CubeSat – Flight unit
<p>(1) Dynamic Environments random MPE envelopes a P95/50 or mean + 5 dB of flight environments. Sinusoidal levels envelope loads predictions and flight environments. Shock MPE envelopes P95/50 for at least (3) samples, with 4.5 dB uncertainty factor applied where less than (3) samples are used.</p> <p>(2) Thermal MPE = Max predicted via simulation + 11° C for uncertainty.</p> <p>(3) Shock testing is not required when the following conditions are met: 1) The qualification random vibration test spectrum when converted to an equivalent shock response spectrum (3-sigma response for Q=10) exceeds the qualification shock spectrum requirement at all frequencies below 2000 Hz. 2) The maximum expected shock spectrum above 2000 Hz does not exceed (g) values equal to 0.8 times the frequency in Hz at all frequencies above 2000 Hz, corresponding to the velocity of (50 inches/second).</p> <p>(4) Maximum bake out temperature set to same maximum temperature for thermal cycle test for consistency, assuming bake out would be performed during same vacuum exposure.</p> <p>(5) If the CubeSat cannot achieve these temperature levels, the CubeSat shall hold a minimum temperature of 60°C for a minimum of 6 hours.</p> <p>(6) Levels are defined to be at the dispenser to Launch Vehicle mechanical interface.</p> <p>(7) Thermal bake out temperatures are not to exceed qualification temperatures</p> <p>(8) CubeSat Thermal vacuum bakeout is required unless LSP removes the requirement for individual CubeSats based on material selection, quantities and manifesting.</p>			

**Figure 1 Dispenser and CubeSat Qualification Acceptance Flow Diagram****Table 2, Strength Qualification Requirements**

Qualification Method	Qualification Factors of Safety
Strength Analysis Only	1.6 X Limit load with respect to material yield strength 2.0 x limit load with respect to material ultimate strength
Structural Test*	1.1 X Limit load with respect to material yield strength with no detrimental yielding of test article 1.25 x limit load with respect to material ultimate strength with no structural failure of test article

Note: Material Strength properties shall be "A" basis allowable as shown in either MIL-HDBK-5 or MMPDS. Limit loads are worst-case combination of flight loads and environments occurring during the launch phase of a mission.

* A combination of structural test and analysis maybe used for qualification. Factors of safety used in the analysis are those shown above for Structural Test.

6.4. LV Technical Requirements

- 6.4.1. LV shall integrate and/or install Dispenser System onto a NASA/Launch Vehicle Contractor agreed upon location.
- 6.4.2. LV integration of a dispensers System shall not delay primary mission integration cycle.
- 6.4.3. LV shall not modify the Primary Spacecraft interface to accommodate a Dispenser.
- 6.4.4. LV shall accommodate Dispenser door position indicator in the flight telemetry stream.
- 6.4.5. Deleted
- 6.4.6. LV shall provide fault tolerance for inadvertent actuation equal to or better than that used on the primary/secondary spacecraft.
- 6.4.7. LV shall not alter the mechanical and electrical interface design of the Dispensers.
- 6.4.8. LV shall design, qualify and acceptance test the LV Dispenser interface.
- 6.4.9. LV shall command deployment of the dispenser's CubeSats.
- 6.4.10. LV trajectory design shall not result in LV contact with deployed CubeSats.
- 6.4.11. LV shall not deploy the CubeSats in a trajectory that will contact the Primary Mission or LV.
- 6.4.12. LV shall define the CubeSat allowable deployment cone for each dispenser.

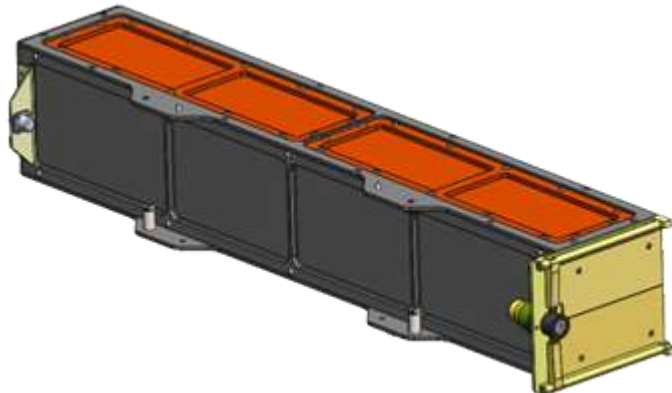
Appendix A

Acronyms

Cal Poly	California Polytechnic State University
cm	Centimeter
ELV	Expendable Launch Vehicle
ICD	Interface Control Document
kg	Kilograms
LSP	Launch Services Program
LV	Launch Vehicle
MCR	Mandatory Compliance Requirements
MPE	Maximum Predicted Environments
NEA	Non-Explosive Actuator
RF	Radio Frequency

B.2 NanoRacks CubeSat Deployer Interface Control Document

Document: NR-SRD-029	NRCSD ICD	NANORACKS
Classification: Public Domain	Date: December 10, 2013	Revision 0.36



NanoRacks CubeSat Deployer (NRCSD) Interface Control Document

NanoRacks, LLC
18100 Upper Bay Road, Suite 150
Houston, TX 77058
(815) 425-8553
www.NanoRacks.com



Document: NR-SRD-029	NRCSD ICD	NANORACKS
Classification: Public Domain	Date: December 10, 2013	Revision 0.36

Document: NR-SRD-029	NRCSD ICD	NANORACKS
Classification: Public Domain	Date: December 10, 2013	Revision 0.36

Acronyms

CTB	Crew Transfer Bag
kgf	kilogram-force
NRCSD	NanoRacks CubeSat Deployer
RBF	Remove Before Flight

Document: NR-SRD-029	NRCSD ICD	NANORACKS
Classification: Public Domain	Date: December 10, 2013	Revision 0.36

Table of Contents

1	Introduction	5
1.1	Document Purpose	5
1.2	Scope.....	5
2	Timeline.....	5
3	General Requirements	5
4	Physical Interfaces	6
4.1	NanoRacks CubeSat Deployer (NRCSD) Description.....	6
4.2	NRCSD Coordinate System.....	7
4.3	Access to CubeSat Inhibit Switches and Service Ports.....	7
4.4	Mass Properties	7
4.5	CubeSat Dimensional Requirements	8
4.6	CubeSat Rails.....	10
4.7	Deployment Switches	12
4.8	Separation Springs	12
4.9	Deployment Compatibility.....	13
5	Electrical Interfaces.....	13
5.1	Electrical System Design	13
5.2	Batteries.....	14
6	Launch Loads.....	15
7	Thermal Interfaces	15
8	Hazardous Materials	15
9	CubeSat Integration	15

List of Figures

Figure 1 NRCSD	6
Figure 2 NRCSD Coordinate System.....	7
Figure 3: Lateral view of NRCSD and access panel dimensions	7
Figure 4 CubeSat Envelope Dimensions.....	8
Figure 5 NRCSD Axial Cross-Section (+Z view).	9
Figure 6 CubeSat Rail and NRCSD Rails Clearances (+Z view, +Y top).....	10
Figure 7 CubeSat Rail Standoff Clearance.....	11
Figure 8 Dimensional fit check gauge cross section view	11
Figure 9 Roller/Slider Switch NRCSD Geometry.....	12
Figure 10 Separation spring placement options	13
Figure 11 Separation spring rail standoff geometry	13
Figure 12 CubeSat Electrical Subsystem Block Diagram (note: RBF switch not shown).....	14

Document: NR-SRD-029	NRCSD ICD	NANORACKS
Classification: Public Domain	Date: December 10, 2013	Revision 0.36

1 Introduction

1.1 Document Purpose

This Interface Control Document (ICD) defines the interface requirements between the NanoRacks CubeSat Deployer (NRCSD) and CubeSats for developers utilizing NanoRacks CubeSat deployment services.

1.2 Scope

The ICD provides the minimum requirements for compatibility with the NRCSD and International Space Station (ISS) flight safety program when using NanoRacks CubeSat deployment services. NanoRacks verifies compliance on behalf of CubeSat developers based on incremental data requests.

2 Timeline

The following timeline of launch-minus dates are provided as template example when using the NanoRacks CubeSat deployment services. Tailored agreements can be discussed as part of contract negotiations.

Launch-minus dates	Activity
L – 12 to 14 months	Contract Signing
L – 10 months	<ul style="list-style-type: none"> • Functional Description • Interface Drawings • Material Identification and Usage List
L – 8 months	First data call to CubeSat developer for ISS safety process
L – 4 months	Environmental testing
L – 1 to 3 months	Delivery to NanoRacks

3 General Requirements

- 1) CubeSats shall be passive and self-contained from the time they are loaded into the NRCSD for transport to the ISS and until after deployment from the NRCSD. No charging of batteries, support services, and or support from ISS crew is provided after final integration.
- 2) CubeSats shall not contain pyrotechnics unless the design approach is pre-approved by NanoRacks. Electrically operated melt-wire systems for deployables that are necessary controls for hazard potentials are permitted.
- 3) CubeSats must have a timer (set to a minimum of 30 minutes) before satellite operation or deployment of appendages. If deploy switches should be released causing the timer to run, the timer must automatically re-set whenever the Remove Before Flight (RBF) feature is replaced and/or the deploy switches are returned to the open state.
- 4) CubeSats should not have detachable parts or create any space debris during launch or normal mission operations.
- 5) CubeSats shall use a secondary locking feature for fasteners external to the CubeSat chassis. An acceptable secondary locking compound is LocTite. Contact NanoRacks for the proper locking compound application procedure. Other secondary locking methods must be approved by NanoRacks.

- 6) A description of frangible materials (e.g. solar cells) must be provided to NanoRacks for approval.

4 Physical Interfaces

4.1 NanoRacks CubeSat Deployer (NRCSD) Description

The NRCSD is a self-contained CubeSat deployer system that mechanically and electrically isolates CubeSats from the ISS, cargo resupply vehicles, and ISS crew. The NRCSD design is compliant with NASA ISS flight safety requirements and is space qualified.

The NRCSD is a rectangular tube that consists of anodized aluminum plates, base plate assembly, access panels and deployer doors. The NRCSD deployer doors are located on the forward end, the base plate assembly is located on the aft end, and access panels are provided on the top. The inside walls of the NRCSD are smooth bore design to minimize and/or preclude hang-up or jamming of CubeSat appendages during deployment should these become released prematurely. However, deployable systems shall be designed such that there is no intentional contact with the inside walls of the NRCSD.

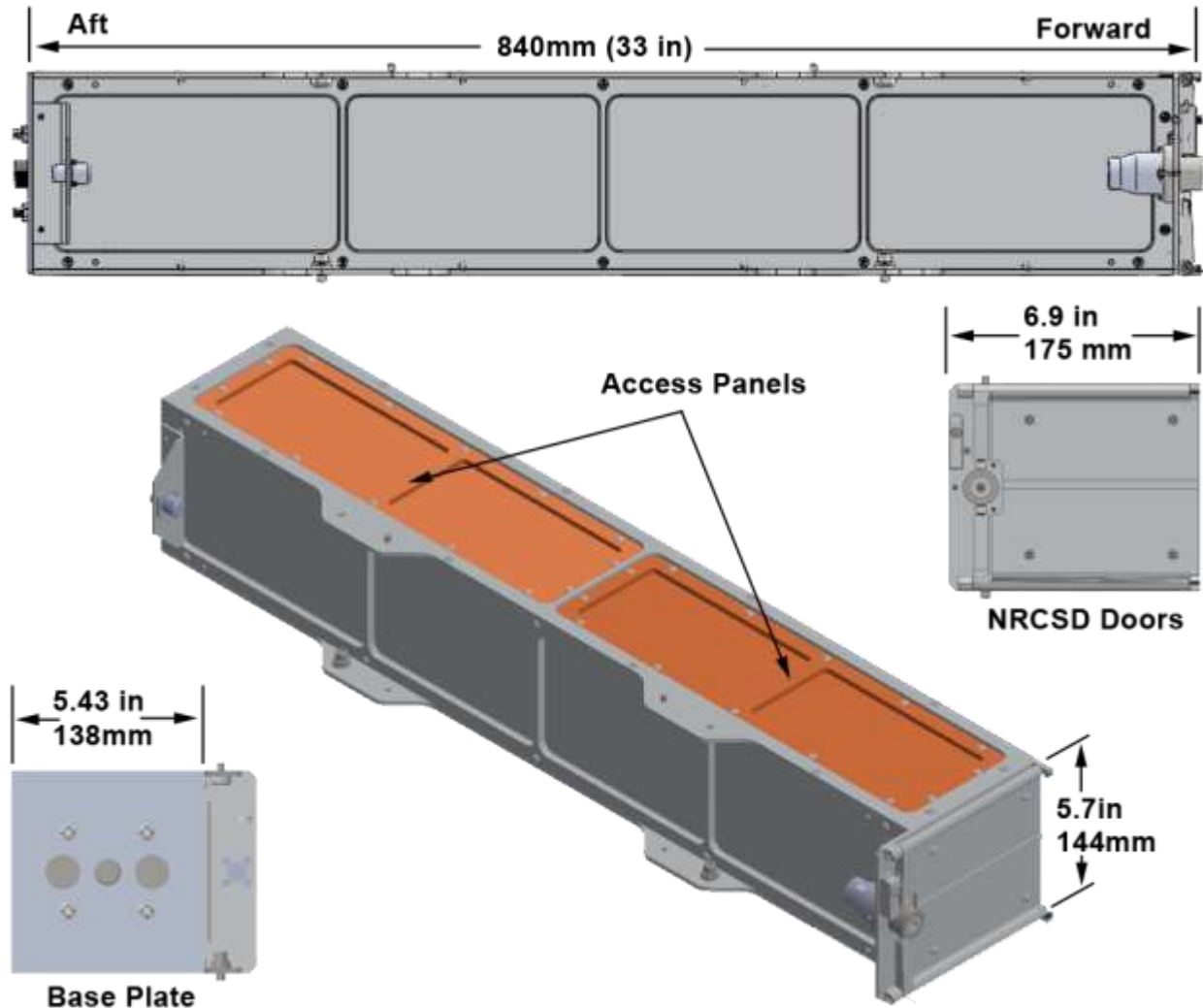


Figure 1 NRCSD

4.2 NRCSD Coordinate System

The coordinate system of the NRCSD is a right-handed system shown in Figure 2. The +X-axis is orientated as shown in the figure, the +Y axis points out of the top of the NRCSD normal to the access panels and the +Z-axis points forward to the NRCSD the deployer doors.

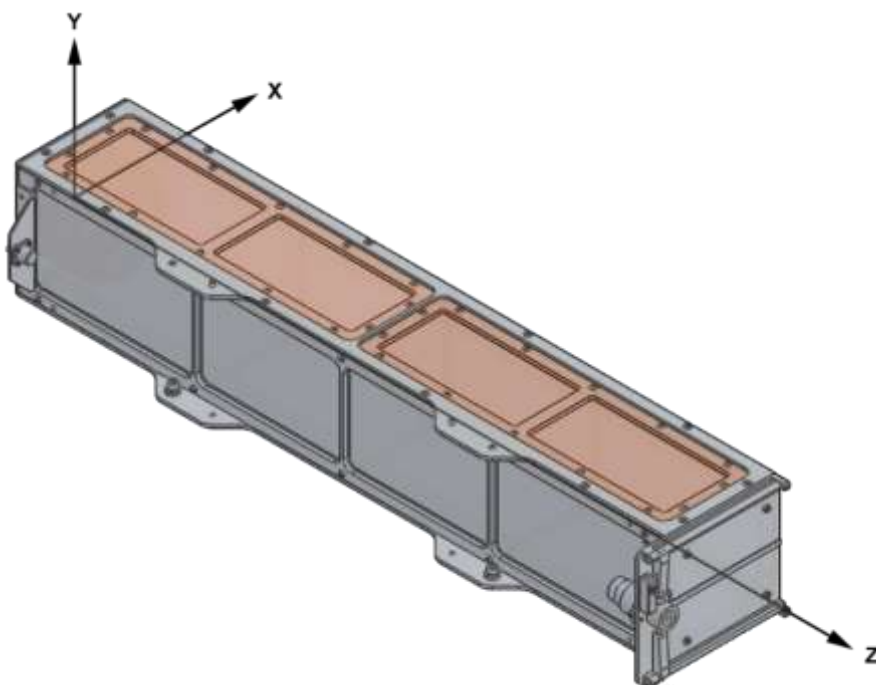


Figure 2 NRCSD Coordinate System

4.3 Access to CubeSat Inhibit Switches and Service Ports

Access for RBF pins and charging systems during the integration process is provided through access panels located on the topside (+Y axis) of the NRCSD as shown in Figure 3. CubeSats are accessible only through the access panels when integrated with the NRCSD.

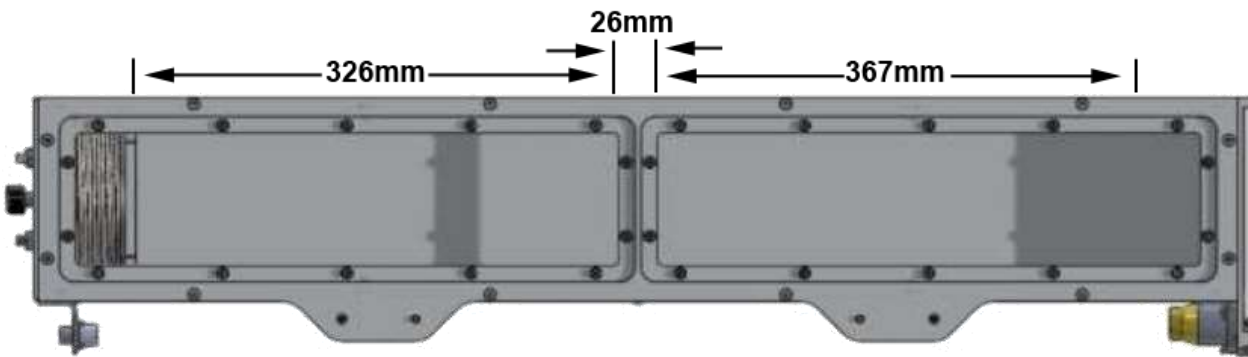


Figure 3: Lateral view of NRCSD and access panel dimensions

4.4 Mass Properties

Mass properties guidelines for CubeSats deployed by NanoRacks are summarized in Table 1. Mass limits are derived from the maximum ballistic number (BN) allowed for ISS deployed payloads. Exceeding

these values requires approval by NanoRacks. The CubeSat center of gravity shall be within 2cm of its geometric center.

Table 1 CubeSat Mass Properties	
Form Factor	Maximum Mass (Kg)
1U	2.82
2U	5.657
3U	8.485
4U	11.314
5U	14.142
6U	16.971

4.5 CubeSat Dimensional Requirements

CubeSats nominal envelope maximum dimensions are shown in Figure 5. No external components other than CubeSat rails or rail roller/slider switch, if used, shall contact the NRCSD interior. Additional envelope provided by a cylindrical recess within the NRCSD pusher plate is available subject to approval.

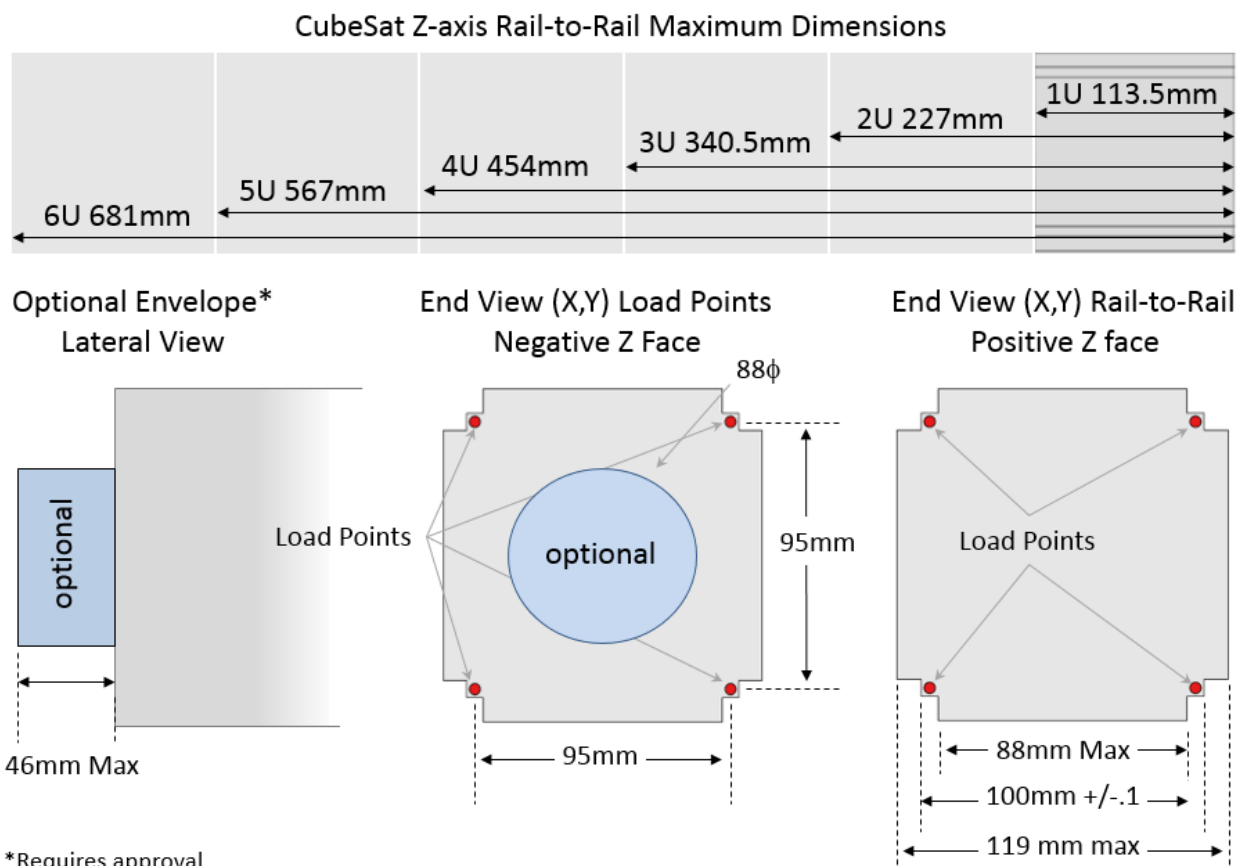


Figure 4 CubeSat Envelope Dimensions

The NRCSD interior envelope is shown in Figure 5.

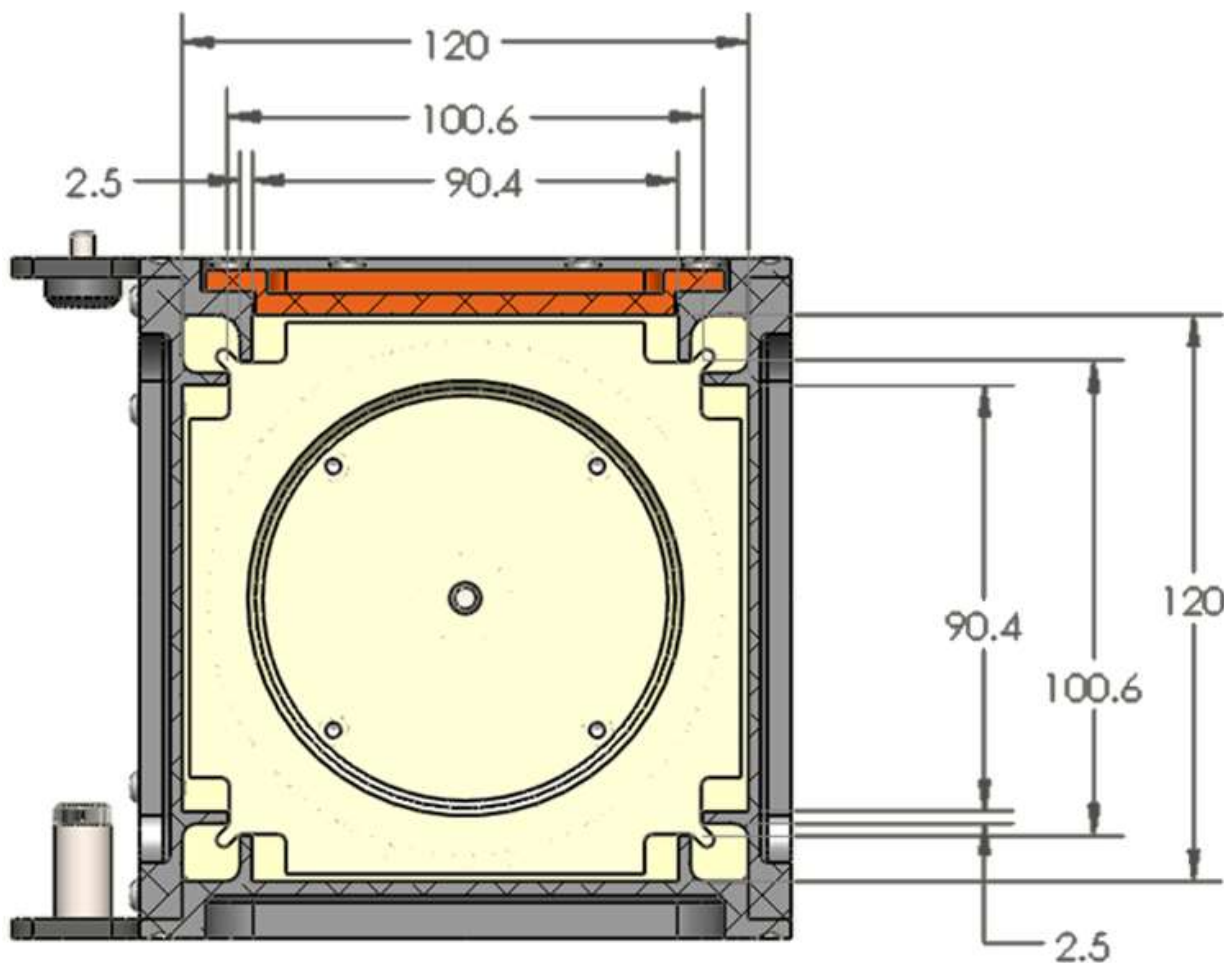


Figure 5 NRCSD Axial Cross-Section (+Z view).

The clearances between NRCSD guide rails and CubeSat rails is shown in Figure 6.

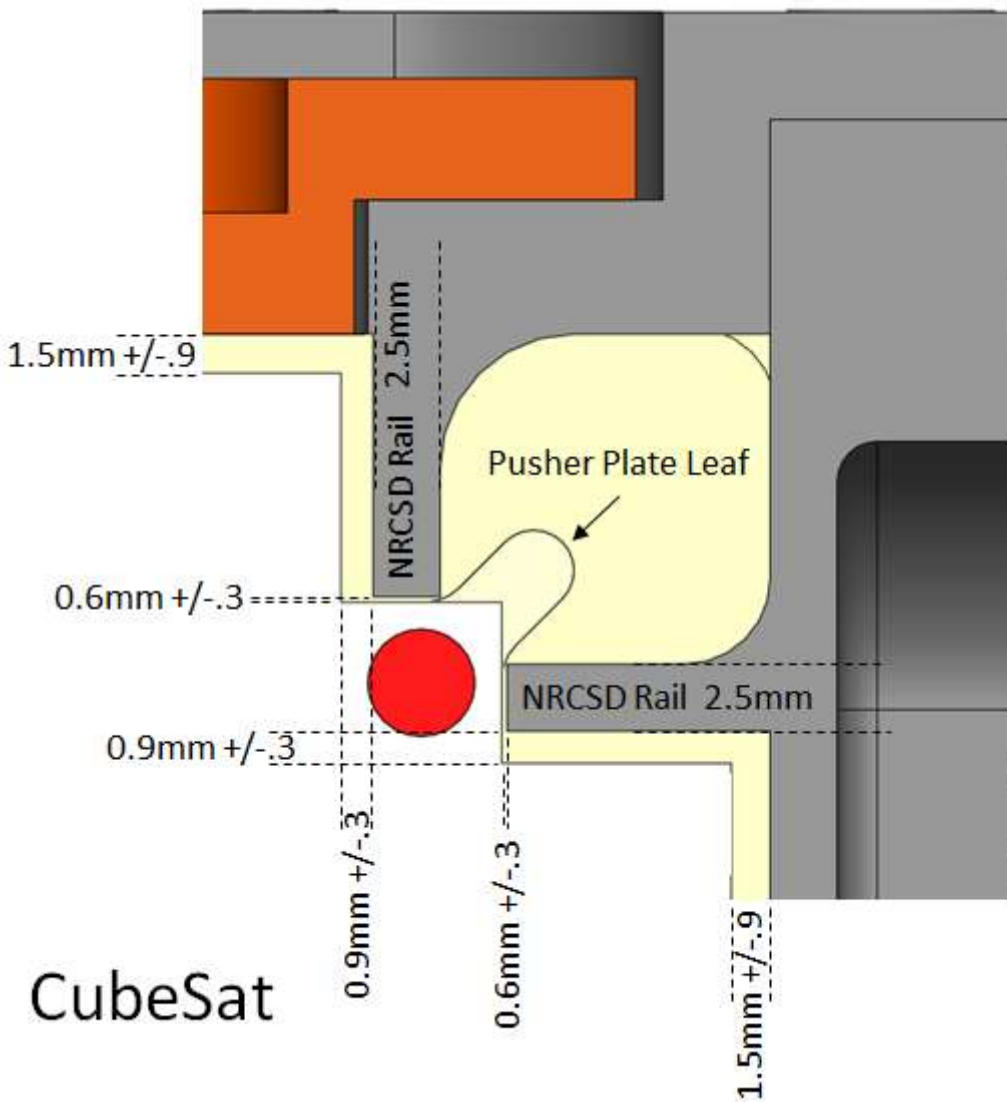


Figure 6 CubeSat Rail and NRCSD Rails Clearances (+Z view, +Y top).

4.6 CubeSat Rails

- 1) A CubeSat shall have four (4) rails, one per corner, along the Z axis.
- 2) Each rail shall have a minimum width of 6mm +0.1mm/ -0.0mm tolerance.
- 3) The edges of the rails shall be rounded to a radius of at least 0.5mm +/- .1mm.
- 4) Each rail end face shall have a minimum surface area of 4mm x 4mm for contact with the adjacent CubeSats.
- 5) The minimum extension of the CubeSat rail standoffs beyond the CubeSat +/- Z face shall be 6.5mm (see Figure 7).

- 6) Rail length variance in the Z axis between rails shall not exceed ± 0.1 mm
- 7) CubeSat rail surfaces that contact the NRCSD guide rails shall have a hardness equal to or greater than hard anodized aluminum (Rockwell C 65-70).

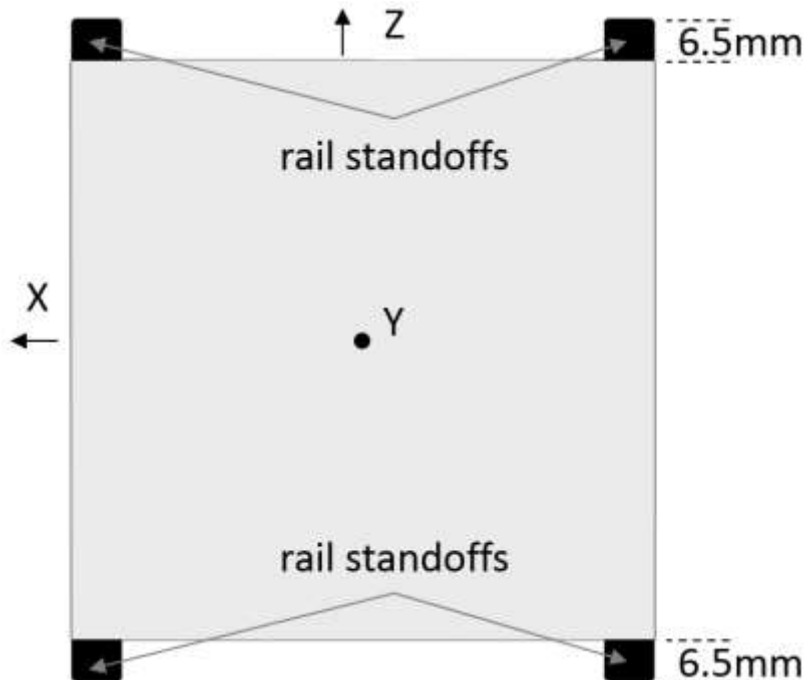


Figure 7 CubeSat Rail Standoff Clearance

- 8) CubeSat developers can verify mechanical compatibility by a fit check with a gauge built to the requirements in Figure 8.

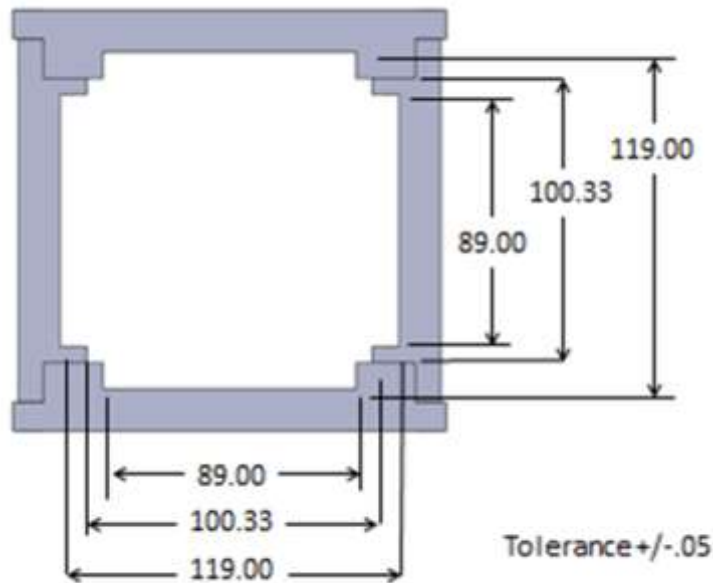


Figure 8 Dimensional fit check gauge cross section view

4.7 Deployment Switches

- 1) CubeSats shall have a minimum of three (3) mechanical deployment switches corresponding to inhibits in the main electrical system (see section on electrical interfaces).
- 2) Deployment switches can be of the pusher variety, located on the -Z face on one or more of the rail end faces, or roller/lever switches embedded in a CubeSat rail and riding along the NRCSD guide rail.
- 3) A roller or slider shall be centered on the deployer guide rail, allowing for placement accuracy, the roller or slider shall maintain a minimum of 75% (ratio of roller/slider width-to-guide rail width) contact along the entire Z-axis (see Figure 9)
- 4) Deployment switches force exerted shall not exceed 3N.

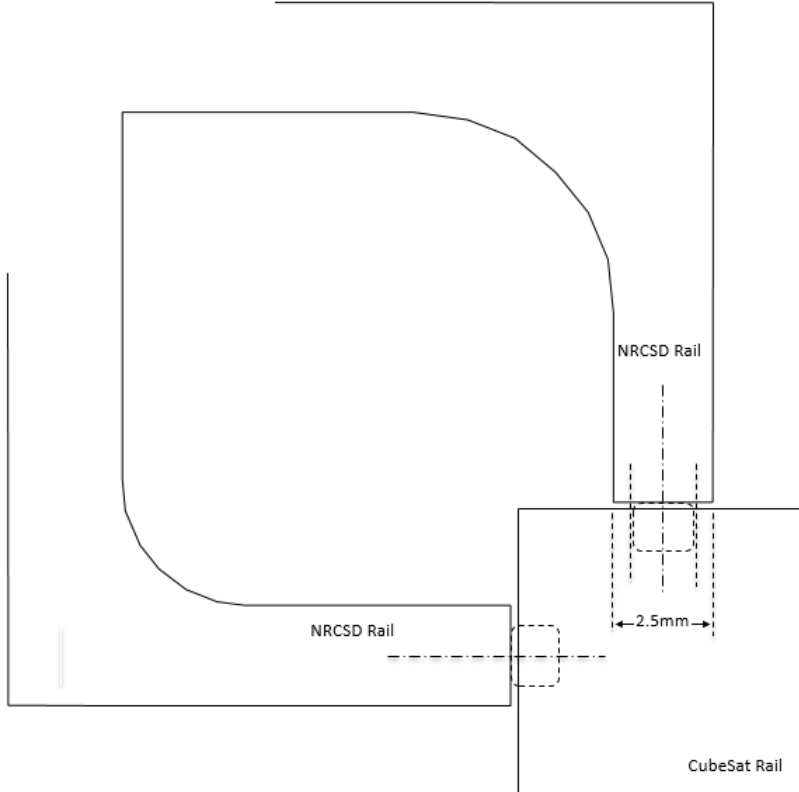
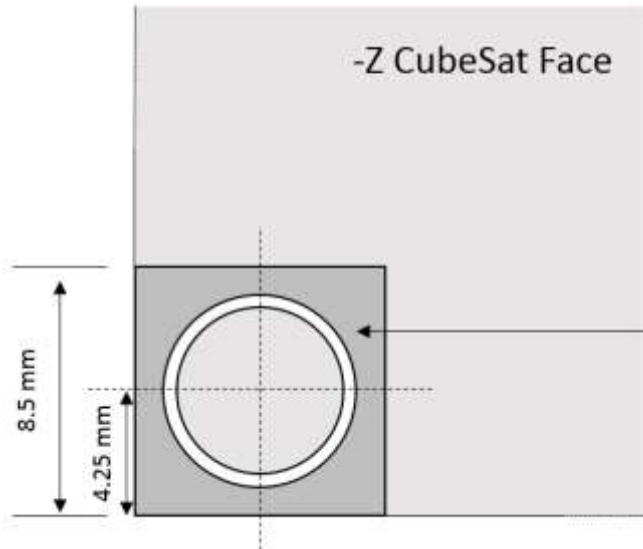
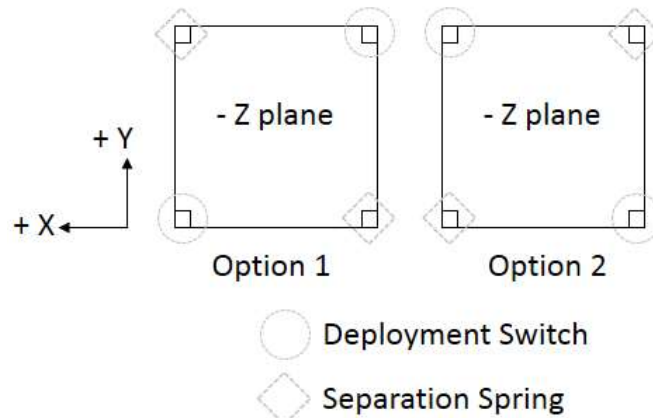


Figure 9 Roller/Slider Switch NRCSD Geometry

4.8 Separation Springs

- 1) CubeSats, except 6U, shall have separation springs. Separation springs shall be located at the -Z end face of a diagonal pair of CubeSat rails as shown in Figure 10.
- 2) Each spring shall be captive. When compressed the spring shall be contained within the maximum rail length. Separation spring and the rail end face alignment are shown in Figure 11.
- 3) Individual separation spring force shall not exceed 3.34 N (0.75 lbs) with the total force for both springs not to exceed 6.67 N (1.5 lbs).



4.9 Deployment Compatibility

During deployment, the CubeSats must be compatible with deployment velocities between 0.5 m/s to 1.5 m/s and accelerations no greater than 2g's in the +Z direction.

5 Electrical Interfaces

5.1 Electrical System Design

The NRCSD does not accommodate an electrical interface to CubeSats. All electrical power shall be internal to CubeSats. CubeSat electronics systems design shall adhere to the following requirements.

- 1) The CubeSat operations shall not begin until a minimum of 30 minutes after deployment from the ISS. Only an onboard timer system may be operable during this 30-minute post deploy time frame.
- 2) The CubeSat electrical system design shall incorporate a minimum of three (3) inhibit switches actuated by physical deployment switches (see Deployment Switches section 4.7) as shown in Figure 12.
- 3) The CubeSat electrical system design shall not permit the ground charge circuit to energize the satellite systems (load), including flight computer (see Figure 12). This restriction applies to all charging methods.
- 4) RBF pins are required. Arming switch or captive jumpers may be an acceptable alternative; contact NanoRacks.
- 5) The RBF pin shall preclude any power from any source operating any satellite functions with the exception of pre-integration battery charging.
- 6) RBF pins must be capable of remaining in place during integration with NRCSD. It shall not be necessary to remove the RBF to facilitate loading into the NRCSD.
- 7) All RBF pins, switches, or jumpers utilized as primary electrical system and RBF inhibits must be accessible from the access panels (see Figure 1) for removal at the completion of loading into the NRCSD.

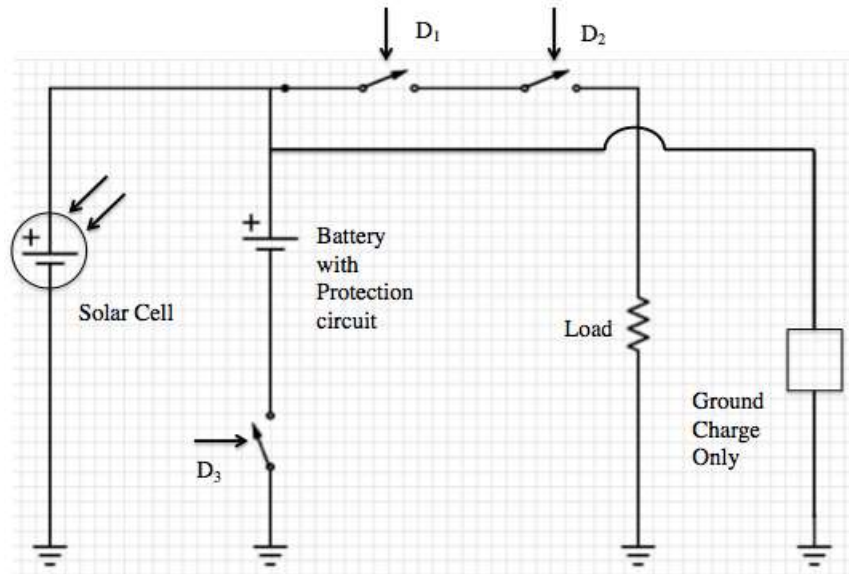


Figure 12 CubeSat Electrical Subsystem Block Diagram (note: RBF switch not shown)

5.2 Batteries

CubeSats that utilize on-board batteries shall comply with NASA requirements for battery safety. This requirement applies for main power batteries and for batteries associated with real-time clocks or watch-dog circuits i.e. "coin cell" batteries. Contact NanoRacks for the appropriate battery test procedure. Batteries should maintain charge for a minimum of 6 months from time of integration into the NRCSD by NanoRacks.

Document: NR-SRD-029	NRCSD ICD	NANORACKS
Classification: Public Domain	Date: December 10, 2013	Revision 0.36

6 Launch Loads

CubeSats shall be tested for random vibration to comply with NASA guidelines per the random vibration profile shown in Table 2 .

Frequency (Hz)	Hard Mount Configuration (g ² /Hz)
20	0.057 (g ² /Hz)
20-153	0 (dB/oct)
153	0.057 (g ² /Hz)
153-90	+7.67 (dB/oct)
190	0.099 (g ² /Hz)
190-250	0 (dB/oct)
250	0.099 (g ² /Hz)
250-270	-1.61 (dB/oct)
750	0.055 (g ² /Hz)
750-2000	-3.43 (dB/oct)
2000	0.018 (g ² /Hz)
OA (grms)	9.47

Table 2 Random Vibration Test Profile

7 Thermal Interfaces

CubeSats shall be designed to withstand overall temperature range of -40C to +65C.

8 Hazardous Materials

CubeSats shall comply with NASA guidelines for hazardous materials. CubeSat developers shall submit a Bill of Materials (BOM) to NanoRacks for assessment.

9 CubeSat Integration

NanoRacks conducts final integration on behalf of the Customer. CubeSat developers shall include their integration requirements in memo format along with the CubeSat.

Document: NR-SRD-052	NRCSD ICD Change Notice	NANORACKS
Classification: Public Domain	Date: April 30, 2014	Revision 0.1



Document Change Notice (DCN)

Maximum CubeSat Mass and Vibration Test Spectra

NanoRacks, LLC
18100 Upper Bay Road, Suite 150
Houston, TX 77058
(815) 425-8553
www.NanoRacks.com

Document: NR-SRD-052	NRCSD ICD Change Notice	NANORACKS
Classification: Public Domain	Date: April 30, 2014	Revision 0.1

Table of Contents

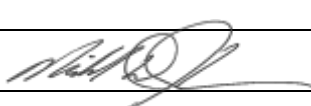
1	Document Purpose	3
2	DCN Summary	3
3	Change Notification	4
3.1	CubeSat Maximum Mass Limits	4
3.2	Vibration Spectrum	4

Document: NR-SRD-052	NRCSD ICD Change Notice	NANORACKS
Classification: Public Domain	Date: April 30, 2014	Revision 0.1

1 Document Purpose

This Document Change Notice (DCN) notifies changes made to the NanoRacks CubeSat Deployer (NRCSD) Interface Control Document (NR-SRD-029). Developers utilizing NanoRacks CubeSat deployment services shall comply with all changes presented in this document, unless otherwise approved by NanoRacks. These changes will be incorporated into the next revision of the NRCSD ICD (Revision 0.37).

2 DCN Summary

DCN Number	NR-SRD-052
Document Affected	NRCSD ICD REV36, NR-SRD-029
Change Description	<ol style="list-style-type: none"> 1. Updated CubeSat maximum mass values for the NRCSD ICD, page 8, Section 4.4, Table 1 2. Corrected frequency ranges NRCSD ICD, page 15, Section 6, Table 2 of the NRCSD ICD
Reason for Change	<ol style="list-style-type: none"> 1. CubeSat maximum mass values revised to comply with NASA guidance issued March 2014. 2. Correction of typographical errors
DCN Distribution	Current and previous external payload developers; NanoRacks Internal
Originator	Kirk Woellert, External Payloads Manager, NanoRacks
Reviewers	NanoRacks Flight Safety: Bob Alexander, 5-7-2014 NanoRacks Safety: NA NanoRacks Operations: NA
Approval	Mike Johnson, CTO, NanoRacks:  5-8-2014

Document: NR-SRD-052	NRCSD ICD Change Notice	NANORACKS
Classification: Public Domain	Date: April 30, 2014	Revision 0.1

3 Change Notifications

3.1 CubeSat Maximum Mass Limits

NASA issued new guidelines for calculation of Ballistic Number (BN) for payloads deployed from the ISS. This affects the mass properties requirements for CubeSats deployed by NanoRacks listed in Section 4.4, Table 1 of the NRCSD ICD. The updated CubeSat maximum mass limits are displayed in the Table 1. Exceeding these mass limits requires approval by NanoRacks.

Table 1 CubeSat Mass Properties	
Form Factor	Maximum Mass (Kg)
1U	2.40
2U	3.60
3U	4.80
4U	6.00
5U	7.20
6U	8.40

3.2 Vibration Spectrum Corrections

The vibration spectrum outlined in Section 6, Table 2 of the NRCSD ICD contained typographical errors in the frequency ranges. Payload developer should plan flight acceptance vibration tests to the correct vibration test profile displayed in Table 2 below.

Table 2 Random Vibration Test Profile	
Frequency (Hz)	Maximum Flight Envelope (g ² /Hz)
20	0.057 (g ² /Hz)
20-153	0 (dB/oct)
153	0.057 (g ² /Hz)
153-190	+7.67 (dB/oct)
190	0.099 (g ² /Hz)
190-250	0 (dB/oct)
250	0.099 (g ² /Hz)
250-750	-1.61 (dB/oct)
750	0.055 (g ² /Hz)
750-2000	-3.43 (dB/oct)
2000	0.018 (g ² /Hz)
OA (grms)	9.47

End of Document

Document: NR-SRD-063	NRCSD ICD Change Notice	NANORACKS
Classification: Public Domain	Date: August 11, 2014	Revision 0.1



Document Change Notice (DCN)

NRCSD Guide Rail Width

NanoRacks, LLC
555 Forge River Road, Suite 120
Webster, TX 77598
(815) 425-8553
www.NanoRacks.com

Document: NR-SRD-063	NRCSD ICD Change Notice	NANORACKS
Classification: Public Domain	Date: August 11, 2014	Revision 0.1

Table of Contents

1	Document Purpose	3
2	DCN Summary	3
3	Change Notifications.....	4
3.1	NRCSD Guide Rail Dimensions	4

Document: NR-SRD-063	NRCSD ICD Change Notice	NANORACKS
Classification: Public Domain	Date: August 11, 2014	Revision 0.1

1 Document Purpose

This Document Change Notice (DCN) notifies changes made to the NanoRacks CubeSat Deployer (NRCSD) Interface Control Document (NR-SRD-029). Developers utilizing NanoRacks CubeSat deployment services shall comply with all changes presented in this document, unless otherwise approved by NanoRacks. These changes will be incorporated into the next revision of the NRCSD ICD (Revision 0.37).

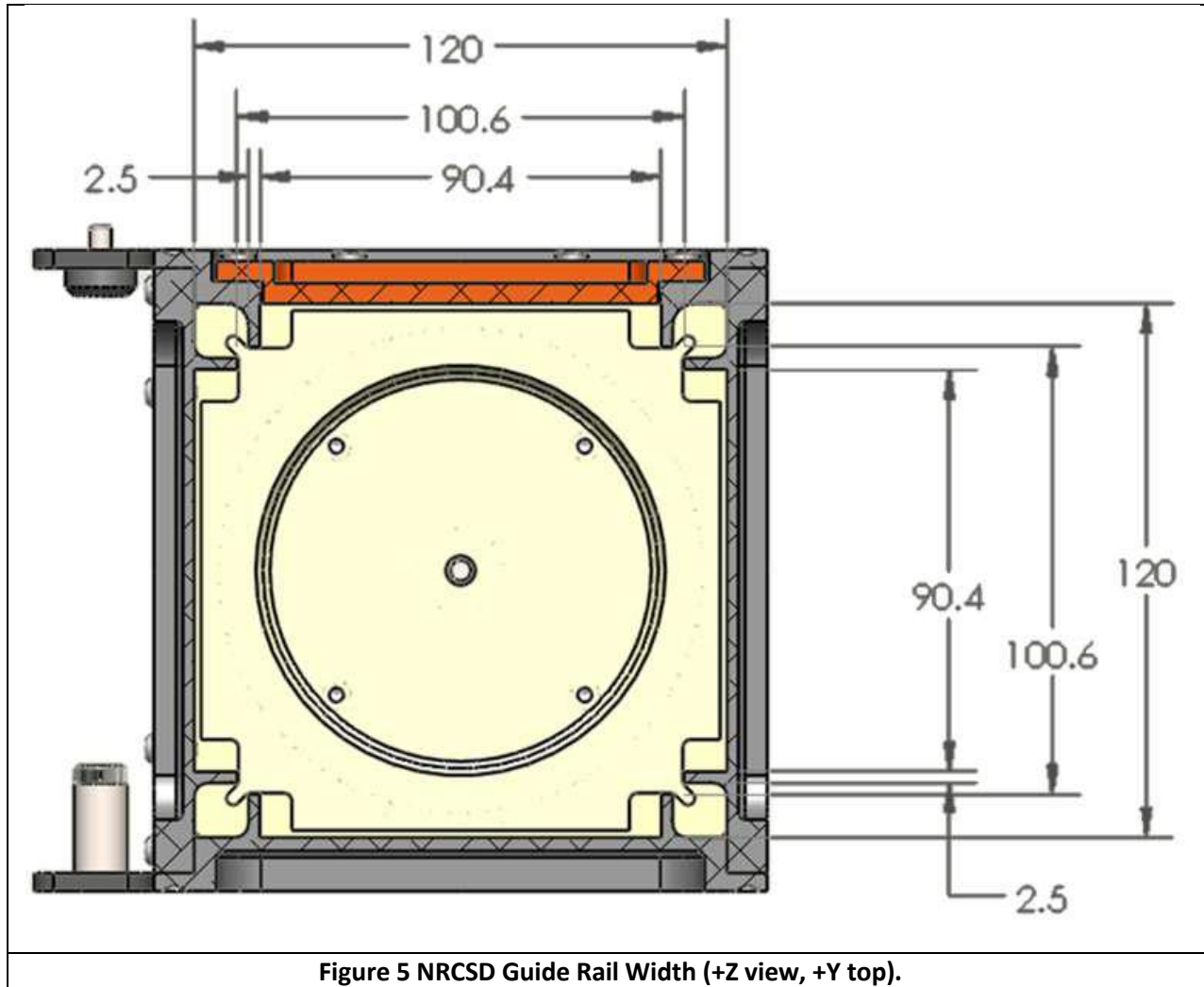
2 DCN Summary

DCN Number	NR-SRD-063	
Document Affected	NRCSD ICD REV36, NR-SRD-029	
Change Description	1. NRCSD guide rail width change	
Reason for Change	1. ICD update	
DCN Distribution	Current and previous external payload developers; NanoRacks Internal	
Originator	Kirk Woellert, External Payloads Manager, NanoRacks	
Reviewers	NanoRacks Flight Safety: Bob Alexander, 7-28-2014	
	NanoRacks Avionics: NA	
	NanoRacks Operations: NA	
	Other: Victor Dube, Quad-M, inc. 8-2-2014	
Approval	Mike Johnson, CTO, NanoRacks:	 8-11-2014

3 Change Notifications

3.1 NRCSD Guide Rail Dimensions

The NanoRacks CubeSat Deployer (NRCSD) interior structure has four sets of guide rails which interface to corresponding CubeSat rails. Section 4.5, Figure 5 of the NRCSD ICD Rev 36, depicts the NRCSD guide rails having width of 2.5mm.



NRCSDs manufactured after June 2014 (NanoRacks CubeSat Mission 2 and thereafter) have guide rail width of 2.25mm as shown in Figure 5 below. There is a difference between the physical envelope and allowable envelope due to the addition of the Keep Out Zone depicted in red. There is no change to the allowable envelope which is denoted in Figure 5 below as dimensions proceeded by an asterisk (*).

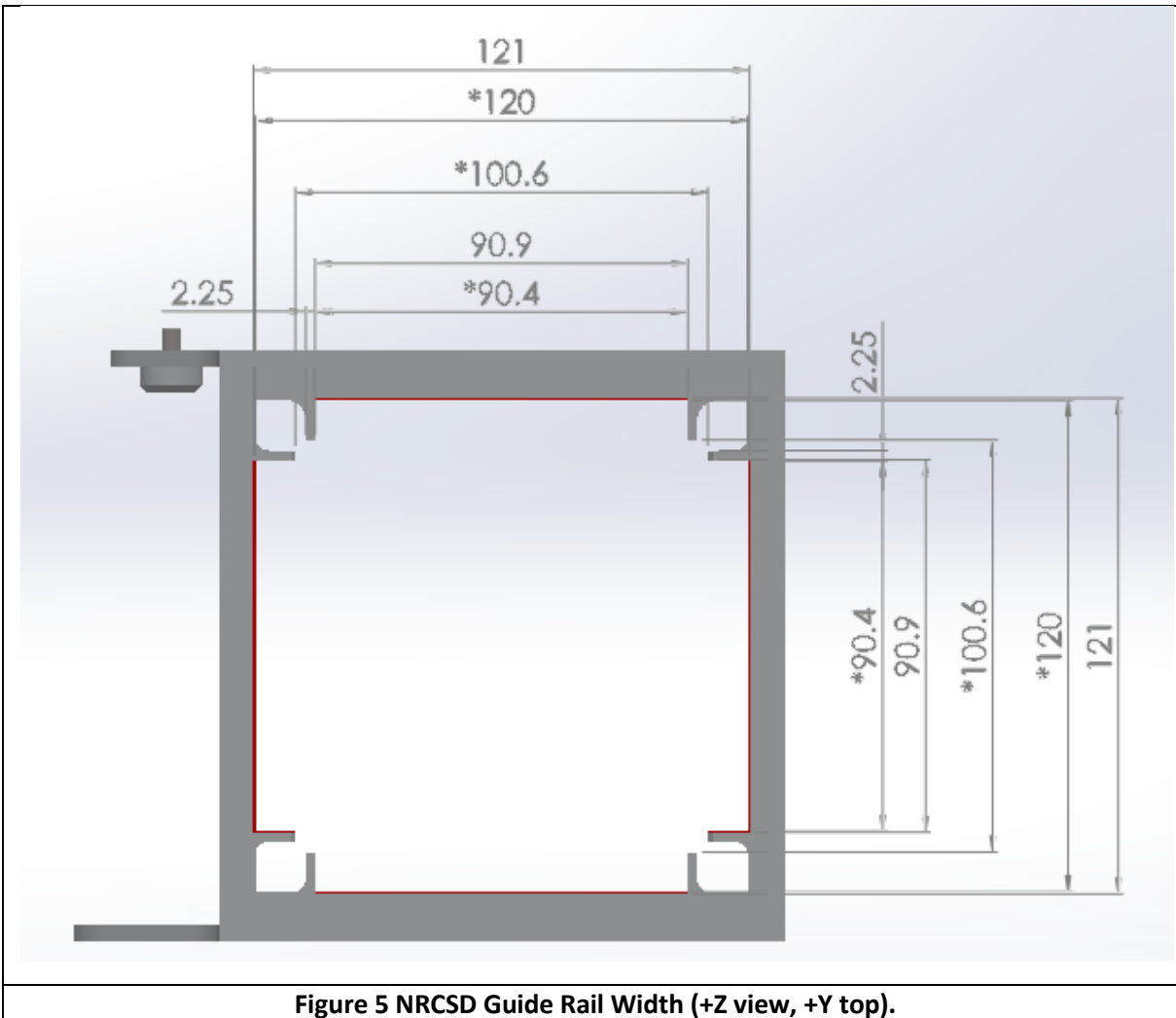
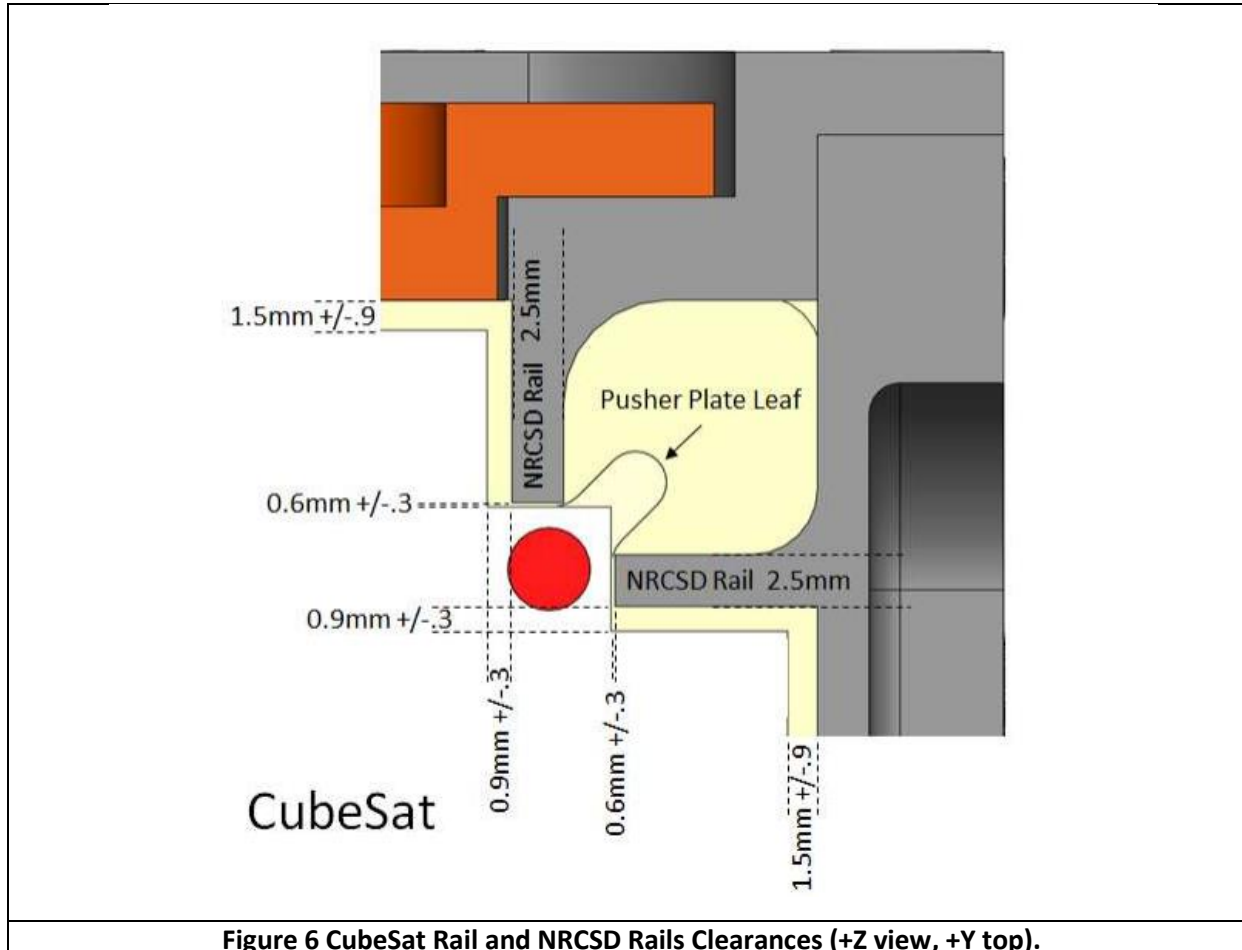


Figure 5 NRCSD Guide Rail Width (+Z view, +Y top).

Section 4.5, Figure 6 of the NRCSD ICD Rev 36, depicts the NRCSD guide rails having width of 2.5mm.



NRCSDs manufactured after June 2014 (NanoRacks CubeSat Mission 2 and thereafter) have guide rail width of 2.25mm as shown in Figure 6 below.

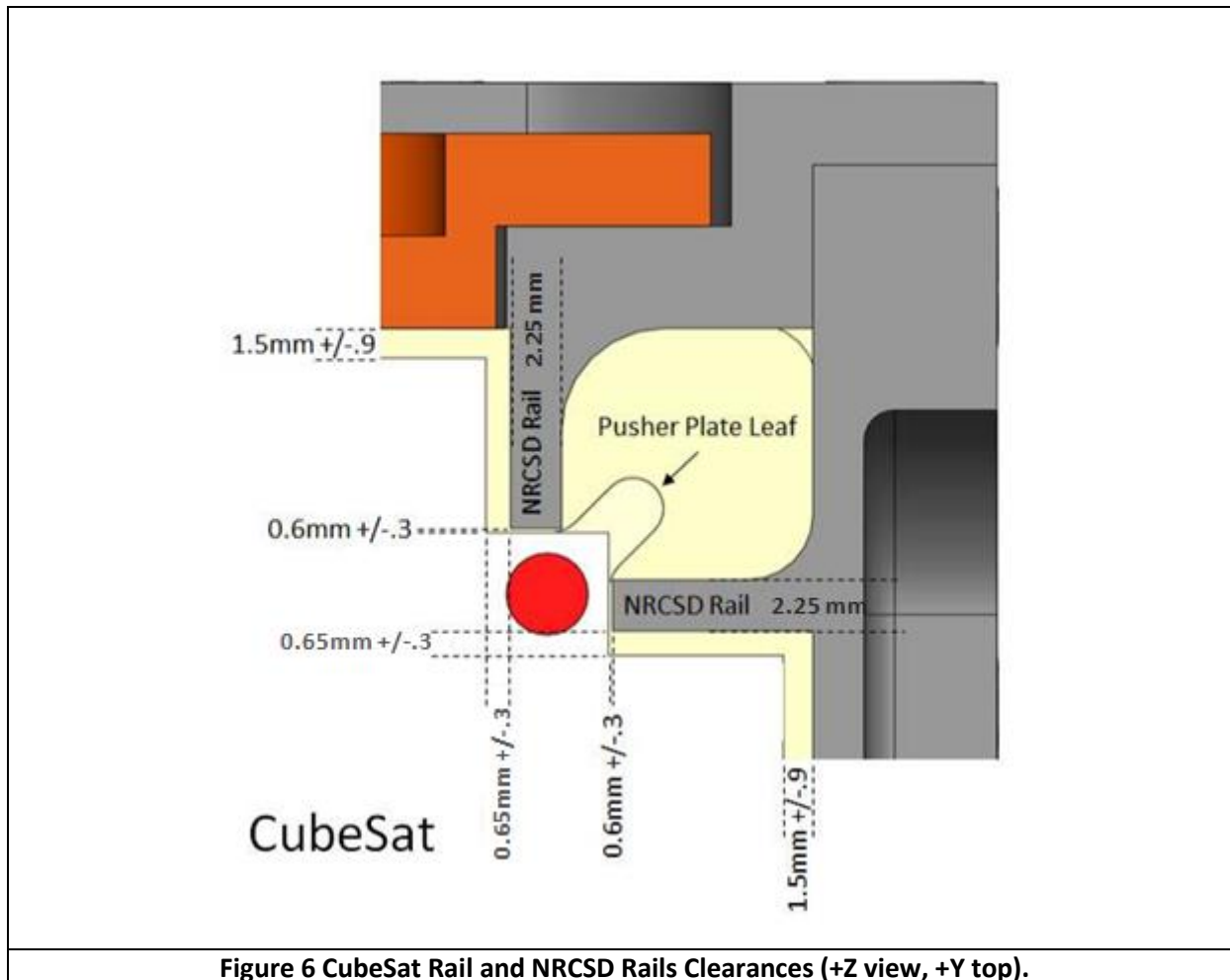


Figure 6 CubeSat Rail and NRCSD Rails Clearances (+Z view, +Y top).

Section 4.7, Figure 9 of the NRCSD ICD Rev 36, depicts the NRCSD guide rails having width of 2.5mm.

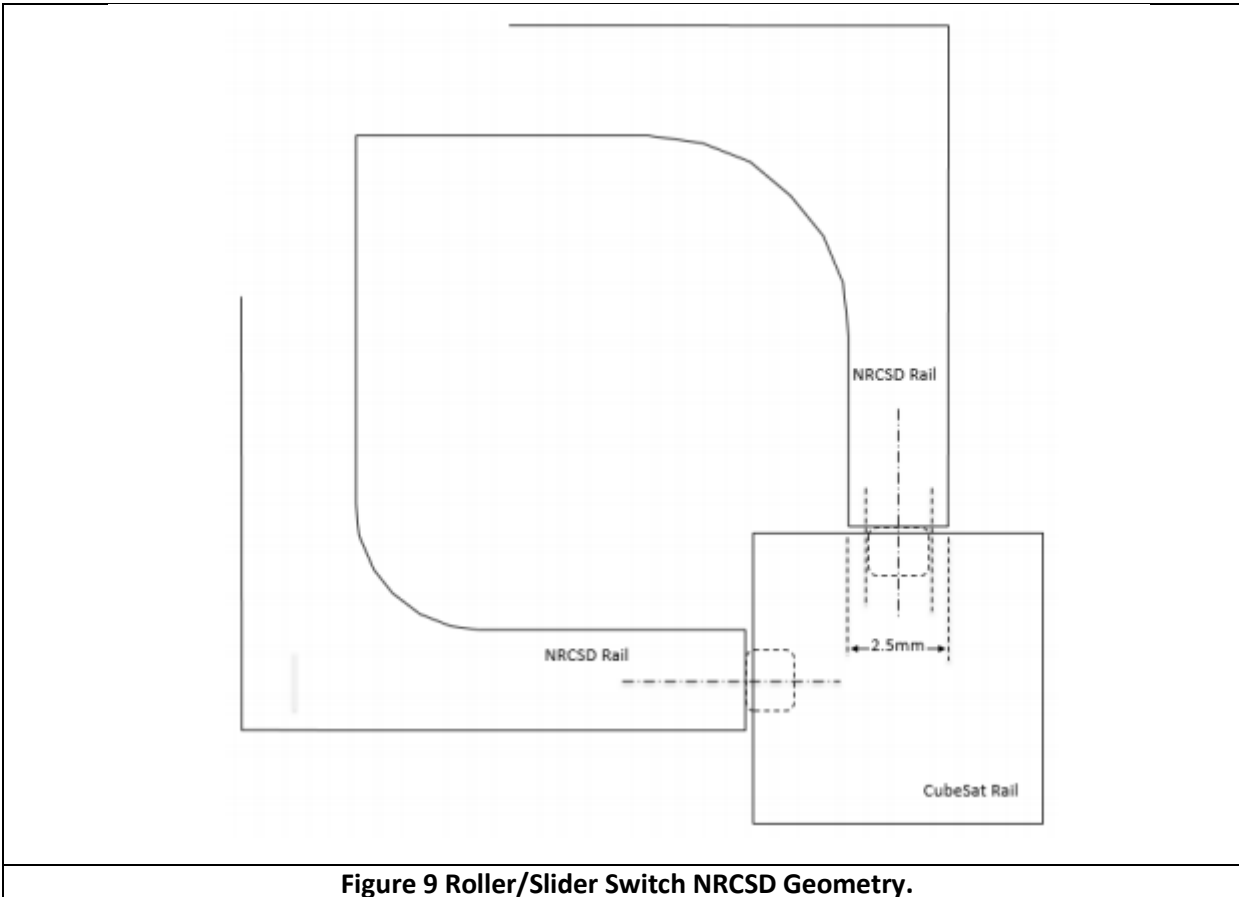


Figure 9 Roller/Slider Switch NRCSD Geometry.

NRCSDs manufactured after June 2014 (NanoRacks CubeSat Mission 2 and thereafter) have guide rail width of 2.25mm as shown in Figure 9 below.

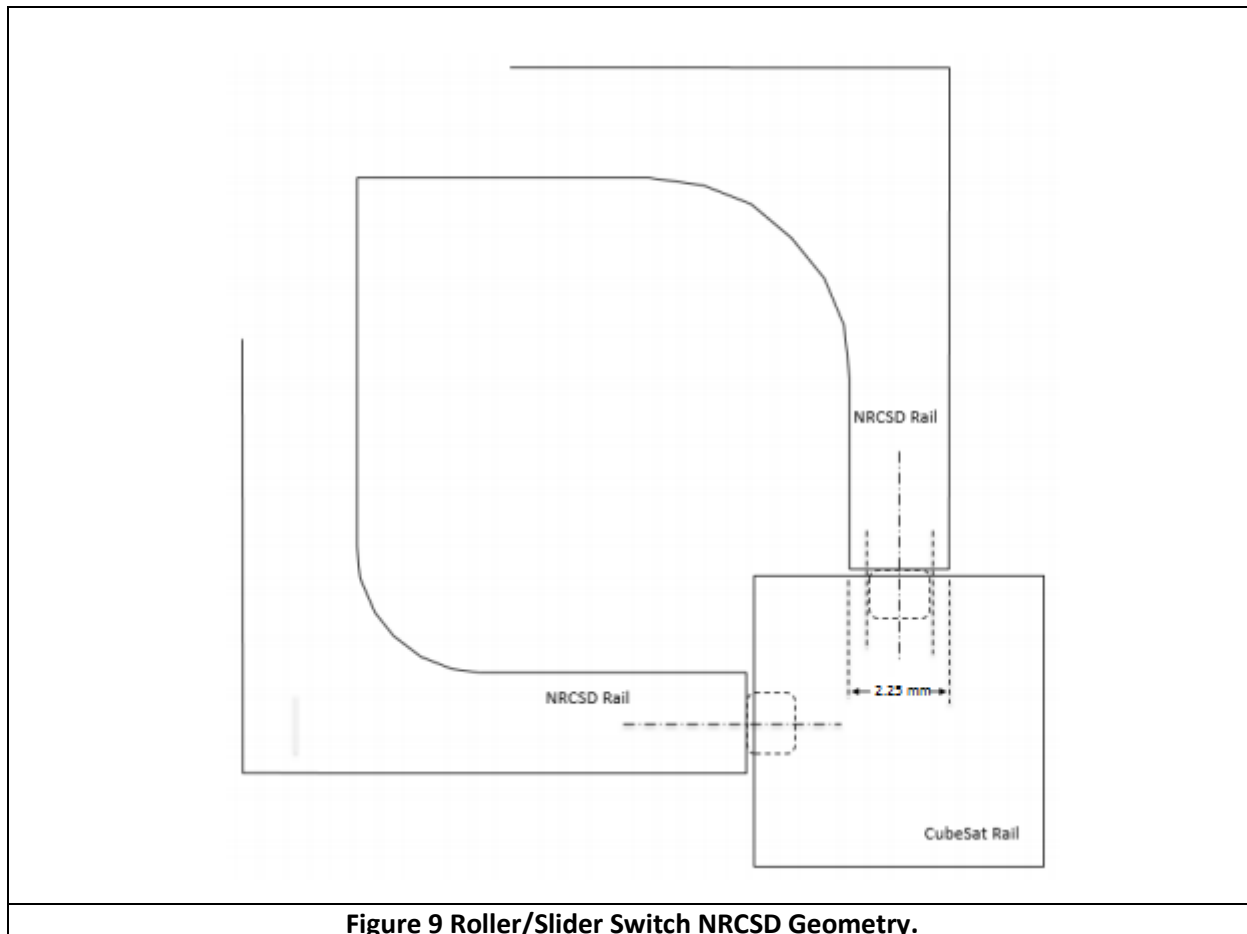


Figure 9 Roller/Slider Switch NRCSD Geometry.

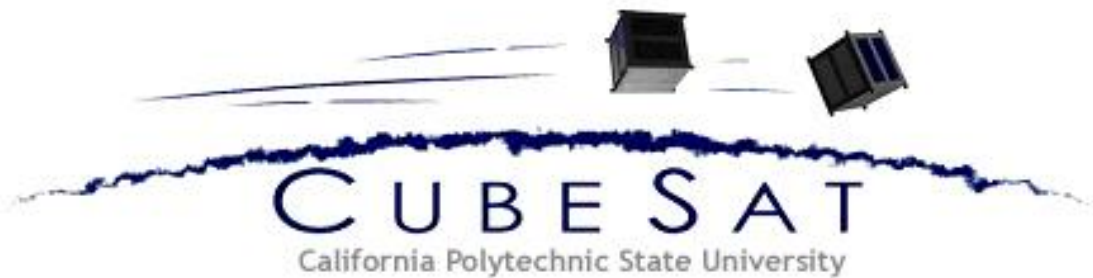
End of Document

B.3 CubeSat Design Specification

Document Classification	
X	Public Domain
	ITAR Controlled
	Internal Only

CubeSat Design Specification

(CDS)
REV 13



CHANGE HISTORY LOG

Effective Date	Revision	Author	Description of Changes
N/A	8	Simon Lee	N/A
5/26/05	8.1	Amy Hupputanasin	Formatting updated.
5/15/06	9	Armen Toorian	Information and presentation revised.
8/2/07	10	Wenschel Lan	Information updated.
10/02/08	11	Riki Munakata	Format, Design specification and Mk.III P-POD compatibility update.
8/1/09	12	Riki Munakata	Requirements update, waiver form requirements, and 3U CubeSat Specification drawing.
3/30/12	12.1	Justin Carnahan	Reformatted document to improve readability, updated to include 1.5U, 2U, and 3U+. Added and modified some req.
7/12/13	13-draft	David Pignatelli	Added applicable documents section. Removed restrictions on propulsion, added guidance for propulsion systems and hazardous materials. Added magnetic field restrictions and suggestions. Cleaned Section 3.2. Added custom spring plunger specs and recommendation. Extended restrictions on inhibits. Added links to outside resources. Cleaned Section 4.
2/20/14	13	Arash Mehrparvar	Fixed page numbering, error in spring plunger thread callout, other minor edits based on external suggestions.

TABLE OF CONTENTS

INTRODUCTION	5
1.1 Overview	5
1.2 Purpose.....	5
1.3 Waiver Process.....	5
2. POLY PICOSATELLITE ORBITAL DEPLOYER	7
2.1 Interface	7
3. CUBESAT SPECIFICATION.....	7
3.1 General Requirements	7
3.2 CubeSat Mechanical Requirements	8
3.3 Electrical Requirements.....	12
3.4 Operational Requirements	13
4. TESTING REQUIREMENTS.....	14
4.1 Random Vibration	14
4.2 Thermal Vacuum Bakeout	14
4.3 Shock Testing	14
4.4 Visual Inspection	14
4.5 CubeSat Testing Philosophy	14
5. CONTACTS.....	16

List of Acronyms

AFSPCMAN	Air Force Space Command Manual
CAC	CubeSat Acceptance Checklist
Cal Poly	California Polytechnic State University, San Luis Obispo
CDS	CubeSat Design Specification
cm	Centimeters
CVCM	Collected Volatile Condensable Mass
DAR	Deviation Wavier Approval Request
FCC	Federal Communication Commission
GSFC	Goddard Space Flight Center
IARU	International Amateur Radio Union
kg	Kilogram
LSP	Lunch Services Program
LV	Launch Vehicle
MIL	Military
mm	Millimeters
NASA	National Aeronautics and Space Administration
NPR	NASA Procedural Requirements
P-POD	Poly Picosatellite Orbital Deployer
RBF	Remove Before Flight
Rev.	Revision
RF	Radio Frequency
SLO	San Luis Obispo
SSDL	Space Systems Development Lab
STD	Standard
TML	Total Mass Loss
μm	Micrometer

Applicable Documents

The following documents form a part of this document to the extent specified herein. In the event of conflict between the documents referenced herein and the contents of this document, the contents of this document shall take precedence.

LSP Program Level P-POD and CubeSat Requirements Document (LSP-REQ-317.01)

General Environmental Verification Standard for GSFC Flight Programs and Projects (GSFC-STD-7000)

Military Standard Test Requirements for Launch, Upper-stage, and Space Vehicles (MIL-STD-1540)

Air Force Space Command Manual 91-710, Range Safety User Requirements Manual (AFSPCMAN 91-710)

Metallic Material Properties (MIL-HDBK-5)

Standard Materials and Processes Requirements for Spacecraft (NASA-STD-6016)

NASA Procedural Requirements for Limiting Orbital Debris (NPR 8715.6)

Introduction

1.1 Overview

Started in 1999, the CubeSat Project began as a collaborative effort between Prof. Jordi Puig-Suari at California Polytechnic State University (Cal Poly), San Luis Obispo, and Prof. Bob Twiggs at Stanford University's Space Systems Development Laboratory (SSDL). The purpose of the project is to provide a standard for design of picosatellites to reduce cost and development time, increase accessibility to space, and sustain frequent launches. Presently, the CubeSat Project is an international collaboration of over 100 universities, high schools, and private firms developing picosatellites containing scientific, private, and government payloads. A CubeSat is a 10 cm cube with a mass of up to 1.33 kg. Developers benefit from the sharing of information within the community. If you are planning to start a CubeSat project, please contact Cal Poly. Visit the CubeSat website at <http://cubesat.org> for more information.



Figure 1: Six CubeSats and their deployment systems.

1.2 Purpose

The primary mission of the CubeSat Program is to provide access to space for small payloads. The primary responsibility of Cal Poly, as the developer of the Poly Picosatellite Orbital Deployer (P-POD), is to ensure the safety of the CubeSat and protect the launch vehicle (LV), primary payload, and other CubeSats. CubeSat developers should play an active role in ensuring the safety and success of CubeSat missions by implementing good engineering practice, testing, and verification of their systems. Failures of CubeSats, the P-POD, or interface hardware can damage the LV or a primary payload and put the entire CubeSat Program in jeopardy. As part of the CubeSat Community, all participants have an obligation to ensure safe operation of their systems and to meet the design and minimum testing requirements outlined in this document. Requirements in this document may be superseded by launch provider requirements.

1.3 Waiver Process

Developers will fill out a "Deviation Waiver Approval Request (DAR)" (see appendix A) if their CubeSat is in violation of any requirements in sections 2 or 3. The waiver process is intended to be quick and easy. The intent is to help facilitate communication and explicit documentation

between CubeSat developers, P-POD integrators, range safety personnel, and launch vehicle providers. This will help to better identify and address any issues that may arise prior to integration and launch. The DAR can be found at <http://www.cubesat.org/> and waiver requests should be sent to standards@cubesat.org.

Upon completion of the DAR, the P-POD Integrator will review the request, resolve any questions, and determine if there are any additional tests, analyses or costs to support the waiver. If so, the Developer, with inputs from the P-POD Integrator, will write a test plan and perform the tests before the waiver is conditionally accepted by the P-POD Integrator. Waivers can only be conditionally accepted by the P-POD Integrator until a launch has been identified for the CubeSat. Once a launch has been identified, the waiver becomes mission specific and passes to the launch vehicle Mission Manager for review. The launch vehicle Mission Manager has the final say on acceptance of the waiver, and the Mission Manager may require more corrections and/or testing to be performed before approving the waiver. Developers should realize that each waiver submitted reduces the chances of finding a suitable launch opportunity.

CubeSat Standard Deviation Waiver Process

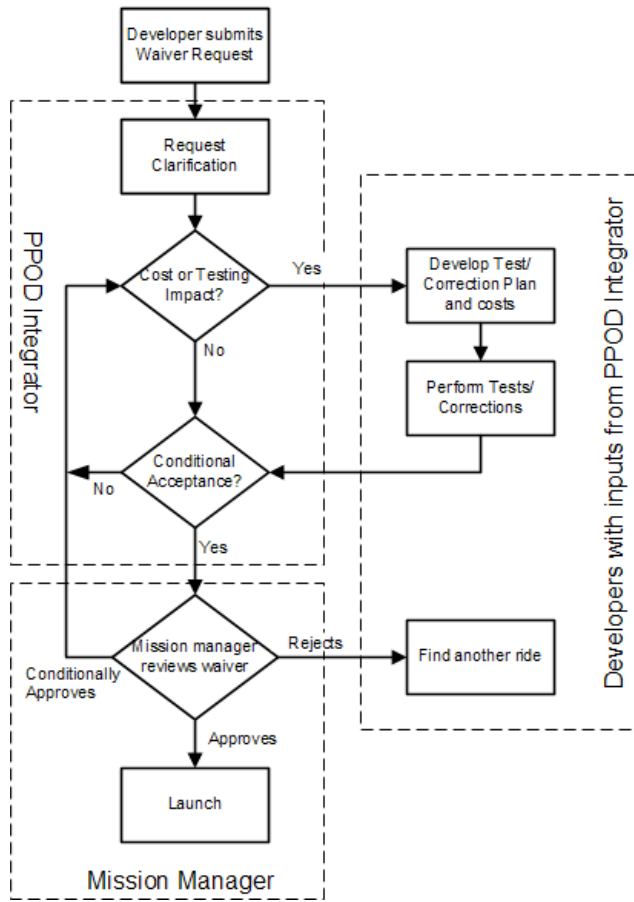


Figure 2: CubeSat Standard Deviation Wavier Process Flow Diagram

2. Poly Picosatellite Orbital Deployer

2.1 Interface

The Poly Picosatellite Orbital Deployer (P-POD) is Cal Poly's standardized CubeSat deployment system. It is capable of carrying three standard CubeSats and serves as the interface between the CubeSats and LV. The P-POD is a rectangular box with a door and a spring mechanism. Once the release mechanism of the P-POD is actuated by a deployment signal sent from the LV, a set of torsion springs at the door hinge force the door open and the CubeSats are deployed by the main spring gliding on its rails and the P-PODs rails (P-POD rails are shown in Figure 3b). The P-POD is made up of anodized aluminum. CubeSats slide along a series of rails during ejection into orbit. CubeSats will be compatible with the P-POD to ensure safety and success of the mission by meeting the requirements outlined in this document. The P-POD is backward compatible, and any CubeSat developed within the design specification of CDS rev. 9 and later will not have compatibility issues. Developers are encouraged to design to the most current CDS to take full advantage of the P-POD features.

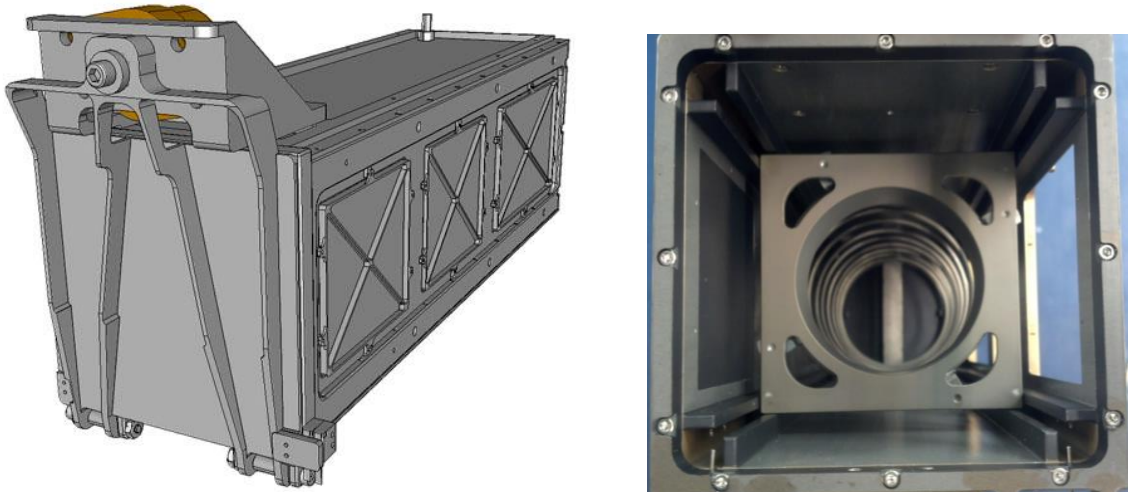


Figure 3a and 3b: Poly Picosatellite Orbital Deployer (P-POD) and cross section

3. CubeSat Specification

3.1 General Requirements

- 3.1.1 CubeSats which incorporate any deviation from the CDS will submit a DAR and adhere to the waiver process (see Section 1.3 and Appendix A).
- 3.1.2 All parts shall remain attached to the CubeSats during launch, ejection and operation. No additional space debris will be created.
- 3.1.3 No pyrotechnics shall be permitted.
- 3.1.4 Any propulsion systems shall be designed, integrated, and tested in accordance with AFSPCMAN 91-710 Volume 3.
- 3.1.5 Propulsion systems shall have at least 3 inhibits to activation.
- 3.1.6 Total stored chemical energy will not exceed 100 Watt-Hours.

- 3.1.6.1 Note: Higher capacities may be permitted, but could potentially limit launch opportunities.
- 3.1.7 CubeSat hazardous materials shall conform to AFSPCMAN 91-710, Volume 3.
- 3.1.8 CubeSat materials shall satisfy the following low out-gassing criterion to prevent contamination of other spacecraft during integration, testing, and launch. A list of NASA approved low out-gassing materials can be found at: <http://outgassing.nasa.gov>
- 3.1.8.1 CubeSats materials shall have a Total Mass Loss (TML) $\leq 1.0\%$
- 3.1.8.2 CubeSat materials shall have a Collected Volatile Condensable Material (CVCM) $\leq 0.1\%$
- 3.1.9 The latest revision of the CubeSat Design Specification will be the official version which all CubeSat developers will adhere to. The latest revision is available at <http://www.cubesat.org>.
- 3.1.9.1 Cal Poly will send updates to the CubeSat mailing list upon any changes to the specification. You can sign-up for the CubeSat mailing list here: www.cubesat.org/index.php/about-us/how-to-join
- 3.1.10 Note: Some launch vehicles hold requirements on magnetic field strength. Additionally, strong magnets can interfere with the separation between CubeSat spacecraft in the same P-POD. As a general guideline, it is advised to limit magnetic field outside the CubeSat static envelope to 0.5 Gauss above Earth's magnetic field.
- 3.1.11 The CubeSat shall be designed to accommodate ascent venting per ventable volume/area < 2000 inches.

3.2 CubeSat Mechanical Requirements

CubeSats are cube shaped picosatellites with dimensions and features outlined in the CubeSat Specification Drawing (Appendix B). The PPOD coordinate system is shown below in Figure 4 for reference. General features of all CubeSats include:

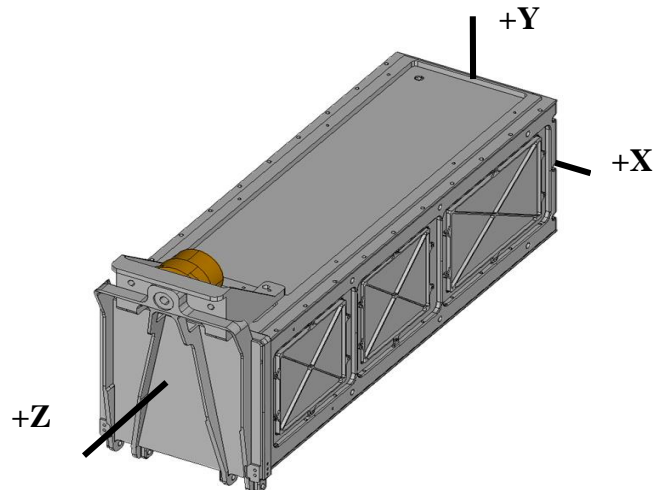


Figure 4: PPOD Coordinate System

- 3.2.1 The CubeSat shall use the coordinate system as defined in Appendix B for the appropriate size. The CubeSat coordinate system will match the P-POD coordinate system while integrated into the P-POD. The origin of the CubeSat coordinate system is located at the geometric center of the CubeSat.
 - 3.2.1.1 The CubeSat configuration and physical dimensions shall be per the appropriate section of Appendix B.
 - 3.2.1.2 The extra volume available for 3U+ CubeSats is shown in Figure 6.
- 3.2.2 The -Z face of the CubeSat will be inserted first into the P-POD.
- 3.2.3 No components on the green and yellow shaded sides shall exceed 6.5 mm normal to the surface.
 - 3.2.3.1 When completing a CubeSat Acceptance Checklist (CAC), protrusions will be measured from the plane of the rails.
- 3.2.4 Deployables shall be constrained by the CubeSat, not the P-POD.
- 3.2.5 Rails shall have a minimum width of 8.5mm.
- 3.2.6 Rails will have a surface roughness less than 1.6 μm .
- 3.2.7 The edges of the rails will be rounded to a radius of at least 1 mm
- 3.2.8 The ends of the rails on the +/- Z face shall have a minimum surface area of 6.5 mm x 6.5 mm contact area for neighboring CubeSat rails (as per Figure 6).
- 3.2.9 At least 75% of the rail will be in contact with the P-POD rails. 25% of the rails may be recessed and no part of the rails will exceed the specification.
- 3.2.10 The maximum mass of a 1U CubeSat shall be 1.33 kg.
 - 3.2.10.1 Note: Larger masses may be evaluated on a mission to mission basis.
- 3.2.11 The maximum mass of a 1.5U CubeSat shall be 2.00 kg.
 - 3.2.11.1 Note: Larger masses may be evaluated on a mission to mission basis.
- 3.2.12 The maximum mass of a 2U CubeSat shall be 2.66 kg.
 - 3.2.12.1 Note: Larger masses may be evaluated on a mission to mission basis.
- 3.2.13 The maximum mass of a 3U CubeSat shall be 4.00 kg.
 - 3.2.13.1 Note: Larger masses may be evaluated on a mission to mission basis.
- 3.2.14 The CubeSat center of gravity shall be located within 2 cm from its geometric center in the X and Y direction.
 - 3.2.14.1 The 1U CubeSat center of gravity shall be located within 2 cm from its geometric center in the Z direction.
 - 3.2.14.2 The 1.5U CubeSat center of gravity shall be located within 3 cm from its geometric center in the Z direction.
 - 3.2.14.3 The 2U CubeSat center of gravity shall be located within 4.5 cm from its geometric center in the Z direction.
 - 3.2.14.4 3U and 3U+ CubeSats' center of gravity shall be located within 7 cm from its geometric center in the Z direction.
- 3.2.15 Aluminum 7075, 6061, 5005, and/or 5052 will be used for both the main CubeSat structure and the rails.
 - 3.2.15.1 If other materials are used the developer will submit a DAR and adhere to the waiver process.
- 3.2.16 The CubeSat rails and standoff, which contact the P-POD rails and adjacent CubeSat standoffs, shall be hard anodized aluminum to prevent any cold welding within the P-POD.

3.2.17 The 1U, 1.5U, and 2U CubeSats shall use separation springs to ensure adequate separation.

3.2.17.1 Note: Recommended separation spring specifications are shown below in Table 1.
These are a custom part available through Cal Poly. Contact cubesat@gmail.com in order to obtain these separation springs.

3.2.17.2 The compressed separation springs shall be at or below the level of the standoff.

3.2.17.3 The 1U, 1.5U, and 2U CubeSat separation spring will be centered on the end of the standoff on the CubeSat's -Z face as per Figure 7.

3.2.17.4 Separation springs are not required for 3U CubeSats.

Table 1: CubeSat Separation Spring Characteristics

Characteristics	Value
Plunger Material	<i>Stainless Steel</i>
End Force Initial/Final	<i>0.14 lbs. / 0.9 lbs.</i>
Throw Length	<i>0.16 inches minimum above the standoff surface</i>
Thread Pitch	<i>8-36 UNF-2B</i>

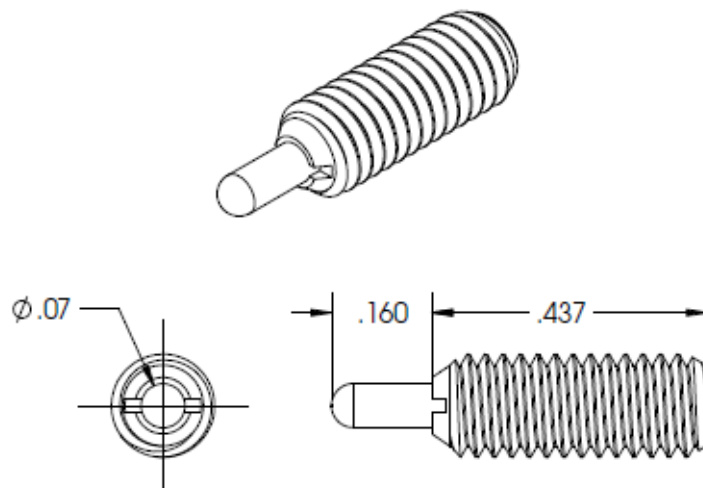


Figure 5: Custom Spec Spring Plunger (Separation Spring)

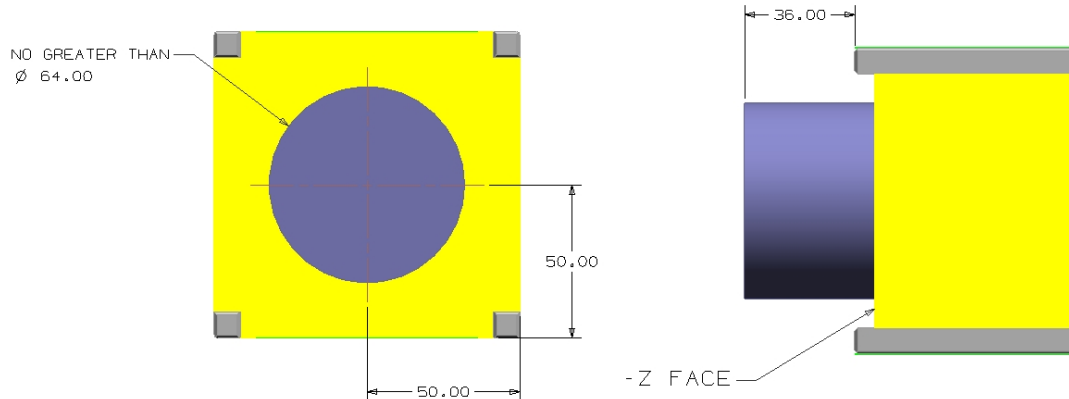


Figure 6: 3U+ Extra Volume ("Tuna Can")

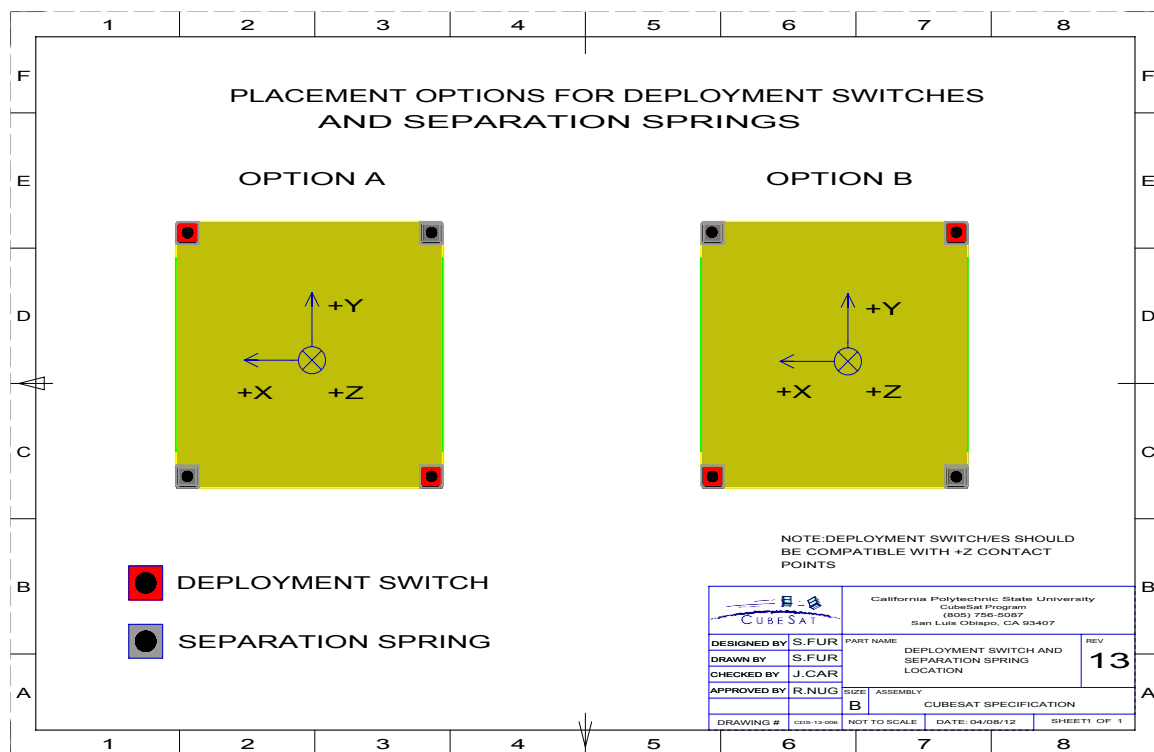


Figure 7: Deployment Switches and Separation Spring Locations

3.3 Electrical Requirements

Electronic systems will be designed with the following safety features.

- 3.3.1 The CubeSat power system shall be at a power off state to prevent CubeSat from activating any powered functions while integrated in the P-POD from the time of delivery to the LV through on-orbit deployment. CubeSat powered function include the variety of subsystems such as Command and Data Handling (C&DH), RF Communication, Attitude Determine and Control (ADC), deployable mechanism actuation. CubeSat power systems include all battery assemblies, solar cells, and coin cell batteries.
- 3.3.2 The CubeSat shall have, at a minimum, one deployment switch on a rail standoff, per Figure 7.
- 3.3.3 In the actuated state, the CubeSat deployment switch shall electrically disconnect the power system from the powered functions; this includes real time clocks (RTC).
- 3.3.4 The deployment switch shall be in the actuated state at all times while integrated in the P-POD.
 - 3.3.4.1 In the actuated state, the CubeSat deployment switch will be at or below the level of the standoff.
- 3.3.5 If the CubeSat deployment switch toggles from the actuated state and back, the transmission and deployable timers shall reset to t=0.
- 3.3.6 The RBF pin and all CubeSat umbilical connectors shall be within the designated Access Port locations, green shaded areas shown in Appendix B.
 - 3.3.6.1 Note: All diagnostics and battery charging within the P-POD will be done while the deployment switch is depressed.
- 3.3.7 The CubeSat shall include an RBF pin.
 - 3.3.7.1 The RBF pin shall cut all power to the satellite once it is inserted into the satellite.
 - 3.3.7.2 The RBF pin shall be removed from the CubeSat after integration into the P-POD.
 - 3.3.7.3 The RBF pin shall protrude no more than 6.5 mm from the rails when it is fully inserted into the satellite.
- 3.3.8 CubeSats shall incorporate battery circuit protection for charging/discharging to avoid unbalanced cell conditions.
- 3.3.9 The CubeSat shall be designed to meet at least one of the following requirements to prohibit inadvertent radio frequency (RF) transmission. The use of three independent inhibits is highly recommended and can reduce required documentation and analysis.
An inhibit is a physical device between a power source and a hazard. A timer is not considered an independent inhibit.
 - 3.3.9.1 The CubeSat will have one RF inhibit and RF power output of no greater than 1.5W at the transmitting antenna's RF input.
 - 3.3.9.2 The CubeSat will have two independent RF inhibits

3.4 Operational Requirements

CubeSats will meet certain requirements pertaining to integration and operation to meet legal obligations and ensure safety of other CubeSats.

- 3.4.1 Operators will obtain and provide documentation of proper licenses for use of radio frequencies.
 - 3.4.1.1 For amateur frequency use, this requires proof of frequency coordination by the International Amateur Radio Union (IARU). Applications can be found at www.iaru.org.
- 3.4.2 CubeSats will comply with their country's radio license agreements and restrictions.
- 3.4.3 CubeSats mission design and hardware shall be in accordance with NPR 8715.6 to limit orbital debris.
 - 3.4.3.1 Any CubeSat component shall re-enter with energy less than 15 Joules.
 - 3.4.3.2 Developers will obtain and provide documentation of approval of an orbital debris mitigation plan from the FCC (or NOAA if imager is present).
 - 3.4.3.2.1 Note: To view FCC amateur radio regulations, go to <http://www.arrl.org/part-97-amateur-radio>
 - 3.4.3.3 Note: Analysis can be conducted to satisfy the above with NASA DAS, available at <http://orbitaldebris.jsc.nasa.gov/mitigate/das.html>
- 3.4.4 All deployables such as booms, antennas, and solar panels shall wait to deploy a minimum of 30 minutes after the CubeSat's deployment switch(es) are activated from P-POD ejection.
- 3.4.5 No CubeSats shall generate or transmit any signal from the time of integration into the P-POD through 45 minutes after on-orbit deployment from the P-POD. However, the CubeSat can be powered on following deployment from the P-POD.
- 3.4.6 Private entities (non-U.S. Government) under the jurisdiction or control of the United States who propose to operate a remote sensing space system (satellite) may need to have a license as required by U.S. law. For more information visit <http://www.nesdis.noaa.gov/CRSRA/licenseHome.html>. Click on the Application Process link under the Applying for a License drop down section to begin the process.
- 3.4.7 Cal Poly will conduct a minimum of one fit check in which developer hardware will be inspected and integrated into the P-POD or TestPOD. A final fit check will be conducted prior to launch. The CubeSat Acceptance Checklist (CAC) will be used to verify compliance of the specification (Found in the appendix of this document or online at <http://cubesat.org/index.php/documents/developers>).

4. Testing Requirements

Testing will be performed to meet all launch provider requirements as well as any additional testing requirements deemed necessary to ensure the safety of the CubeSats, P-POD, and the primary mission. If the launch vehicle environment is unknown, The General Environmental Verification Standard (GEVS, GSFC-STD-7000) and MIL-STD-1540 can be used to derive testing requirements. GSFC-STD-7000 and MIL-STD-1540 are useful references when defining testing environments and requirements, however the test levels defined in GSFC-STD-7000 and MIL-STD-1540 are not guaranteed to encompass or satisfy all LV testing environments. Test requirements and levels that are not generated by the launch provider or P-POD Integrator are considered to be unofficial. The launch provider testing requirements will supersede testing environments from any other source. The P-POD will be tested in a similar fashion to ensure the safety and workmanship before integration with the CubeSats. At the very minimum, all CubeSats will undergo the following tests.

4.1 Random Vibration

Random vibration testing shall be performed as defined by the launch provider

4.2 Thermal Vacuum Bakeout

Thermal vacuum bakeout shall be performed to ensure proper outgassing of components. The test specification will be outlined by the launch provider.

4.3 Shock Testing

Shock testing shall be performed as defined by the launch provider.

4.4 Visual Inspection

Visual inspection of the CubeSat and measurement of critical areas will be performed per the appropriate CAC (Appendix C).

4.5 CubeSat Testing Philosophy

The CubeSat shall be subjected to either a qualification or protoflight testing as defined in the CubeSat Testing Flow Diagram, shown in Figure 88. The test levels and durations will be supplied by the launch provider or P-POD integrator.

4.5.1 Qualification

Qualification testing is performed on an engineering unit hardware that is identical to the flight model CubeSat. Qualification levels will be determined by the launch vehicle provider or P-POD integrator. Both MIL-STD-1540 and LSP-REQ-317.01 are used as guides in determining testing levels. The flight model will then be tested to Acceptance levels in a TestPOD then integrated into the flight P-POD for a final acceptance/workmanship random vibration test. **Additional testing may be required if modifications or changes are made to the CubeSats after qualification testing.**

4.5.2 Protolight

Protolight testing is performed on the flight model CubeSat. Protolight levels will be determined by the launch vehicle provider or P-POD integrator. Both MIL-STD-1540 and LSP-REQ-317.01 are used as guides in determining testing levels. The flight model will be tested to Protolight levels in a TestPOD then integrated into the flight P-POD for a final acceptance/workmanship random vibration test. The flight CubeSat **SHALL NOT** be disassembled or modified after protolight testing. Disassembly of hardware after protolight testing will require the developer to submit a DAR and adhere to the waiver process prior to disassembly. **Additional testing will be required if modifications or changes are made to the CubeSats after protolight testing.**

4.5.3 Acceptance

After delivery and integration of the CubeSat into the P-POD, additional testing will be performed with the integrated system. This test ensures proper integration of the CubeSat into the P-POD. Additionally, any unknown, harmful interactions between CubeSats may be discovered during acceptance testing. The P-POD Integrator will coordinate and perform acceptance testing. Acceptance levels will be determined by the launch vehicle provider or P-POD integrator. Both MIL-STD-1540 and LSP-REQ-317.01 are used as guides in determining testing levels. The P-POD **SHALL NOT** be deintegrated at this point. If a CubeSat failure is discovered, a decision to deintegrate the P-POD will be made by the developers, in that P-POD, and the P-POD Integrator based on safety concerns. The developer is responsible for any additional testing required due to corrective modifications to deintegrated P-PODs and CubeSats.

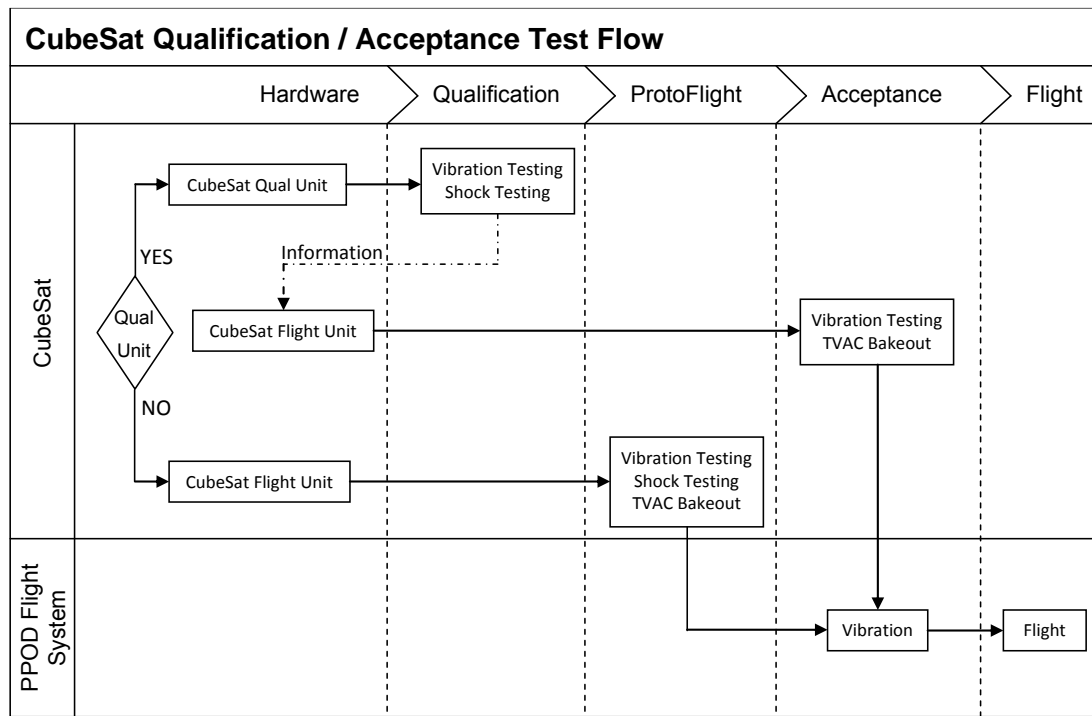


Figure 8: CubeSat General Testing Flow Diagram

5. Contacts

Cal Poly - San Luis Obispo

Prof. Jordi Puig-Suari
Aerospace Engineering Dept.
(805) 756-5087
(805) 756-2376 fax
jpuigsua@calpoly.edu

Cal Poly Program Manager

Roland Coelho
(805) 756-5087
(805) 756-5165 fax
rcoelho@calpoly.edu

SRI International

Dr. Scott Williams, Program Manager
Engineering Systems Division
(650) 859-5057
(650) 859-3919 fax
scott.williams@sri.com

Cal Poly Student Contacts

(805) 756-5087
(805) 756-5165 fax
cubesat@gmail.com

Appendix A:

Waiver Form

CubeSat Design Specification

Deviation Waiver Approval Request (DAR)

Date: August 1, 2009

Rev. 12

CubeSat Developers only fill out sections 1 through 9 and 15(optional). Email to: standards@cubesat.org

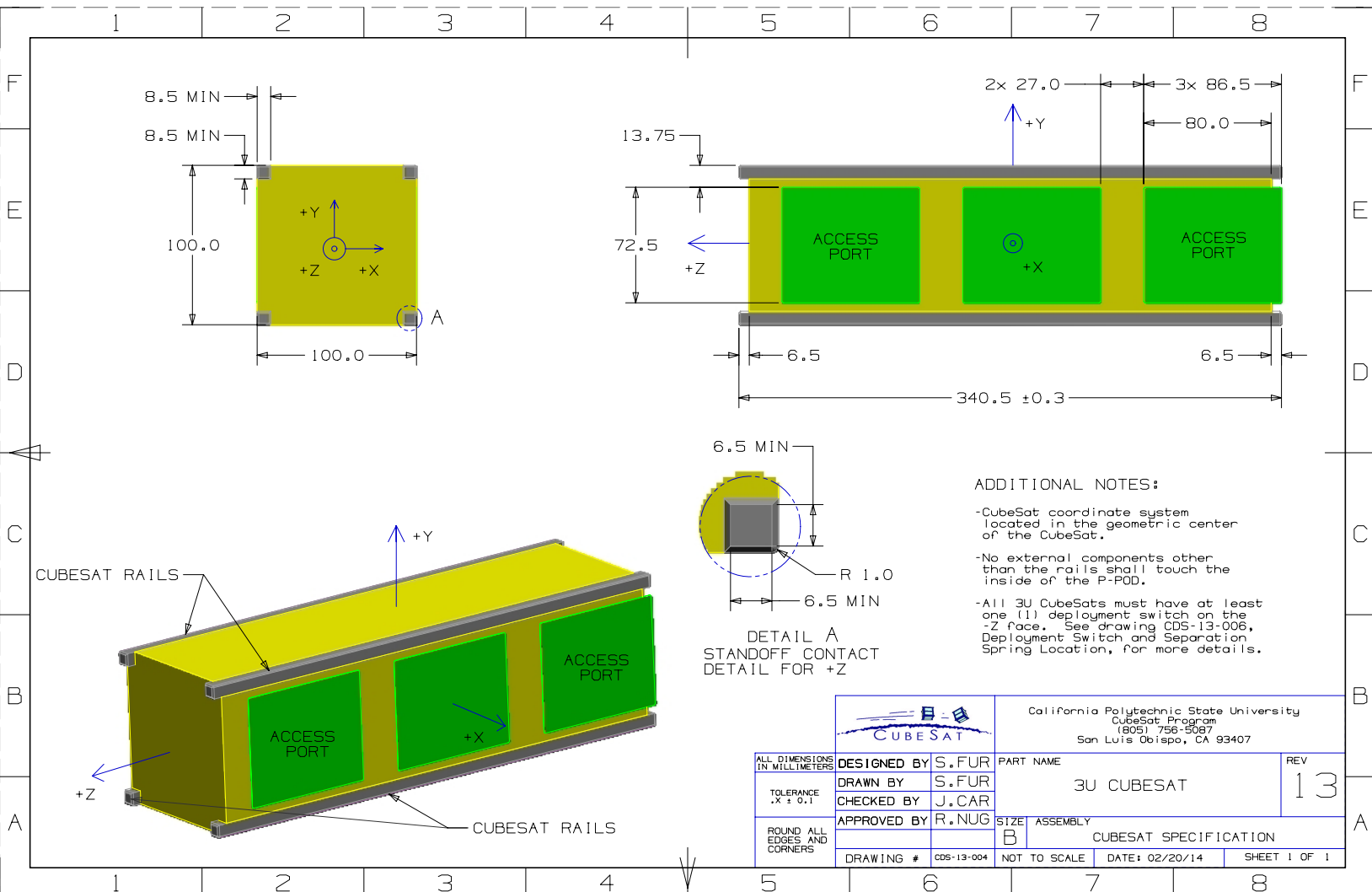
1. MISSION NAME:	2. DAR NUMBER:	3. DATE:		
4. INITATOR	5. INITIATING ORGANIZATION:			
6. SPECIFIED REQUIREMENTS NUMBERS:	7. JUSTIFICATION FOR DAR:	8. WAIVER TYPE <input type="checkbox"/> DIMENSIONS or MASS <input type="checkbox"/> STRUCTURE <input type="checkbox"/> ELECTRICAL <input type="checkbox"/> OPERATIONS <input type="checkbox"/> TESTING <input type="checkbox"/> OTHER		
9. DESCRIPTION OF DEPARTURE FROM REQUIREMENTS:				
10. CSEP DISPOSITION: <input type="checkbox"/> ACCEPTED <input type="checkbox"/> REJECTED <input type="checkbox"/> CONDITIONALLY ACCEPTED	11. ACCEPT/REJECT JUSTIFICATION:			
CSEP AUTHORIZED REP.		SIGNATURE	ORGANIZATION	DATE
12. ACCEPTANCE CONDITIONS				
13. LAUNCH VEHICLE INTEGRATOR APPROVAL AUTHORITY: <input type="checkbox"/> APPROVED <input type="checkbox"/> DISAPPROVED <input type="checkbox"/> CONDITIONALLY APPROVED	14. LVI APPROVAL/DISAPPROVAL JUSTIFICATION:			
LVI AUTHORIZED REP.		SIGNATURE	ORGANIZATION	DATE
15. APPROVAL CONDITIONS				

1. MISSION NAME:	DEVIATION WAIVER APPROVAL REQUEST CONTINUATION PAGE	2. DAR NO.	3. DATE:
16. CONTINUATION (indicate item or block number):			

Appendix B:
1U, 1.5U, 2U, 3U, and 3U+
CubeSat Specification Drawing

Section 4

3U CubeSat Design Specification Drawing



Appendix C:
1U, 1.5U, 2U, 3U, and 3U+
CubeSat Acceptance Checklist

Section 4
3U CubeSat Acceptance Checklist

3U CubeSat Acceptance Checklist

Project:

Date/Time:

Engineers:

Organization:

Location:

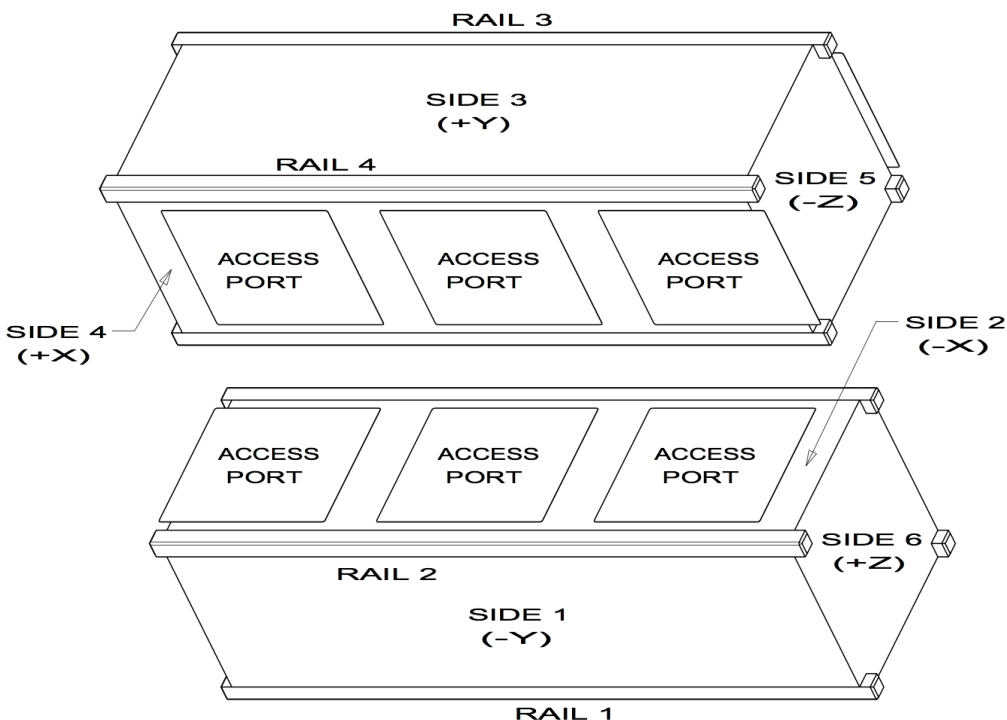
Satellite Name:

Satellite S/N:

Revision Date: 02/20/2014

Mass (< 4.00 kg)	_____	RBF Pin ($\leq 6.5\text{mm}$)	_____
Spring Plungers (Depressed)	Functional Y / N Flush with Standoff Y / N	Rails Anodized	Y / N
Deployment Switches (Depressed)	Functional Y / N Flush with Standoff Y / N	Deployables Constrained	Y / N

Mark on the diagram the locations of the RBF pin, connectors, deployables, and any envelope violations.



Authorized By:

IT #1: _____

IT #2: _____

Passed: Y / N

List Item	As Measured				Required	
Width [x-y]	Side 1 (-Y)	Side 2 (-X)	Side 3 (+Y)	Side 4 (+X)		
+Z	_____	_____	_____	_____	$100.0 \pm 0.1\text{mm}$	
Middle	_____	_____	_____	_____	$100.0 \pm 0.1\text{mm}$	
-Z	_____	_____	_____	_____	$100.0 \pm 0.1\text{mm}$	
Height [x-y]	Rail 1 (+X, -Y)	Rail 2 (-X, -Y)	Rail 3 (-X, +Y)	Rail 4 (+X, +Y)	$340.5 \pm 0.3\text{mm}$	
	_____	_____	_____	_____		
	Rail 1 (+X, -Y) length x width	Rail 2 (-X, -Y) length x width	Rail 3 (-X, +Y) length x width	Rail 4 (+X, +Y) length x width		
+Z Standoffs	____ x ____	____ x ____	____ x ____	____ x ____	$\geq 6.5\text{mm}$	
-Z Standoffs	____ x ____	____ x ____	____ x ____	____ x ____	$\geq 6.5\text{mm}$	
Protrusions	Side 1 (-Y)	Side 2 (-X)	Side 3 (+Y)	Side 4 (+X)	Side 5 (-Z)	Side 6 (+Z)
	_____	_____	_____	_____	_____	_____
						$\leq 6.5\text{mm}$